Ternary Alloys

Volume 21

MSI
Science Simplified

Ternary Alloys

A Comprehensive Compendium of Evaluated Constitutional Data and Phase Diagrams

critically evaluated by MSIT®

Volume 21

Selected Al-Fe-X Ternary Systems for Industrial Applications

Editors
Frank Stein, Martin Palm

Associate Editors
Liya Dreval, Oleksandr Dovbenko, Svitlana Iljenko

Authors
Materials Science International Team, MSIT®

MSI
Science Simplified

Editors: Frank Stein,
Martin Palm
Associate Editors: Liya Dreval
Oleksandr Dovbenko
Svitlana Iljenko

ISBN 978-3-932120-51-0

Vol. 21. Selected Al-Fe-X Ternary Systems for Industrial Applications. – 2022

This volume is part of the book series:
Ternary Alloys: A Comprehensive Compendium of Evaluated Constitutional Data and Phase Diagrams/
Materials Science International Services GmbH, Stuttgart, Germany

Group ISBN for the Ternary Alloys book series: 978-3-932120-41-1

Published by
MSI, Materials Science International Services GmbH, Stuttgart (Federal Republic of Germany)
Am Wallgraben 100, D-70565 Stuttgart, Germany
Postfach 800749, D-70507, Stuttgart, Germany
http://www.msiport.com
http://www.msi-eureka.com/

Printed on acid-free paper.

Printing and binding:
WIRmachenDRUCK GmbH, Mühlbachstraße 7, 71522 Backnang

Printed in the Federal Republic of Germany

Authors: Materials Science International Team, MSIT®

This volume results from collaborative evaluation programs performed by MSI and authored by MSIT®. In this program, data and knowledge are contributed by many individuals and have accumulated over almost thirty five years, up to the present day. The content of this volume is a subset of the ongoing MSIT® Evaluation Programs. Authors of this volume are:

Nataliya Bochvar, Moscow, Russia
Anatoliy Bondar, Kyiv, Ukraine
Gabriele Cacciamani, Genova, Italy
Lesley Cornish, Johannesburg, South Africa
Oleksandr Dovbenko, Stuttgart, Germany
Liya Dreval, Stuttgart, Germany
Yong Du, Changsha, China
Kiyaasha Dyal Ukabhai, Johannesburg, South Africa
Olga Fabrichnaya, Freiberg, Germany
Lorenzo Fenocchio, Genova, Italy
Sergio Gama, Campinas, Brasil
Gautam Ghosh, Evanston, USA
Bernd Grieb, Tübingen, Germany
Kiyohito Ishida, Sendai, Japan
Hermann A. Jehn, Stuttgart, Germany
Kostyantyn Korniyenko, Kyiv, Ukraine
Mario J. Kriegel, Freiberg, Germany
Ortrud Kubaschewski†, Aachen, Germany
K.C. Hari Kumar, Chennai, India
Bernard Legendre, Paris, France
Xiaojing Li, Changsha, China
Shuhong Liu, Changsha, China
Xing Jun Liu, Sendai, Japan
Annelies Malfliet, Heverlee, Belgium
Niraja Moharana, Chennai, India
Martin Palm, Düsseldorf, Germany
Jian Peng, Wuhan, China
Pierre Perrot, Lille, France
Alexander Pisch, Grenoble, France
Qingsheng Ran, Stuttgart, Germany
Maximilian Rank, Karlsruhe, Germany
Peter Rogl, Vienna, Austria
Lazar Rokhlin, Moscow, Russia
Rainer Schmid-Fetzer, Clausthal-Zellerfeld, Germany
Frank Stein, Düsseldorf, Germany
Vasyl Tomashyk, Kyiv, Ukraine
Lyudmila Tretyachenko†, Kyiv, Ukraine
Mikhail Turchanin, Kramatorsk, Ukraine
Oksana Tymoshenko, Kyiv, Ukraine
Thomas Vaubois, Chatillon, France
Alexander Walnsch, Freiberg, Germany
Chuanbin Wang, Wuhan, China
Cui Ping Wang, Sendai, Japan
Junjun Wang, Wuhan, China
Andrew Watson, Chesterfield, UK
Liming Zhang, München, Germany

Contents

Ternary Alloys
A Comprehensive Compendium of Evaluated Constitutional Data and Phase Diagrams

Volume 21
Selected Al-Fe-X Ternary Systems for Industrial Applications

Aluminium – Iron – Silicon

Gautam Ghosh, updated by Xiaojing Li, Shuhong Liu, Yong Du, Mikhail Turchanin and Liya Dreval

Introduction

The ternary system is the basis for many engineering alloys, such as grain refined cast Al-alloys, aluminization of steels, soft magnetic alloys for transformers *etc.* In addition, iron and silicon originating from bauxite ore and anode materials are present in nearly all industrial Al-alloys, and the metallurgical grade silicon contains, among others, aluminum and iron as impurities.

Iron has a strong influence on the porosity, mechanical properties and extrusion characteristics of Al-Si castings, which are governed by the amount and morphology of Fe containing intermetallics. In commercial Al-Si castings these are affected by other transition metals, such as Co, Cr, Mn and Sr that may be present either as alloying additions or as impurities. It is generally agreed that the elimination of plate-shaped and Chinese-script intermetallic phases results in an improvement of mechanical properties of Al-Si castings.

Due to these reasons, there have been numerous experimental studies on the characterization of intermetallics (morphology, composition and crystal structure) and phase equilibria of the ternary system. A summary of experimental studies of phase equilibria is given in Table 1. The experimental results have been reviewed from time to time [1934Fus, 1943Mon, 1950Gme, 1952Han, 1959Phi, 1968Dri, 1981Riv, 1981Wat, 1985Riv, 1987Pri, 1988Ray, 1992Gho, 1992Zak, 1994Rag, 2002Rag, 2004Gho, 2007Gho, 2007Kre, 2009Rag, 2010Rag, 2012Rag]. Recent MSIT Evaluation Report was written in 2013 by [2013Gho].

The system is characterized by a large number of ternary phases, both stable and metastable, and more than twenty ternary invariant reactions during solidification, which impart difficulties in establishing the phase equilibria of the system. In addition, there are effects of metastability, impurity elements, incomplete reactions, undercooling, and many solid-state reactions, which are not well understood.

Many earlier works by [1923Dix, 1923Han, 1923Wet, 1924Fus, 1934Roe, 1941Pan] reported primarily the microstructures of Al rich alloys. [1951Ran] determined the phase boundaries of the Al corner at 475°C by diffusional anneal technique. Due to extensive investigations [1927Gwy, 1933Nis, 1936Jae, 1937Ura, 1951Hol, 1951Now, 1967Mun, 1987Gri1, 1987Ste], the phase equilibria of Al corner are well established.

The first comprehensive study of phase equilibria of the entire system was performed by [1940Tak]. They used electrolytic iron, pure aluminium and metallic silicon (unspecified purity). Over 150 ternary alloys were prepared using master alloys of selected compositions in an arc furnace, under hydrogen atmosphere with NaCl as flux on the molten surface of the alloys, followed by cooling at a rate of 2 to 3°C per 5 to 10 sec. In some cases, in order to confirm and identify solid-state reactions, the cooling curves were supplemented by heating runs. [1940Tak] employed metallography, thermal, X-ray, magnetic and dilatometric analyses to establish the phase equilibria. They reported six ternary phases that form by peritectic reactions. They also presented several vertical sections from 500°C up to the liquidus temperature. Based on these results, [1981Riv, 1988Ray] constructed a probable isothermal section at 1000°C.

[1968Lih] studied the Fe corner up to 50 at.% Al and 35 at.% Si using DTA, magnetometry, microhardness and X-ray diffraction techniques. The phase equilibria involving ordered and disordered phases in Fe rich alloys were determined by [1982Miy] and [1986Miy] in the temperature range of 450 to 700°C using transmission electron microscopy.

Due to their importance in commercial Al alloys, there have been renewed interests on the phase equilibria of Al corner. [1987Gri1] and [1987Ste] studied the phase equilibria of Al corner, using alloys up to 14 at.% Si and 35 at.% Fe, by means of thermal analysis, X-ray diffraction and electron probe microanalysis techniques. They reported a partial liquidus surface, and partial isothermal sections at 570 and 600°C. However, the latter results were slightly modified by [1987Pri] to make them consistent with the thermodynamic rules of phase diagram construction.

[1981Zar] reported ten ternary phases, and an isothermal section at 600°C. [2001Kre] determined a partial isothermal section at 550°C. About 100 alloys, containing up to 50 at.% Fe and 50 at.% Si, were used [2001Kre]. In their later work, [2007Kre] summarized the available data and constructed the liquidus surface projection of the system. This projection does not include phase equilibria involving ordered phases. The phase relations were established by means of optical metallography, EDS analysis of the phases, and X-ray diffraction methods. [2002Gup, 2002Mai] performed diffusion couple (between pure Fe and Al-Si alloy) experiments in the temperature range of 600 to 1100°C, followed by quenching the specimens. They reported five isothermal sections based on the microstructural observations and

composition analysis (by EPMA) of phases in as-quenched specimens. [2008Du] prepared five ternary alloys along the section Al-15 mass% Fe-10 mass% Si. They studied phase equilibria using DTA, EPMA and XRD techniques. More recently, [2011Mar] prepared seventy-three ternary alloys using 99.95% Fe, 99.999% Al, 99.9999% Si, and investigated phase equilibria using SEM, EPMA, DTA and X-ray diffraction techniques. They reported two isothermal sections, at 800 and 900°C, and six vertical sections. [2011Rog1] determined the crystal structure of the α-FeAlSi phase by XRD and reported a peritectic reaction by DTA: α-FeAlSi ⇌ Fe_4Al_{13}+γ-$FeAl_3Si$+L. [2014Hao] prepared two alloys annealed at 500°C for 30 days in the Al-rich corner and they analyzed the alloys in both annealed and as-cast states by XRD, SEM/EDS and EPMA. Using XRD and SEM/EDS. [2014Li] determined the isothermal section of the Al-rich corner at 650°C by three Al-rich alloys. Utilizing the same method, [2015Zho] and [2015Zou] determined the isothermal sections of the Al-rich corner at 700°C and 600°C, respectively.

Thermodynamic properties of ternary alloys were investigated by emf method [1970Mit, 1973Nag, 1980Sud, 1984Ber, 1989Bon, 2004Kan], calorimetry [1937Koe, 1937Oel, 1997Vyb, 2000Li1, 2000Li2, 2003Kan], using first-principles methods [2010Du, 2010Fri, 2014Ami]. In addition, thermodynamic datasets of the ternary system have been assessed within the Calphad formalism [1994Ang, 1998Kol, 1999Liu, 2008Du, 2010Ele, 2014Che].

Binary Systems

The Al-Si binary phase diagram is accepted from [2004Luk]. The Al-Fe phase diagram is accepted from the binary evaluation report of [2022Ste] and presented in the chapter "*Al - Fe (Aluminium – Iron)*" of this volume. The Fe-Si binary phase diagram is essentially based on the results of [2017Cui] but with certain amendments to take the homogeneity ranges of certain binary compounds into account and better reproduce the order-disorder transition in the Fe-rich part. The amendments were introduced considering the results of [1943Wei, 1960Aro, 1976Ber, 1977Kud, 1982Kub, 2012Ohn]. The final diagram is shown in Fig. 1. The tetragonal high-temperature modification of $FeSi_2$ was denoted as "Fe_3Si_7".

Solid Phases

The complexity of phase equilibria of the Al-Fe-Si system is primarily due to the occurrence of many ternary phases, and the associated reactions during solidification, and also in the solid state. While some of these ternary phases are stable, some are metastable. In recent years, the detailed crystallographic characterization of stable phases has been performed, however, the current crystallographic data of many metastable ternary phases are far from being complete. The difficulties of complete crystallographic characterization of these phases are due to (i) the occurrence of several phases over a relatively narrow composition range in the Al corner, (ii) their complex crystal structures along with the presence of high density of planar defects, (iii) the order-disorder reactions in the Fe corner, (iv) many invariant reactions which under normal experimental conditions (both during solidification and during heat treatments) do not undergo completion, and (v) the effect of heterogeneous nucleation on the phase selection during solidification. In the past decades a large number of ternary phases in the Al-Fe-Si system have been reported. A chronological survey of these ternary phases was presented in the MSIT evaluation of [2013Gho]. It may be noted that some of the results reported by different research groups are still controversial.

The information on the binary phases could be summarized as following. At 550°C, the solubility of Fe and Si in (Al) is less than 1 at.% [2001Kre], and that of Fe and Al in (Si) is extremely small.

The Fe_4Al_{13} phase is reported to dissolve 0.8 mass% Si [1955Arm], 0.2 mass% Si [1967Sun], 1.0 mass% Si [1984Don], 2.9 mass% Si [1987Skj1], up to 6.0 mass% Si at 600°C [1987Ste], 4 at.% (3.4 mass%) Si at 550°C [2001Kre], and 5 to 6 at.% (4.2-5.1 mass%) Si in the temperature range of 800 to 1115°C [2002Mai]. The maximum solubility of Si in the Fe_4Al_{13} phase at 650°C was 2 at.% as reported by [2014Li]. This is associated with an increase in the *a* lattice parameter and a decrease in the *b*-lattice parameter, whereas no significant changes in the *c* lattice parameter and β were detected by [1987Ste]. The composition dependence of *a* and *b* lattice parameters in Fe_4Al_{13} is expressed by [1987Ste] as

a (in pm) = $1505.0 + 1.14 \cdot W_{Fe} - 0.41 \cdot W_{Si}$

b (in pm) = $862.8 - 1.41 \cdot W_{Fe} - 1.3 \cdot W_{Si}$

where W_{Fe} and W_{Si} are the mass% of Fe and Si, respectively.

A detailed crystallographic analysis of the Fe_4Al_{13}, by means of convergent beam electron diffraction and high-resolution electron microscopy, has been performed by [1987Skj3]. Lattice images revealed that the Fe_4Al_{13} crystals are divided into tiny domains (few thousand pm) that are separated by lattice displacements such as stacking faults [1987Skj2, 1987Skj3].

Available data indicate that the solid solubility of Si in Fe_2Al_5 decreases from about 4.5 at.% at 1020°C [2002Gup, 2002Mai] to about 2.5 at.% at 550°C [2007Kre]. At 550°C, $FeAl_2$ dissolves about 1 at.% Si [2001Kre].

Initial studies showed that the Fe_3Si_7 phase dissolves up to about 0.5 mass% (0.7 at.%) Al [1961Sab, 1965Sab, 1965Skr, 1968Sab1, 1968Sab2] which is accompanied by a small increase in both the *a* and *c* lattice parameters. According to [2001Kre, 2007Kre, 2011Mar], low-temperature $FeSi_2$ dissolves up to 1 at.% Al between 900 and 550°C. The FeSi phase dissolves substantial amount of Al [1996Szy, 1998Dit, 2001Kre, 2007Kre, 2011Mar]. Between 550 and 900°C, it is about 10 at.% with Al substituting Si [2001Kre, 2007Kre, 2011Mar]. The lattice parameters of FeSi, Fe_3Si_7 and $FeSi_2$ as functions of Al content were reported by [1996Szy]:

For FeSi:

a (in pm) = $448.1 + 5.4 \cdot x_{Al}$

For Fe_3Si_7:

a (in pm) = $269.1 + 17.9 \cdot x_{Al}$

c (in pm) = $515.7 + 30.2 \cdot x_{Al}$

For $FeSi_2$(r):

a (in pm) = $986.6 + 7.3 \cdot x_{Al}$

b (in pm) = $778.7 + 10.3 \cdot x_{Al}$

c (in pm) = $782.1 + 27.6 \cdot x_{Al}$

where x_{Al} is the atomic fraction of Al.

Ordered phases. Fe_3Al and Fe_3Si (the ordered $D0_3$ structure), as well as FeAl and FeSi (the ordered *B*2 structure), form continuous solid solutions denoted as Fe_3(Al,Si) and Fe(Al,Si). The ordered $D0_3$, *B*2 and disordered *bcc* (the latter is characteristic of the (αδFe) phase) structure are interrelated since $D0_3$ and *B*2 can be presented as a superlattice based on a simple *bcc* cell.

The lattice parameter of the alloys along Fe_3Al-Fe_3Si and $Fe_{73}Al_{27}$-$Fe_{73}Si_{27}$ sections and also for the commercial SENDUST and ALSIFER 32 alloys were determined systematically and accurately by [1979Cow]. The composition dependence of the lattice parameter can be expressed as:

Along the Fe_3Al-Fe_3Si section

a (in pm) = $565.54 + 12.846 \cdot W + 1.896 \cdot W^2 - 0.7245 \cdot W^3 = 565.54 + 12.776 \cdot C + 1.9522 \cdot C^2 - 0.7094 \cdot C^3$

where W = mass fraction of Fe_3Al and C = mole fraction of Fe_3Al.

Along the $Fe_{73}Al_{27}$-$Fe_{73}Si_{27}$ section

a (in pm) = $564.462 + 11.964 \cdot W + 5.3929 \cdot W^2 - 2.5 \cdot W^3 = 564.462 + 11.915 \cdot C + 5.3183 \cdot C^2 - 2.321 \cdot C^3$

where W = mass fraction of $Fe_{73}Al_{27}$ and C = mole fraction of $Fe_{73}Al_{27}$.

[1979Cow] attributed a small, but consistent, deviation from the linear dependence on composition, along both sections, to the incomplete ordering as Al is replaced by Si. [1979Bur] also reported limited lattice parameter data along Fe_3Al-Fe_3Si section that are in reasonable agreement with those of [1979Cow], but [1979Bur] assumed a linear dependence of lattice parameter on composition (see also [1977Nic1], [1977Nic2]). [1968Lih] reported lattice parameters of ternary alloys up to 30 at.% Si and 47 at.% Al at 20, 500, 600 and 900°C. [1946Sel] also measured the lattice parameter of ternary alloys up to 18 mass% Si and 13 mass% Al. The lattice parameter of Fe_3(Al,Si) containing about 10 mass% Al and 5 mass% Si is reported to be 570 ± 3 pm [1978Xu]. The lattice parameter of an Fe-5.5 mass% Al-9.7 mass% Si alloy is reported to be 568.4 pm after water quenching and 568.54 pm after annealing for 24 h at 600°C.

Following the experimental works [2001Kre, 2007Kre, 2011Mar] and the previous critical evaluations [1992Gho, 2004Gho, 2013Gho] and review [2022Mar], eleven ternary phases considered to be stable. The composition ranges, in which they were reported experimentally, are shown in Fig. 2. The provided boundaries are schematical and cannot be attributed to a particular temperature. They encircle the compositions, corresponding to the homogeneity range of a ternary phase, as reported in the original papers. For the papers, in which a significant number of compositions were reported, only the highest concentrations of elements are shown in the figure. The ternary compounds were differently denominated by various research groups. Some of the older denominations are reported in Table 2.

$Fe_3Al_2Si_3$. The identification of this phase using the XRD method is especially complicated, because it shows a significant homogeneity range together with a low symmetry structure. This results in the XRD powder pattern

changing drastically over the composition range. It is then of no surprise that, for a long time, two ternary phases belonging to the Fe rich and Fe poor regions of the homogeneity range were considered as two different ternary intermetallic compounds by [1974Mur, 1981Zar, 2002Gup, 2002Mai]. In 2001, [2001Kre] found that these compounds were the same phase ($Fe_3Al_2Si_3$) with an extended homogeneity range. [2004Bos] later confirmed this result. The crystal structure and lattice parameters of $Fe_3Al_2Si_3$ were established for the first time by [1996Yan]. The authors performed the measurements for single crystals and found that this compound has a triclinic structure (*aP*16, $P\overline{1}$, $Fe_3Al_2Si_3$). [2001Kre, 2007Kre, 2011Mar] confirmed the crystal structure proposed by [1996Yan]. [2011Mar] measured the variation of the lattice parameters of $Fe_3Al_2Si_3$ across the homogeneity range. These results are reproduced in the present work in Fig. 3 and listed in Table 2. The *a* and γ parameters decrease with increasing Si-content while *b*, *c*, α, and β increase. The variation of the cell volume with the composition is practically linear. The cell volume decreases with increasing Si-content, which is consistent with the substitution of the larger Al- by smaller Si-atoms. According to [2011Mar], the homogeneity range of this phase extends from $Fe_{37.5}Al_{21.0}Si_{41.5}$ (at.%) to $Fe_{37.5}Al_{41.5}Si_{21.0}$ (at.%) at 800°C while [2004Bos] reported the homogeneity range between $Fe_{37.5}Al_{21.0}Si_{41.5}$ (at.%) and $Fe_{36.5}Al_{45.0}Si_{18.5}$ (at.%) at 727°C.

γ-*$FeAl_3Si$.* This compound also shows a significant homogeneity range as follows from the data of [1967Mun, 1974Mur, 1981Zar, 2001Kre, 2011Rog2]. The crystal structure and stoichiometry of this phase was a subject of numerous experimental efforts. [1952Arm], [1955Arm], who denoted this compound as α_3, reported that it had a cubic structure. Later, [1967Mun] proposed that this phase (denoted as γ-FeAlSi) possessed *C*-face-centered monoclinic structure. This type of the crystal structure has been accepted by many other research groups. In particular, [2001Kre] used the monoclinic unit cell to index diffraction patterns measured from a three-phase $Fe_{22}Al_{61}Si_{17}$ (at.%) sample. This sample contained predominantly γ-$FeAl_3Si$ and small amounts of $FeAl_2Si$ and Fe_4Al_{13}. Until 2004, no single crystal studies were reported for this ternary phase. [2004Sug] measured the intensity patterns of a single crystal with a composition of $Fe_{20.9}Al_{63.0}Si_{16.1}$ (at.%), which was cut out from an as-cast sample. [2004Sug] reported that the observed patterns lead to a rhombohedral structure $R\overline{3}$. Although, this phase was considered to be unknown and was denoted as λ-FeAlSi, its composition fell into a homogeneity range of γ-$FeAl_3Si$. [2011Rog2], who determined the crystal structure from single crystals grown from ternary melts using XRD, later confirmed the finding of [2004Sug]. The authors also determined the composition of the compound and "$FeAl_3Si$" stoichiometry for it. The γ-$FeAl_3Si$ denomination of [2011Rog2] is used in the present evaluation. The lattice parameters and space group of [2011Rog2] agree fairly well with those of [2004Sug]. They are also compatible with the previously reported monoclinic cell, since every monoclinic structure allows setting up basis vectors in different ways. [2016Yu] also found a ternary phase having the $R\overline{3}$ space group by examining thin films produced from as-cast $Fe_{0.2}Al_{90.2}Si_{9.6}$ (at.%) sample. The examination was performed using TEM. Although space group and lattice parameters agree with the data of [2004Sug, 2011Rog2], the composition of the phase ($Fe_{15.74\pm0.61}Al_{68.54\pm1.22}Si_{15.72\pm0.82}$ (at.%)) measured by EDX spectroscopy corresponds to the region of β-$FeAl_{4.5}Si$. [2016Yu] themselves attributed this composition to the region of γ-$FeAl_3Si$ as reported by [2007Kre]. The reasons for such discrepancies in the composition of the phase reported by [2016Yu] and other authors are not clear. [2011Rog2] also measured the homogeneity range of γ-$FeAl_3Si$ and variation of the lattice parameters with composition (Fig. 4). The reported homogeneity range extends from $Fe_{20.1}Al_{64.7}Si_{15.2}$ (at.%) to $Fe_{21.5}Al_{52.4}Si_{26.1}$ (at.%).

$FeAl_2Si$. This phase was for the first time reported by [1940Tak]. In earlier studies of [1974Mur, 1981Zar], it was claimed to have rhombic structure. In latter work of [1989Ger2], the orthorhombic structure (*Cmca*) was reported for this phase. Although [1989Ger2] proposed the $FeAl_2Si$ stoichiometry for this compound, which agree well with that reported by [1940Tak, 1974Mur, 1981Zar], its homogeneity range measured by [2001Kre, 2007Kre, 2011Mar] at 550, 800°C using EDX or EPMA never covers the $Fe_{25}Al_{50}Si_{25}$ (at.%) composition corresponding to this stoichiometry. The homogeneity range of $FeAl_2Si$ extends from $Fe_{25.2}Al_{51.8}Si_{23}$ (at.%) to $Fe_{26.6}Al_{54.5}Si_{18.9}$ (at.%) at 800°C [2011Mar]. The $Fe_{44.18}Al_{32.24}Si_{23.55}$ (at.%) composition reported for $FeAl_2Si$ by [2002Gup] seems to be erroneous especially considering the fact the authors did not perform any XRD measurements in their study.

$FeAl_3Si_2$. This phase was reported in a number of works starting from at least 1931. Since it has extended homogeneity range, the reported stoichiometries, as well as compositions, varied from $Fe_2Al_6Si_3$ and $FeAl_3Si_2$ to $FeAl_4Si_2$. Its crystal structure was refined as tetragonal *I*4/*mcm* structure of $PdGa_5$ by [1969Pan]. [1995Gue1] referring to [1969Pan] noted the existence of superstructure reflections suggesting ordering between Al and Si atoms. [1995Gue1] came to a conclusion that the single crystals, which were studied in this work, showed the 4/*mmm* Laue symmetry and weak reflections indicating a superstructure with a primitive unit cell. The structure could be solved in two stages. As [1995Gue1] explained, if the superstructure reflections were neglected (the first stage), the average structure was refined in the tetragonal *I*4/*mcm* space group of $PdGa_5$. This is in full agreement with the results of [1969Pan, 1974Mur, 1981Zar, 2007Kre]. At the second stage, the superstructure was solved. Consequently, [1995Gue1] concluded that $FeAl_3Si_2$ has ordered orthorhombic *Pbcn* superstructure. The results of [1995Gue1] were

adopted in the present evaluation. [2007Kre] suggested that the homogeneity range of $FeAl_3Si_2$ extends from $Fe_{15.5}Al_{54}Si_{30.5}$ to $Fe_{16.5}Al_{45.5}Si_{39}$ (at.%).

α-FeAlSi. This compound with average formula $Fe_2Al_{7.1}Si$ as reported by [2011Rog1] is known to form very easily by crystallization from ternary Al-rich melts. According to [2007Kre], the homogeneity range of this compound is between $Fe_{18}Al_{72}Si_{10}$ to $Fe_{19.5}Al_{68}Si_{12.5}$ (at.%).

β-FeAl$_{4.5}$Si. This compound, as well as $FeAl_3Si_2$, form as plate-shaped particles in secondary Fe-containing Al-Si alloys during solidification or occur during bonding of Al-Si alloys to cast iron or steel. As [2019Bec] notes, the correct identification of these two phases is sometimes doubted for the following reasons. β-$FeAl_{4.5}Si$ occurs at approximately the same Fe content, at lower Si and higher Al but approximately similar (Al+Si) molar fraction as $FeAl_3Si_2$. Thereby, depending on the formation conditions, the plates might be reported to be $FeAl_3Si_2$ instead of β-$FeAl_{4.5}Si$ if the phase identification is based on the morphology and/or chemical compositions of the particles.

The crystal structure of β-$FeAl_{4.5}Si$ is still under discussion. This unsolved issue is in particular related to the fact that β-$FeAl_{4.5}Si$ and $FeAl_3Si_2$ are closely related, consisting of the same basic constituent layers. Furthermore, [1950Phr, 1998Han, 2000Zhe, 2003Gjo] in particular mentioned that the ordered stacking of the layers can lead to superstructure formation that can classified as polytypes. [2019Bec] noted that although the β-$FeAl_{4.5}Si$ is always described with near tetragonal lattice parameters, further details reported by the researchers may vary. This compound can be reported as monoclinic with space group $A12/a1$, orthorhombic or tetragonal with lattice parameter c either around 2080 pm or 4160 pm.

[2019Bec] analyzed the crystallographic data reported in the literature and their own experimental results. The authors formulated structural models based on ordering of the constituting double layers being shifted by $a/2$ or $b/2$ displacements leading to 4 different double layer positions A, B, C, and D. Idealized two polytype structures were proposed. The AB polytype with idealized *Acam* symmetry actually shows a monoclinic distortion towards $A12/a1$ symmetry. The second polytype is ABCD polytype with idealized $I4_1/acd$ symmetry. [2019Bec] also reported stackings with non-periodic sequence A, B, C and D double layers to exist next to the ordered polytypes. These disordered structures might be described with tetragonal $I4/mmm$ space group. [2019Bec] concluded that the observed polytype structures for the β-$FeAl_{4.5}Si$ phase were preventing the distinct characterization of the phase polytypes. [1994Rom] indexed EBSD data using a tetragonal structure mimicking the diffraction effects due to a disordered stacking sequence (Table 3).

$Fe_2Al_3Si_3$. [1995Gue2] found the crystal structure of this compound to be monoclinic. This was later confirmed by [2001Kre, 2007Kre, 2011Mar]. According to [2011Mar], $Fe_2Al_3Si_3$ shows significant homogeneity range at 800°C which extends from $Fe_{24}Al_{41}Si_{35}$ to $Fe_{26}Al_{46.5}Si_{27.5}$ (at.%).

$Fe_3Al_2Si_4$. [1996Yan] reported this phase has orthorhombic crystal structure. [2001Kre, 2007Kre, 2011Mar] confirmed this finding. According to [1974Mur, 1981Zar], the composition of this phase at 600°C is $Fe_{32}Al_{38}Si_{30}$ (at.%) that is much higher than the highest aluminium solubility in this compound ($Fe_{34.1}Al_{28.6}Si_{37.3}$ (at.%)) reported by [2011Mar] for 800°C. More work is required to clarify this issue.

τ_1 ($FeAl_{2.4}Si_{0.6}$) and $Fe_{1.7}Al_4Si$. Several research groups provided their data on the τ_1 crystal structure. [1991Ger] reported a quite simple hexagonal Na_3As-type crystal structure for τ_1 with a composition $FeAl_{2.4}Si_{0.6}$. While [2004Bos] found this phase to be orthorhombic, [2007Kre] stated that it should have hexagonal structure. Recently, [2022Mar] re-evaluated the diffraction data of [2007Kre] using the peak positions reported by [1991Ger] and found that the data of [1991Ger] yield a better description of the τ_1 crystal structure than those of [2007Kre]. The crystallographic data and stoichiometry reported by [1991Ger] are accepted in the present evaluation.

τ_1 and hexagonal $Fe_{1.7}Al_4Si$ (Co_2Al_5 prototype) were several times reported to exist at the same composition ($Fe_{25}Al_{60}Si_{15}$ (at.%)) depending on the production condition [1974Mar, 1981Zar, 2001Kre]. This led to certain problems with the interpretation of the data. [1974Mar, 1981Zar] used the same letter “F” for as-cast Co_2Al_5-type single crystals and for a phase (crystal structure was not reported) included in their isothermal section at 600°C. In their earlier study, [2001Kre] discussed τ_1 and $Fe_{1.7}Al_4Si$ reported by [1989Ger1] as if they were the same compound. In their latter work, [2007Kre] came to the conclusion that τ_1 and $Fe_{1.7}Al_4Si$ should be considered as two different phases.

Available information does not allow to take final decision regarding the low-temperature phase equilibria involving these compounds. τ_1 is probably stable between 550 and 727°C as follows from the isothermal sections reported by [1974Mur, 1981Zar, 2001Kre, 2004Bos], while $Fe_{1.7}Al_4Si$ could be stable at 727°C and higher temperatures according to [2004Bos, 2007Kre, 2011Mar]. It should be however noted that [1989Ger1] claimed the occurrence of the $Fe_{1.7}Al_4Si$ (Co_2Al_5 prototype) compound in their sample after annealing at 597°C. This suggests the stabilization of this phase below 700°C. Both compounds have homogeneity ranges but their precise establishment at different

temperatures requires further experimental efforts. According to [2004Bos], τ_1 shows a homogeneity range of 24-25 at.% Fe, 59-57 at.% Al, 17-18 at.% Si at 727°C. For $Fe_{1.7}Al_4Si$, [2011Mar] reported a solubility range of 26.0 at.% Fe, 62.5-65 at.% Al, 11.5-9.0 at.% Si at 800°C. Future studies are certainly required to understand the phase equilibria involving τ_1.

Fe_2Al_3Si. This compound was for the first time reported by [2011Mar], who also established its crystal structure. [2011Mar] noted that the real composition of the phase as determined by EPMA - 36 at.% Fe, 48 at.% Al, 16 at.% Si - deviates slightly from the ideal composition of the phase.

A number of the metastable ternary phases were listed in the previous MSIT evaluation by [2013Gho]. Some of them are either derivatives of the stable ternary compounds or develop upon small additions of manganese, chromium or other metal, for example, Chinese script α_c ($Im\bar{3}$) [2022Mar]. For more details refer to the MSIT evaluation of [2013Gho].

Quasibinary Systems

[1931Fus] and [1934Fus] proposed a quasibinary section Si-Fe_4Al_{13} with a peritectic reaction L + Fe_4Al_{13} ⇌ $FeAl_3Si_2$ at about 920°C and a eutectic reaction between (Si) and $FeAl_3Si_2$ at 850°C and 32 mass% Si. However, later works failed to confirm the presence of such a quasibinary section and consequently it is disregarded.

Invariant Equilibria

Figure 5 shows the reaction scheme which is based on the reaction scheme proposed by [2007Kre] with certain amendments according to [1988Ray] and [2011Mar]. [2007Kre] constructed their reaction scheme and liquidus surface considering the data available in the literature and their own experimental results. Some of the reactions were not actually measured but deduced from available experimental data.

Since the information on the phase equilibria involving the ordered phases is scarce, no conclusions could be drawn regarding the invariant reactions involving (Fe,Al)Si and Fe_3(Al,Si) phases. Therefore, these phases were denoted as "Ord" and some of the phase transformations with their participation in the Fe-rich part were omitted. The information about compositions of liquid phase involved in the invariant reactions are listed in Table 3.

Based on their results, [1940Tak] suggested that $FeAl_2$ which does not participate in the liquid-solid phase equilibria in the Al-Fe system should appear in the liquidus surface of the ternary system. The presented experimental data are however controversial. They contradict the phase equilibria involving $FeAl_2$ as presented in the Al-Fe phase diagram accepted here and, therefore, allow different interpretations. [1940Tak], for example, stated that the L + Fe_5Al_8 ⇌ Ord + $FeAl_2$ and L + $FeAl_2$ ⇌ Ord + Fe_2Al_5 reactions they proposed could not be distinguished clearly. Therefore, a temperature interval of 5°C was assumed. In this work, the L + Fe_5Al_8 ⇌ Ord + $FeAl_2$ and L + $FeAl_2$ ⇌ Ord + Fe_2Al_5 reactions suggested by [1940Tak] and accepted by [2007Kre, 2011Mar] were substituted by L + Fe_5Al_8 ⇌ Ord + Fe_2Al_5 (U_2 at 1120°C) following the suggestion of [1988Ray] and by Fe_2Al_5 + Fe_5Al_8 ⇌ Ord + $FeAl_2$ (U_3 between 1095 and 1120°C). The U_3 reaction was proposed in this work to take the phase equilibria with $FeAl_2$ into account. Further experimental studies are required to cast light on this matter.

Most ternary compounds form by peritectic reactions. Except for the P_8 reaction, the temperatures invariant reactions were accepted according to [2007Kre]. The P_8 temperature is according to [2011Rog1]. The peritectic temperature of γ-$FeAl_3Si$ was not measured experimentally. [2007Kre] suggested this phase to form between 900 and 934°C. Fe_2Al_3Si form *via* peritectoid reaction at 1005°C as proposed by [2011Mar].

[2007Kre] and [2011Mar] proposed the tentative solid-state invariant reactions between 550 and 800°C based on their own experimental results and earlier data of [1974Mur, 1981Zar, 2004Bos]. However, neither of the proposed sets of reactions accounts for all discrepancies in the three-phase equilibria reported for different isothermal sections. The main reason behind this issue is that the phase equilibria between (Si), $FeSi_2$, Fe_3Si_7, $Fe_2Al_3Si_3$ and $Fe_3Al_2Si_4$ below 800°C reported by different authors are inconclusive and contradictory. It is established by [2007Kre] and [2011Mar] that Fe_3Si_7 is stable in the ternary system at much lower temperatures (up to 700°C according to [2007Kre]) than in the Fe-Si system. However, the phase equilibria involving this phase between 700 and 800°C are barely studied. Neither exact temperature nor phases emerging after the decomposition of Fe_3Si_7 are established.

In view of this insufficiency of the accurate experimental data, [2007Kre, 2011Mar] deduced the solid-state reactions by comparing the phase equilibria at different temperatures. This approach however allows different sets of solid-state reactions depending on the experimental data that were considered reliable. In the present evaluation, it was decided to preserve the reaction scheme as simple as possible since no suggestive information on the phase equilibria below 800°C has been published since 2011. Most of the solid-state invariant reactions proposed by [2011Mar] were

accepted. The estimated temperature range in which these reactions occur was however changed to preserve the internal consistency between different isothermal sections. The (Si)+$Fe_3Al_2Si_4$⇌$Fe_2Al_3Si_3$+$Fe_3Al_2Si_4$ suggested by [2011Mar] was replaced by $Fe_2Al_3Si_3$+$FeAl_2Si$⇌$Fe_3Al_2Si_3$+γ-$FeAl_3Si$ after [2007Kre] to further simplify the reaction scheme and to avoid introduction of additional solid-state reactions below 600°C. The accepted set of reactions requires certain changes to be introduced in the isothermal sections reported by [1974Mur, 1981Zar] and [2004Bos] (see *'Isothermal Sections'* part). In this respect, it should be pointed out that [1974Mur, 1981Zar] and [2004Bos] did not provide the primary data of their experiments, *i.e.* compositions of the phases in equilibrium. [1974Mur, 1981Zar] did not specify their experimental procedure. Therefore, the evaluation of the accuracy of the results presented in these papers is not possible and allow different interpretation. This in turn causes problems with the further assessment of the solid-state invariant reactions. Since very little is known about the reactions involving τ_1, they were not included in the reactions scheme.

As follows from Fig. 5, the reaction scheme of the Al-Fe-Si system is very complex. Not all invariant reactions were measured experimentally, and some of these reactions take place in a very narrow range of temperature, thus, difficult to resolve by thermal analysis. The phase equilibria involving the ordered phases are almost unexplored. Therefore, further experimental studies are required to better understand the phase diagram of the system.

Liquidus and Solidus Surfaces

The liquidus surface is shown in Fig. 6. It is essentially accepted according to [2007Kre], who used the data of [1927Gwy, 1940Tak, 1951Now, 1952Arm, 1981Riv, 2004Pon1, 2004Pon2, 2004Bos] but was slightly amended to preserve the compatibility with the binary systems accepted in this work and to be in agreement with the reaction scheme presented in the *'Invariant Equilibria'* section. As it was already mentioned the main changes are associated with the region close to the $FeAl_2$ phase. The phase equilibria involving the ordered phases was not included in the absence of the corresponding experimental data.

There are no published data for the solidus projection of the entire system, even though a number of vertical projections are available [1927Gwy, 1932Nis, 1933Nis, 1940Tak, 1946Phi1]. The solidus projection of the Fe corner was reported [1968Lih], but their results differ substantially along the Al-Fe binary edge, so they are not accepted here.

Isothermal Sections

Figures 7 and 8 show the isothermal sections at 1100 and 1020°C, respectively. [2002Gup] constructed these two isothermal sections based on the microstructural characterization in diffusion couples that were quenched from the respective temperatures. They also utilized the vertical sections of [1940Tak]. However, several amendments are done to comply with the accepted binary phase diagrams, the reaction scheme in Fig. 5 and vertical sections reported by [2011Mar]. All changes are shown with dashed lines. The tentative phase boundaries between (αδFe) and ordered (Fe,Al)Si, as well as between ordered (Fe,Al)Si and Fe_3(Al,Si), were added. However, the phase equilibria involving ordered phases are not explored in detail for these temperatures. Therefore, it was impossible to rule out which of the ordered phases taking part in some of the three-phase equilibria. Such tie-triangles were labelled using "Ord" denomination. The tentative phase boundaries between (αδFe) and (γFe) were also added. The phase boundary related to the liquid phase and corners of the tie-triangles corresponding to the liquid compositions were adjusted to be in agreement with the accepted liquidus and reaction scheme.

In Fig. 7, all two- and three-phase fields involving Fe_5Al_8, originally proposed by [2002Gup] were preserved as they are in good agreement with the accepted Al-Fe diagram. This observation of [2002Gup] supports to certain extent the invariant reaction U_3 proposed in the present work.

In their original isothermal section at 1020°C, [2002Gup] showed two three-phase fields: L + $FeSi_2$ + $Fe_3Al_2Si_3$ and FeSi + $FeSi_2$ + $Fe_3Al_2Si_3$. But these triangles are incompatible with the reaction scheme in Fig. 5. To be consistent, these are replaced by two three-phase fields: L + FeSi + Fe_3Si_7 (from e_1) and L + FeSi + $Fe_3Al_2Si_3$ (from P_1) in Fig. 8. The homogeneity range of the $Fe_3Al_2Si_3$ compound was also changed since high solubility of iron in this phase as reported by [2002Gup] contradicts the results of the latter studies by [2007Kre, 2011Mar]. The homogeneity ranges of FeSi and Fe_3Si_7 were also adjusted to preserve compatibility with liquidus surface projection constructed in the present work and vertical sections by [2011Mar].

[1981Riv, 1988Ray] constructed an isothermal section at 1000°C utilizing the results of the polythermal sections of [1940Tak]. It should be pointed out that [1940Tak] did not find $Fe_3Al_2Si_4$ and Fe_2Al_3Si during their experimental examinations. These phases were reported latter in the studies of [1974Mur, 1981Zar, 2001Kre, 2007Kre, 2011Mar]. Hence, the isothermal section at 1000°C constructed by [1981Riv, 1988Ray] is not compatible with the reaction

scheme and the liquidus surface accepted in the present evaluation. This section was discarded since the available information is not enough to introduce the corrections required for attaining the agreement between this section and other diagrams.

In Figs. 9 and 10, the isothermal sections at 900 and 800°C are shown. This section is essentially accepted according to [2011Mar]. Solid lines show the phase fields that were actually measured by the authors. The dashed lines show deduced phase equilibria. The tentative phase boundaries between (αδFe), $Fe_3(Al,Si)$ and Fe(Al,Si) were added. A question mark in the doubtful region indicates the need for further experimental data. The homogeneity region of γ-$FeAl_3Si$ was adjusted to be in agreement with the latter data of [2011Rog2]. Some of the phase boundaries were adjusted to be in agreement with the binary phase diagrams accepted in the present chapter. The isothermal sections at 600, 800, and 900°C were also constructed by [2002Mai]. These sections are essentially based on the microstructural characterization in diffusion couples that were quenched from the respective temperature. There is a contradiction in the sections at 800 and 900°C reported by [2011Mar] and [2002Mai]. In the present evaluation, the results of [2011Mar] were preferred since they were obtained using more comprehensive and accurate experimental procedure.

The phase boundary of the liquid phase was changed most significantly in Fig. 9 to be in agreement with the liquidus surface projection in Fig. 6. It should be pointed out that only compositions of the liquid in the tie-triangles, not the phase assemblages were changed. [2011Mar] have not actually measured the composition of the liquid phase (except for the L+(Si)+Fe_3Si_7 tie-triangle). Therefore, the proposed changes are acceptable in view of the data used to construct the liquidus surface and reaction scheme. The corner of the L+(Si)+Fe_3Si_7 tie-triangle corresponding to the liquid was shifted by 5 at.% of Fe and Si comparing to the measured data. Consequently, the corresponding edges of the triangle are shown with dashed lines. Since the composition of the solidified liquid could deviate to some extent from the equilibrium composition, this shift could be considered as acceptable. According to the reaction scheme, the U_{10} (L + $FeAl_2Si$ ⇌ γ-$FeAl_3Si$ + Fe_4Al_{13}) reaction occurs at 900°C. The reaction plane corresponding to this reaction is shown in Fig. 9 and denoted "U_{10}". In Fig. 10, the tentative L+ γ-$FeAl_3Si$+ $Fe_{1.7}Al_4Si$ and L+ $Fe_4Al_{13}Si$+ $Fe_{1.7}Al_4Si$ tie-triangles proposed by [2011Mar] were replaced by the L + γ-$FeAl_3Si$ + Fe_4Al_{13} and $FeAl_2Si$ + γ-$FeAl_3Si$ + Fe_4Al_{13} phase regions to be in agreement with the accepted reaction scheme in Fig. 5.

Figure 11 shows the isothermal section at 727°C. It was essentially accepted after [2004Bos]. However, certain changes were introduced to preserve the consistency with the reaction scheme (see *'Invariant Equilibria'* section). Three (Si)+$FeSi_2$+$Fe_3Al_2Si_4$, FeSi+$FeSi_2$+$Fe_3Al_2Si_3$, and $FeSi_2$+$Fe_3Al_2Si_3$+$Fe_3Al_2Si_4$ tie-triangles were replaced by three-phase fields involving the high-temperature Fe_3Si_7 phase, which was stabilized by Al additions at low temperature. This decision is to certain extent justified by the experimental results of [2007Kre], who have found Fe_3Si_7 to be in equilibrium with (Si) and $Fe_2Al_3Si_3$ at 700°C. However, this three-phase equilibrium reported by [2007Kre] was not accepted in the present evaluation. It would require the introduction of too many unjustified solid-phase invariant reactions. Instead, the tie-triangles including Fe_3Si_7 similar to those reported by [2011Mar] were drawn. There are also contradictions between the results of [2011Mar] and [2004Bos]. According to [2011Mar], Fe_2Al_3Si should exist at 727°C while [2004Bos] did not report the existence of this compound at this temperature. The Fe(Al,Si)+$Fe_3Al_2Si_3$+Fe_2Al_5 tie-triangle reported by [2004Bos] is replaced with three tie-triangles involving Fe_2Al_3Si in the present evaluation. The proposed changes are tentative and require further experimental confirmation. As it was already mentioned in the *'Solid Phases'* section, the information involving the τ_1 phase is contradictory, and further experimental efforts are needed to clarify this issue. According to [2004Bos], this phase is stable at 727°C and is in equilibrium with a number of other ternary phases.

Phase equilibria involving the ordered $Fe_3(Al,Si)$ ($D0_3$) and Fe(Al,Si) ($B2$) phases below 700°C were studied by [1971Gle, 1982Miy, 1984Mat, 1986Miy]. Figures 12 and 13 show the topology of ordered (Fe_3Al, FeAl) and disordered (αδFe) phase fields in the partial isothermal sections at 700 and 650°C. These results are adopted from [1982Miy] and [1986Miy] who studied about 20 ternary alloys, containing up to 40 at.% solute atoms (Al + Si), by means of transmission electron microscopy. According to [1986Miy], the ordered FeSi′ ($B2$) phase in the Fe-Si system is stable up to 450°C, and the FeSi′+ Fe_3Al miscibility gap occurs below 700°C. This contradicts to the Fe-Si phase diagram adopted in the present evaluation, according to which FeSi′ disappears below 700°C, and the miscibility gap occurs at around 1200°C. Therefore, the partial isothermal sections at 700 and 650°C were adjusted to preserve the compatibility with the Fe-Si phase diagram accepted here. In Fig. 12, the miscibility gap originating from the Fe-Si edge was added. In Fig. 13, the $B2$ phase boundary was modified so that it did not originate from in the Fe-Si system. The Fe(Al,Si) to (αδFe) transformation is of the second order. [1982Miy, 1986Miy] reported the phase separation between $Fe_3(Al,Si)$ ($D0_3$) + Fe(Al,Si) ($B2$) and (αδFe) + $Fe_3(Al,Si)$ ($D0_3$) in the ternary system at 650°C. At 700°C, the critical point, at which the $Fe_3(Al,Si)$ ($D0_3$) + Fe(Al,Si) gap disappears, is unknown. Therefore, the phase fields are shown with dashed lines. At 650°C, this change occurs at around 20 at.% Al, 79 at.% Fe, 1 at.%

Si [1986Miy]. [1984Mat] also observed two kinds of ordering processes leading to phase separation. X-ray diffraction data and TEM observations of [1971Gle] concerning various order-disorder transitions in ternary alloys qualitatively agree with those of [1982Miy, 1986Miy].

[1959Phi, 2014Li, 2015Zho, 2015Zou] measured the phase equilibria in the Al rich corner between 620 and 700°C. The phase transformations in this temperature-composition region are very complex due to the occurrence of many invariant reactions involving ternary phases. The three-phase assemblages reported by [1959Phi, 2015Zou] agree with the reactions scheme. [2014Li, 2015Zho] stated that the L + α-FeAlSi + β-$FeAl_{4.5}Si$ equilibrium was observed at 650 and 700°C. This contradicts the accepted reaction scheme according to which the L + α-FeAlSi + β-$FeAl_{4.5}Si$ equilibrium emerged below 648°C – temperature of the L + γ-$FeAl_3Si$ ⇌ α-FeAlSi + β-$FeAl_{4.5}Si$ reaction. Above this temperature, the L + γ-$FeAl_3Si$ + α-FeAlSi region should exist. As it was already discussed in the *'Solid Phases'* section, the discrepancies in the identification of the ternary phases are caused by the fact that they have significant homogeneity ranges and the crystal structures of some of them are still under discussion.

The phase equilibria in the Al rich corner at 700°C are identical to those at 727°C. Therefore, the partial isothermal section at 700°C reported by [2015Zho] is not reproduced here. At 650°C, [2014Li] determined only three tie-triangles. As it was discussed above, the reported L + α-FeAlSi + β-$FeAl_{4.5}Si$ equilibrium is most probably misinterpretation. This phases field was replaced by L + γ-$FeAl_3Si$ + α-FeAlSi to preserve agreement with the reaction scheme and liquidus surface. The data of [2014Li] were complemented with the three-phase equilibria deduced from the liquidus surface and reaction scheme. These tie-triangles are shown with dashed line in Fig. 14. Figures 15 and 16 show the phase equilibria in the Al corner at 640 and 620°C according to [1959Phi] and [2015Zou]. Small adjustments were introduced to preserve compatibility with the accepted binary phase diagrams and liquidus surface projection.

[1987Gri1, 1987Ste] reported the phase equilibria in a set of commercial Al based alloy after heat treating the as-cast samples for one month between 570 and 600°C. The heat-treated state was referred to as 'quasi-equilibrium' condition by [1987Ste]. It is to be noted that some phase equilibria, such as (Al)+β-$FeAl_{4.5}Si$, were derived from the measurements on samples annealed at 570°C. [1987Pri] amended the phase equilibria of the Al corner at 600°C reported by [1987Gri1] and [1987Ste].

[1974Mur, 1981Zar] also studied the phase equilibria at 600°C. The authors presented the phase equilibria in almost whole composition range except for Fe-rich corner. Neither primary experimental results were provided, nor experimental procedure was specified in this work. This raises certain doubts in the accuracy of the constructed section. There are issues with should be mentioned with respect to the results of [1974Mur, 1981Zar]. Firstly, the authors considered Si-rich and Si-poor compositions of $Fe_3Al_2Si_3$ as two different intermetallic compounds. Secondly, no phase equilibria involving the liquid phase were reported. These findings contradict the experimental results of [1940Tak, 1951Now, 2001Kre, 2004Pon1, 2004Pon2, 2007Kre, 2011Mar]. Thirdly, [1974Mur, 1981Zar] did not find the $Fe_3Al_2Si_3$+Fe_2Al_5+Fe_4Al_{13} tie-triangle which was observed by [2004Bos, 2011Mar] and by [2001Kre, 2007Kre] above and below 600°C.

Therefore, the isothermal section as-constructed by [1974Mur, 1981Zar] was significantly amended in the present evaluation (Fig. 17). All changes are shown with dashed lines. The phase equilibria involving $Fe_3Al_2Si_3$ were revised taking into account results of [2004Bos] for 727°C and [2007Kre] for 550°C. The composition of $Fe_3Al_2Si_4$ was accepted according to [2011Mar]. Also, according to the reaction scheme, three-phase fields L+(Si)+$FeAl_3Si_2$, L+$FeAl_3Si_2$+β-$FeAl_{4.5}Si$, and L+(Al)+β-$FeAl_{4.5}Si$ were added. In the Al-rich corner, the phase equilibria involving α-FeAlSi, β-$FeAl_{4.5}Si$, γ-$FeAl_3Si$ and (Al) reported by [1974Mur, 1981Zar] agree with results of [1987Gri1, 1987Ste] and compatible with the reaction scheme. Therefore, they were preserved.

As it was already discussed in the *'Invariant Equilibria'* section, the phase equilibria between (Si), $FeSi_2$, $Fe_2Al_3Si_3$ and $Fe_3Al_2Si_4$ at low temperatures are inconclusive and contradictory. It would require the introduction of many unjustified solid-phase invariant reactions to make the isothermal sections at different temperatures compatible. To avoid such unnecessary complication, it was suggested that the (Si)+$Fe_2Al_3Si_3$+$Fe_3Al_2Si_4$ tie-triangle reported by [2004Bos] also existed at lower temperatures. Thus, the $FeSi_2$+$Fe_2Al_3Si_3$+$Fe_3Al_2Si_4$ and (Si)+$FeSi_2$+$Fe_2Al_3Si_3$ phase fields at 600°C were replaced by (Si)+$Fe_2Al_3Si_3$+$Fe_3Al_2Si_4$ and (Si)+$FeSi_2$+$Fe_3Al_2Si_4$. The latter were also accepted to be stable at 550°C (Fig. 18). In the previous evaluation of [2013Gho], it was stated that the Fe corner involving the ordered phases at 600°C is taken from [1982Miy, 1986Miy]. However, [1982Miy, 1986Miy] did not perform measurements at this temperature. Therefore, the phase boundaries in Fe corner are shown schematically.

Figure 18 shows the partial isothermal section at 550°C according to [2007Kre]. [2007Kre] stated that their section is essentially schematical as available data on the phase equilibria have not been suggestive. The phase equilibria in the Al corner agree with the partial isothermal section at 500°C proposed by [1984Don]. The phase equilibria in the Fe

corner as 550°C, as well as at 450°C (Fig. 19), are accepted according to [1982Miy, 1986Miy]. As follows from Fig. 19, the phase equilibria between the ordered phases are of the first-order at 450°C.

It should be emphasized that the low-temperature phase equilibria and transformations involving the ordered phase require further experimental study.

Temperature – Composition Sections

Figures 20 to 29 show the vertical sections at constant concentrations of aluminium (Fig. 20), silicon (Figs. 21 to 23), and iron (Figs. 24 to 29). The sections are adopted from different sources. To comply with the accepted reaction scheme shown in Fig. 5, the temperatures of invariant reactions in the figures were corrected according to the reaction scheme. The phase boundaries were adjusted to preserve qualitative agreement between the liquidus surface, isothermal and vertical sections and compatibility with the accepted binary systems.

Fig. 20 shows the partial isopleth at 5 at.% Al redrawn for 50-95 at.% Si according to [2011Mar]. [2011Mar] actually constructed the vertical section for the whole composition range. In our opinion, the authors simplified the phase equilibria involving the ordered phases in view of absence of reliable experimental data. Since no detailed information regarding this issue appeared in the literature, the Si-poor part of the isopleth was omitted in the presented evaluation.

The partial isopleths in Figs. 21 to 25 show the phase equilibria in the Al-rich corner. These sections reveal the complexity of the phase transformations involving the liquid phase. The vertical sections isopleths at 0.7 mass% Fe (Fig. 24) and 8.0 mass% Si (Fig. 21) are based on [1949Cru, 1959Phi] and [1959Phi], respectively. The L+(Si) phase boundary in Fig. 21 is shown with dashed line as no reliable DTA data are available for this region. The isopleths at 10.0, 13.5 mass% Si and 5.0 mass% Fe were adopted according to the thermodynamic assessments of [2014Che] and [2010Ele] with small correction according to accepted liquidus surface projection. Although [2010Ele] and [2014Che] calculated their partial section using their own thermodynamic assessment, the calculated phase fields agree well with the reactions scheme and liquidus surface accepted in the present work.

Figs. 26 to 29 show isopleths at 27, 35, 40, and 50 at.% Fe. These sections were presented by [2011Mar] and redrawn in the present evaluation but with certain amendments. In Figs. 26, 27, and 28, the phase equilibria near the Al-Fe side were modified to preserve compatibility with the binary system and the reaction scheme accepted in the present work. For the isopleth at 27 at.% Fe (Fig. 26), the U_{12} reaction was introduced that was required to have agreement with the isothermal sections presented by [2011Mar]. This reaction was probably overlooked by [2011Mar] in their original work. For the isopleth at 50 at.% Fe (Fig. 29), the order-disorder transition was included. The corresponding phase boundary should be considered as tentative as no corresponding data are available to confirm our suggestion. The isopleth at 60 at.% Fe presented by [2011Mar] was not accepted here. This section involves the phase equilibria between different ordered phases that are still to be clarified. For the same reason, we did not distinguish between the ordered phases in Figs. 27 to 29 and denoted them as “Ord”. Also, no attempts have been made to draw the phase equilibria below 800°C because of the absence of the accurate experimental data for lower temperatures (see, *“Invariant Equilibria”* section).

There have been extensive studies of order-disorder transitions of Fe-rich ternary alloys, both experimentally and theoretically. Some of the studies related to this topic by [1946Sel, 1951Sat, 1969Pol, 1973Kat, 1977Nic1, 1977Nic2, 1977Suw, 1982Cha, 1983Gle, 1983Sch, 1986Tak, 1987For, 1987Dob] were discussed by [1988Ray, 2013Gho]. The solid solubility and the magnetic behavior of $Fe_3(Al, Si)$ were correlated with the electron-atom ratio [1977Nic1] and [1977Nic2]. The ordered phases Fe_3Al and Fe_3Si which have $D0_3$ or BiF_3 type order and FeAl and FeSi which have $B2$ or CsCl type order along the Fe_3Al-Fe_3Si section were studied by means of high temperature X-ray diffraction and recording the disappearance of $D0_3$ superlattice reflections as a function of temperature and composition [1969Pol, 1973Kat]. [1946Sel] measured the lattice parameter of alloys up to 13 mass% Al and 18 mass% Si, and observed an inflection point in the lattice parameter versus composition curve which was attributed to the ordering transition and the formation of $Fe_3(Al,Si)$ having $D0_3$ superstructure. These results were further supported by the specific heat measurements as a function of Si/Al ratio by [1951Sat], who found the transformation is accompanied by a small change in Gibbs energy suggestive of a second-order type. However, with the addition of Si in Fe_3Al the ordering energies increase monotonically [1973Kat]. The order-disorder transition along Fe_3Al-Fe_3Si was also studied by transmission electron microscopy (TEM) [1982Cha] and by magnetic method [1986Tak].

Despite these results, there is still some controversy regarding the sequence of ordering transitions along this section. This issue has not been yet solved. Previous studies by [1969Pol] and [1973Kat] indicate that the sequence of ordering transition (on cooling) is always (αδFe) → FeAl → Fe_3Al along the entire Fe_3Al-Fe_3Si section. However, recent studies by [1982Cha] and [1986Tak] indicate that substitution of more than 50% of the Al atoms by Si atoms (αδFe) transforms directly into $D0_3$ structure (Fe_3Al). The effect of Si on the ordering induced phase separation around Fe_3Al

has not been investigated in detail. But it is important to note that [1996Mor] observed (αδFe) + Fe_3Al microstructure in an Fe-17Al-1Si (at.%) alloy in the temperature range of 400 to 600°C.

The results of [1969Pol] also indicate that $Fe_3(Al, Si)$ and liquid should be in equilibrium along the Fe_3Al-Fe_3Si section at 12.5 at.% Si. However, the nature and type of the phase equilibria between the ordered phases and liquid are not clarified. Even though the nucleation and growth of Fe_3Al domain in FeAl domain is easier than in (αδFe) matrix, the direct (αδFe) ⇌ Fe_3Al transformation in certain composition range has been attributed to the lowering of atomic potential energy where Al atoms are substituted by Si atoms. This causes the formation of different types of anti-phase boundaries and the corresponding changes in dislocation configuration leads to double dissociation of superlattice dislocations [1982Cha]. Depending on the composition of an alloy, the nucleation of ordered phases may also take place in the melt. TEM and Mössbauer spectroscopy study [1983Gle] in an Fe-5.4Al-9.6Si (mass%) alloy revealed that the *B*2 type of ordering takes place directly in the melt which subsequently undergoes $D0_3$ ordering. However, [1969Pol] observed that the $D0_3$ superlattice reflections persist up to the melting point in an alloy of Fe_3Al + 12 at.% Si. A similar conclusion was also made by [1954Gar] who investigated the order-disorder transition, after quenching from different temperatures, in an Fe-9.7Si-5.5Al (mass%) alloy. By rapid quenching an Fe-5.4Al-9.6Si (mass%) alloy, [1983Gle] observed that excess vacancies are introduced which occupy ordered sublattice positions, giving rise to a new crystallographic superstructure of the $D0_3$ type.

Mössbauer spectroscopy study of $Fe_{73}Al_{11}Si_{16}$ (ALSIFER27) and $Fe_{68}Al_{22}Si_{10}$ (ALSIFER32), by [1977Suw], revealed that excess diamagnetic atoms (Al and Si) preferentially occupy the Fe site at (0, 0, 0) in the $D0_3$ lattice. They argued that powder methods used in X-ray diffraction experiments may not represent the ordering transitions in the bulk materials. Later, measurements of on-site magnetic moment by neutron diffraction, and also the Mössbauer spectroscopy data suggest that the excess Al and Si atoms occupy the Fe-site at (1/4, 1/4, 1/4) in the $D0_3$ lattice [1987Dob]. Mössbauer spectroscopy results indicate that 'order-annealing' treatment is accompanied by a separation of Fe_3Al and Fe_3Si types of local surroundings [1983Sch]. However, this has only weak influence on the physical properties, and the predominant factor being the composition of the alloy.

In their review, [1988Ray] summarized the experimental data of [1969Pol] and drew the Fe_3Al-Fe_3Si section that should be considered as simplified. [2013Gho] proposed the modified Fe_3Al-Fe_3Si section that however also presents a simplified representation of the phase transitions and does not agree with the Fe-Si system adopted here. For these reasons, this section was not included in the present evaluation.

Thermodynamics

Thermodynamic properties of ternary alloys have been investigated a number of times by measuring the heat of formation of solid alloys [1937Koe, 1937Oel], activity measurements in liquid alloys [1969Bed, 1970Mit, 1973Nag, 1973Per, 1980Sud, 1984Ber, 1985Cao, 1989Bon, 2004Kan], heat of mixing of liquid alloys [2003Kan], and the standard heat of formation of ternary intermetallics [1997Vyb, 2000Li1, 2000Li2].

[1969Bed] determined the activity coefficients at several constant mole fraction ratios (x_{Si}/x_{Fe}) at 1627°C. Activity of Al in liquid alloys in the temperature range of 800 to 1100°C were reported by [1973Nag], and at 900°C by [1973Per]. [1980Sud] reported activity of Al in an Al-Fe-1Si (mass%) alloy at 1485 and 1546°C. Additional experiments were also carried out by [1984Ber] and [1989Bon]. The latter authors measured the chemical potential of Al in alloys containing up to 11.8 at.% Fe and 23.7 at.% Si by the concentration cell method in the temperature range of 577 to 1027°C. The activities of Al show a negative deviation from the ideal behavior. The results of [1984Ber] also show a similar trend. The activity of Al in $Fe_x(Al_{0.879}Si_{0.121})_{1-x}$, $0.0249 \le x \le 0.0512$, shows a transition from positive to negative deviation from the ideal behavior at $x = 0.035$ [2004Kan].

Recently, [2003Kan] measured the heat of mixing of liquid alloys at 1477°C using a high-temperature isoperibolic calorimeter. Some selected data is listed in Table 4, while several isoenthalpic (mixing) lines are plotted in Fig. 30.

Heat of mixing of solid alloys was measured by pouring liquid Al-Si alloy and liquid iron into a calorimeter [1937Koe, 1937Oel]. However, the state of equilibrium in these experiments is uncertain [1999Liu]. The standard heat of formation of ternary intermetallics, except $Fe_2Al_3Si_3$, has been determined by solution calorimetry by [1997Vyb], [2000Li1] and [2000Li2]. These results are summarized in Table 5. [1997Vyb] used 99.99% Al, 99.9% Fe and 99.99% Si to prepare single phase α-FeAlSi and β-$FeAl_{4.5}Si$ samples by annealing cast ingots either at 550°C (α-FeAlSi) or at 600°C (β-$FeAl_{4.5}Si$) for 1 month. They used an aluminum bath at 1070°C for solution calorimetry. [2000Li1, 2000Li2] used 99.99% Al, 99.999% Fe and 99.999% Si to prepare the intermetallics. Levitation melting followed by annealing, the conditions of which varied, were employed to obtain single phase alloys of $Fe_3Al_2Si_3$, α-FeAlSi and τ_1 [2000Li1], and γ-$FeAl_3Si$, $FeAl_2Si$, $FeAl_3Si_2$, β-$FeAl_{4.5}Si$, and $Fe_3Al_2Si_4$ [2000Li2]. Unlike [1997Vyb], [2000Li1, 2000Li2] used an aluminum bath at a lower temperature of 800°C for solution calorimetry.

There are differences between the results of [1997Vyb] and [2000Li1, 2000Li2]. For example, [1997Vyb] reported that the standard heat of formation of α-FeAlSi ($Fe_{19.2}Al_{71.2}Si_{9.6}$) and β-$FeAl_{4.5}Si$ ($Fe_{15.4}Al_{69.2}Si_{15.4}$) are –34.3 ± 2 and –24.5 ± 2 kJ·(g-at)$^{-1}$, respectively. The corresponding values are –24.44 ± 1.387 kJ·(g-at)$^{-1}$ for α-FeAlSi at $Fe_{18}Al_{72}Si_{10}$ [2000Li1] and –20.209 ± 0.926 kJ·(g-at)$^{-1}$ for β-$FeAl_{4.5}Si$ at $Fe_{15}Al_{70}Si_{15}$ [2000Li2]. Even though the α-FeAlSi and β-$FeAl_{4.5}Si$ compositions of [1997Vyb] and [2000Li1, 2000Li2] are not identical, large differences in heat of formation are unexpected. Apparently, [2000Li1, 2000Li2] were unaware of the results of [1997Vyb], and they did not discuss this discrepancy. Nonetheless, it is not clear if a higher bath temperature (causing oxidation) and relatively impure starting materials used by [1997Vyb] compared to [2000Li1, 2000Li2] have contributed to more negative heat of formation. [2010Du] calculated formation energy of $FeAl_3Si_2$ and $Fe_3Al_2Si_4$ using first-principles methods. Their calculated results agree within ±5 kJ/mol-atoms with the experimental values of [2000Li2].

[1994Ang] determined the enthalpy of fusion of $FeAl_3Si_2$ and $Fe_2Al_3Si_3$.

Thermodynamic modeling of the ternary system has also been carried out by the CALculation of PHase Diagram (CALPHAD) method [1994Ang, 1995Gue3, 1998Kol, 1999Liu], where the Gibbs energies of the relevant phases are described by simple analytical functions. [1949Cru] reported calculated solubility isotherms of Fe and Si in solid (Al). They suggested the formation of a ternary compound Fe_2Al_7Si whose composition is close to the α-FeAlSi phase at low Si content. On the other hand, their calculation seems to suggest the ternary phase $FeAl_5Si$ that is close to the β-$FeAl_{4.5}Si$ phase [1981Riv]. Calculation of the liquidus surface from a purely thermodynamic approach [1946Phi2] seems to produce good result near the binary edges. However, their approach can neither predict the composition of the precipitating phase nor calculate the solidus curves.

[1994Ang] employed the CALPHAD technique and calculated two vertical sections corresponding to x_{Al}/x_{Si}=3/1 and at x_{Si} = 0.85. [1995Gue3] calculated two partial isothermal sections at 600 and 900°C, and a vertical section at x_{Si} = 0.78 by the CALPHAD method. They considered only two ternary phases: $FeAl_3Si_2$ and $Fe_5Al_8Si_7$. In our classification, these correspond to $FeAl_3Si_2$ and $Fe_2Al_3Si_3$, respectively.

[1998Kol] and [1999Liu] carried out detailed thermodynamic assessments of the ternary system by the CALPHAD method. [1998Kol] considered six ternary phases that in our classification correspond to α-FeAlSi, β-$FeAl_{4.5}Si$, $FeAl_3Si_2$, γ-$FeAl_3Si$, $Fe_3Al_2Si_3$, and $FeAl_2Si$. In their CALPHAD modeling, [1999Liu] considered seven ternary intermetallics that correspond to $Fe_3Al_2Si_3$, γ-$FeAl_3Si$, $FeAl_2Si$, $FeAl_3Si_2$, α-FeAlSi, β-$FeAl_{4.5}Si$, and $Fe_2Al_3Si_3$ in our classification. [1999Liu] argued that γ-$FeAl_3Si$ and $FeAl_2Si$ have very similar Fe contents, and wondered, if they are the same phase with a small homogeneity range. This view was also accepted by [2002Rag]. However, as summarized in Table 2, γ-$FeAl_3Si$ and $FeAl_2Si$ have different crystal structures. [1999Liu] computed the liquidus surface, isothermal sections at 600 and 1000°C, and vertical sections at 1.3, 2, 5, 10 mass% Fe and 2 mass% Si.

[2008Du] also performed CALPHAD modeling of the system considering ten ternary intermetallics ($Fe_3Al_2Si_3$, γ-$FeAl_3Si$, $FeAl_2Si$, $FeAl_3Si_2$, α-FeAlSi, β-$FeAl_{4.5}Si$, $Fe_2Al_3Si_3$, $Fe_3Al_2Si_4$, τ_1 and $Fe_{1.7}Al_4Si$). They reported liquidus surface, reaction scheme, isothermal sections at 550, 727, 800°C, vertical sections at 15 mass% Fe, 10 mass% Si, and at a constant ratio of w(Fe)/w(Si)=0.133. More recently, [2010Ele] re-assessed Al-corner of the system using the CALPHAD approach. They considered four ternary intermetallics: α-FeAlSi, β-$FeAl_{4.5}Si$, γ-$FeAl_3Si$ and $FeAl_3Si_2$. They reported following calculated results: (i) liquidus surface of Al-corner, (ii) isothermal sections at 590 and 727°C, and (iii) vertical sections at 13.5 mass% Si and 5 mass% Fe.

In the CALPHAD modeling by [1994Ang, 1998Kol, 1999Liu, 2008Du, 2010Ele, 2014Che] of the ternary system, several sublattice models have been used to describe Gibbs energy of ternary intermetallics. For example, [1994Ang] used a three-sublattice model for $FeAl_3Si_2$ and $Fe_2Al_3Si_3$. [1998Kol] used a four-sublattice model for the α-AlFeSi phase while a three-sublattice model for other compounds considered in the study. On the other hand, [1999Liu] used a three-sublattice model for $Fe_3Al_2Si_3$, γ-$FeAl_3Si$, $FeAl_2Si$, $FeAl_3Si_2$, and $Fe_2Al_3Si_3$, while a four-sublattice model for β-$FeAl_{4.5}Si$ and α-FeAlSi. [2008Du] used a two-sublattice model for $Fe_3Al_2Si_3$, γ-$FeAl_3Si$, $FeAl_3Si_2$, $Fe_2Al_3Si_3$ and $Fe_3Al_2Si_4$, while a three-sublattice model for $FeAl_2Si$, α-FeAlSi, β-$FeAl_{4.5}Si$, τ_1 and $Fe_{1.7}Al_4Si$. Later, [2014Che] improved this assessment by taking the data of [2007Kre] into account. [2010Ele] used a four-sublattice model for all four ternary phases mentioned above. Notwithstanding these differences, the heat of formation of ternary intermetallics calculated by CALPHAD method agree reasonably well with available calorimetry data.

Theoretical analysis of phase separation involving the ordered (Fe_3Al, FeAl) and disordered (αδFe) phases was carried out by [1991Fuk, 1994Koz]. They described free energy of ternary alloys using a statistical model that uses pair-wise interaction up to second nearest neighbor. Both chemical and magnetic interactions based on Bragg-Williams-Gorsky model were used. The calculated phase diagrams are found to be consistent with the experimental ones. These theoretical studies underscore the influence of ferromagnetic ordering on phase separation.

Also, [2010Ele] reported calculated isothermal section of Al-corner at 727°C. Since [2010Ele] considered only four ternary phases (γ-$FeAl_3Si$, $FeAl_2Si$, $FeAl_3Si_2$ and α-FeAlSi), their calculated isothermal section of Al-corner at 727°C does not show phase fields involving $Fe_2Al_3Si_3$, τ_1 and $Fe_{1.7}Al_4Si$ phases.

[2010Fri] employed first-principles methods to calculate structural and elastic properties of $D0_3$-Fe_3Al alloyed with Si. Substitution of Si at both Fe and Al sites is associated with a decrease in formation energy and an increase in Young's modulus.

[2010Mal] proposed thermodynamic and kinetic arguments for the formation of ternary phases during rapid solidification of Al-Fe-Si alloys. [2010Mor] modeled microsegregation and precipitation of ternary intermetallics. Their model considers α-FeAlSi and β-$FeAl_{4.5}Si$ phases, and an effective interdiffusion coefficient in solid (*fcc*-Al) and liquid phases.

[2011Spr] investigated interdiffusion between an Al-5 mass% Si alloy and a mild steel at 600 and 675°C using optical microscopy, SEM, Electron backscatter diffraction (EBSD), orientation imaging (OIM), XRD, analytical TEM, scanning transmission electron microscopy (STEM). In the interdiffusion zone, they observed $Fe_3Al_2Si_3$, $FeAl_2Si$, α-FeAlSi and β-$FeAl_{4.5}Si$ phases, and confirmed that the addition of Si to Al retard growth of α-FeAlSi phase.

[2014Ami] performed density functional theory (DFT) calculations for the intermetallic phase $FeAl_3Si_2$ which is stable in the Al-Fe-Si system up to the temperature of 875°C and they also determined the heat capacity of this phase by DSC measurement.

[2019Zie] calculated the heat capacity of Fe_2Al_5, Fe_5Al_8 and $FeAl_3Si_2$ by an algorithm based on zero-Kelvin properties (V_0, B_0), the Debye temperature and the thermal expansion coefficient at the Debye temperature.

Notes on Materials Properties and Applications

A summary of experimental investigation of properties is given in Table 6. [1951Oga1, 1951Oga2, 1983Sch] reported the ferromagnetic behavior of Fe_3Al-Fe_3Si alloys. [1968Aru1, 1968Aru2, 1970Aru] reported that the occupation of ordered sites by all three Al, Fe and Si atoms accompanied with a minimum in electrical resistivity at $Fe_{75}Al_{18}Si_7$. [1996Szy] reported that dissolved Al in $FeSi_2$ increases its magnetic susceptibility, and both FeSi and $FeSi_2$ exhibit Van Vleck paramagnetism even at very low temperature (up to 4.2 K). [1996Fri] and [1998Dit] studied the metal-insulator transition in Al doped FeSi. [1998Dit] reported lattice constant, thermoelectric effect, Hall effect, electrical conductivity, magnetic susceptibility, specific heat and magnetoresistance in $FeSi_{1-x}Al_x$, with $0 \le x \le 0.08$. All these properties confirm a metal to insulator transition of FeSi, which is otherwise a Kondo insulator. [1999Oht] have reported that doping of $FeSi_2$ with 3 at.% Al improves its thermoelectric figure of merit. [1986Tak] and [1988Dor] have discussed magnetic properties of ternary alloys. However, recent studies of magnetic properties due to Si/Al substitution in $Fe_{75}Al_{25}$, $Fe_{70}Al_{30}$ and $Fe_{60}Al_{40}$ alloys using Mössbauer spectroscopy and X-ray diffraction by [2010Leg] demonstrate a complex interplay between atomic ordering and magnetic heterogeneity. [2010Ma] studied electronic structure of $D0_3$-$Fe_3Al_{1-x}Si_x$ alloys using first-principles methods. As Al is replaced with Si, both lattice parameter and saturation magnetization decrease linearly. Associated change in magnetic properties is related to changes in local moment of Fe caused by its local environment causing charge transfer and bonding type as demonstrated by Mulliken charge analysis.

[1993Sch] investigated the plastic deformation of single-crystal $Al_{20}Fe_{75}Si_5$ alloy as a function of temperature. The critical resolved shear stress exhibits a non-monotonic behavior with a maximum around 530°C. The non-monotonic behavior was correlated with the temperature-dependent dislocation mobility rather than a decrease in $D0_3$ long-range order parameter. [1996Cho, 2001Cho] reported the microstructure, hardness and tensile properties of Al-5 mass% Fe-16 mass% Si alloy, processed by powder metallurgy, up to 520°C.

[2003Cie] observed Portevin-Le Chatelier Effect in biaxially strained Al-Fe-Si foils. This effect is attributed to the diffusion of Si rather than Fe, as the latter has much slower diffusivity and low solubility in (Al). [2003Mur] reported the hardness and indentation fracture toughness of γ-$FeAl_3Si$ and α-FeAlSi phases, both have hardness much higher than binary aluminides and they have very similar indentation fracture toughness.

[1948Jen] demonstrated a relationship between the constitutional diagram and the susceptibility to cracking of the Al-Fe-Si alloys. A key factor in determining the corrosion behavior of Al rich alloys is the Fe/Si ratio. At a low Fe/Si ratio, ternary alloys exhibit better corrosion resistance in both industrial and marine environment [2000Bha].

[2012Leg] reported the influence of different Al/Si ratios on the magnetic and structural properties of $Fe_{75}Al_{25-x}Si_x$, $Fe_{70}Al_{30-x}Si_x$ and $Fe_{60}Al_{40-x}Si_x$ alloys. The results indicated that addition of Si to binary Al-Fe alloys makes the disordering more difficult. The magnetic measurements indicate that addition of Si to binary $Fe_{75}Al_{25}$ and $Fe_{70}Al_{30}$ alloys opposes the magnetic behavior induced by Al in the magnetism of Fe.

[2015Che] measured the thermal and electrical conductivity of the gravity castings of the Al-10Si-Fe alloy. It was shown that the thermal conductivity was affected by several factors, such as microstructures, composition, and distribution of each phase.

[2017Raj] investigated the phase fractions, microstructure and thermoelectric properties of $FeSi_2$ with different aluminium concentrations. The results illustrated that the Al-doping in Si dispersed $FeSi_2$ results in the increased hole-carrier concentration thereby enhancing the electrical conductivity without compromising the Seebeck coefficient.

Miscellaneous

In recent years, the solidification of Al rich ternary alloys has been investigated rather extensively.

[1983Per] discussed the effect of metastable liquid miscibility gaps, metastable eutectic and metastable peritectic on the rapid solidification processing and alloy design. Addition of up to 0.11 mass% Fe in an Al-0.5Si (mass%) alloy is reported to favor the formation of the metastable phase $FeAl_6$ [1978Suz].

[1995Bel] proposed a non-equilibrium solidification method to analyze the cast microstructure of ternary alloys. This method utilizes equilibrium phase diagram, but assumes that the peritectic reactions are suppressed and the eutectic reactions occur according to the equilibrium phase diagram. The role of heterogeneous nucleation on phase selection, solidification, and grain refinement of Al has been investigated in detail [1996All, 1997All, 1997Can, 2004Kha]. In particular, [2004Kha] investigated the nucleation potency of Al on the surface of MgO, TiB_2, TiC, α-Al_2O_3 and SiC inclusions. They showed that in dilute hypoeutectic alloys (Al+Fe less than 1.5 mass%) these inclusions act as efficient grain refiner caused by a decrease in liquid/inclusion interfacial energy due to the segregation of Si. [2005Kha] investigated heterogeneous nucleation of ternary intermetallics ($FeAl_3Si_2$, α-FeAlSi, β-$FeAl_{4.5}Si$) on the surface of CaO, MgO, TiB_2, TiC, Al_4C_3, α-Al_2O_3, γ-Al_2O_3 and SiC inclusions. They found that reactive inclusion such as CaO and SiC are potent nucleants for the intragranular ternary intermetallics. Also, the potent nucleants for the primary phase, (Al), such as γ-Al_2O_3 exhibit poor potency for the nucleation of ternary phases. [2002Dut] reported the effect of cooling rate on the amount of ternary eutectic, and also the effect of Fe/Si ratio on the morphology of intermetallics in cast Al alloys.

[1997Sto] studied the effect of cooling rate and solidification velocity on the microstructure selection of Al-3.5Fe-(1 to 8.5)Si (mass%) alloys by wedge chill casting and Bridgman directional solidification techniques. In the latter case, the front growth velocity was in the range of 0.01 to 2 mm·s^{-1} under a temperature gradient of 15°C·mm^{-1}. Also, at front velocities greater than 1 mm·s^{-1}, the primary intermetallics were suppressed. The results of Al-3.5Fe-8.5Si (mass%) were summarized in terms of a kinetically based solidification microstructure selection diagram.

[1999Tay] applied Scheil equation to predict the defect-onset (porosity) during solidification of Al rich alloys as a function of Fe and Si contents. The effect of Fe and other elements on the porosity of hypoeutectic Al-Si castings has also been discussed by [2005Lu]. Taylor et al [1999Tay] found that a defect-free casting can be obtained if the solidification proceeds directly to the invariant reaction E_1 (L ⇌ β-$FeAl_{4.5}Si$ + (Al) + (Si)), whereas poor casting may result when the solidification proceeds *via* the (Al)-β-$FeAl_{4.5}Si$ eutectic valley. The critical Fe content at which the porosity is minimized is a function of Si content in the alloy. [2001Sha] also carried out Bridgman directional solidification of a model 6xxx alloy (Al-0.3Fe-0.6Si-0.8Mg (mass%)), and obtained solidification front velocity in the range of 5 to 120 mm·min^{-1}. They observed two ternary phases, α-FeAlSi and β-$FeAl_{4.5}Si$, of which the latter is metastable. At low front velocity, such as 30 to 60 mm·min^{-1}, β-$FeAl_{4.5}Si$ dominate the microstructure, while at high front velocity, such as 120 mm·min^{-1}, β-$FeAl_{4.5}Si$ dominates the phase selection. Hegde and Prabhu [2008Heg] have discussed possible mechanisms of grain refinement in Al-Fe-Si casting alloys.

Since both Al-Fe and Fe-Si binary systems form γ loops, a ternary γ loop is expected. [1931Wev] reported the coordinates of the phase boundaries of the ternary γ loop and these are listed in Table 7. [1960Voz] reported the effect of impurities on the solid solubility of Al alloys by means of electrical resistivity. [1972Ere] studied the dissolution kinetics of Fe in Al-Si melts at 700, 750 and 800°C, the kinetics of which was correlated with the formation of various intermediate phases.

[2000Sri] reported synthesis of bulk ternary intermetallics using elemental powder mixture by self-propagating high temperature synthesis. They used cold compacted powder mixtures that were heated to 650°C in a vacuum furnace. Both stable (γ-$FeAl_3Si$, α-FeAlSi and β-$FeAl_{4.5}Si$) and metastable phases were obtained in this process. They also reported hardness of the intermetallics.

[1998Akd] proposed that the value of activity coefficient of Al in (αδFe) alloys has a strong influence on the formation and growth kinetics of interfacial diffusion layer. [1999Oht] have discussed the sintering mechanism of

Al-Fe-Si alloys, particularly the role of liquid phase, in the context of fabricating an Al doped $FeSi_2$ phase. [2001Jha] has discussed the diffusion path of Al in ternary *bcc* alloys.

[2004Kaj] calculated time-temperature-precipitation diagram of α-FeAlSi during processing of an Al-0.51Fe-0.07Si alloy employing heterogeneous nucleation theory within Johnson-Mehl-Avrami formalism by considering stored energy including the effects due to recovery and recrystallization. [2005Bar] developed a model for Si and Al diffusion in iron by reducing coupled system of diffusion equations to a single partial differential equation. They predicted diffusion paths at 800 and 1100°C during galvanizing process. [2005Lu] reported that addition of Sr changes the mode of eutectic nucleation, depresses the precipitation temperature of β-$FeAl_{4.5}Si$, while addition of Mn suppresses the formation of coarse β-$FeAl_{4.5}Si$ replaces it with more compact and less harmful α-FeAlSi phase. [2009Gom] discussed the roles of Al and Si in designing TRIP (TRansformation Induced Plasticity) steels.

[2011Lee1, 2011Lee2] investigated the effects of Fe content and cooling rate on the solidification path and formation behavior of the β-$FeAl_{4.5}Si$ phase in two Fe-containing eutectic and hypoeutectic Al-Si alloys based on thermodynamic analysis and pertinent experiments.

[2017Tod] studied the effect of ultrasonic melt treatment (USMT) on macro-segregation and primary Fe-containing intermetallic peritectic transformations in an Al-19 mass% Si-4 mass% Fe alloy. USMT had a significant impact on the constitution of the primary Fe-containing intermetallics, where complex particles of $FeAl_3Si_2$/β-$FeAl_{4.5}Si$ were prominent without USMT, while few $FeAl_3Si_2$ particles were observed after USMT and the primary Fe-containing intermetallics existed mostly as the single-phase β-$FeAl_{4.5}Si$. It also leads to enhanced peritectic transformation $FeAl_3Si_2$ → β-$FeAl_{4.5}Si$ due to the significant reduction in the average size of the primary $FeAl_3Si_2$ particles.

[2020Zha] investigated the microstructural evolution of an as-cast Al-7Si-2Fe alloy by optical microscope (OM) and SEM/EDS and thermodynamic calculations.

Acknowledgments

The authors would like to thank gratefully Prof. Andreas Leineweber (the Institute of Materials Science, TU Bergakademie Freiberg, Germany) for his comments and help with the critical evaluation of the Al-Fe-Si system.

References

[1923Dix] Dix, Jr., E.H., "Observations on the Occurrence of Iron- and Silicon in Aluminium", *Trans. AIME*, **69**, 957-971 (1923) (Phase Relations, Experimental, 12)

[1923Han] Hanson, D., Gayler, M.L.V., "The Heat-treatment and Mechanical Properties of Alloys of Aluminium with Small Percentages of Copper", *J. Inst. Met.*, **29**, 491-506 (1923) (Experimental, 1)

[1923Wet] Wetzel, E., "Advances in Aluminium Research" (in German), *Die Metallboerse*, **13**, 737-738 (1923) (Phase Diagram, Experimental, 6)

[1924Fus] Fuss, V., "On the Constitution of Ternary Al Alloys" (in German), *Z. Metallkd.*, **16**, 24-25 (1924) (Phase Relations, Experimental, 3)

[1927Gwy] Gwyer, A.G.C., Phillips, H.W.L., "The Ternary System: Aluminium-Silicon-Iron" in "*The Constitution of Alloys with Silicon and Iron*", *J. Inst. Met.*, **38**, 44-83 (1927) (Phase Diagram, Phase Relations, Experimental, *, 9)

[1928Dix] Dix Jr., E.H., Heath Jr., A.C., "Equilibrium Relations in Aluminium-Silicon and Aluminium-Iron-Silicon Alloys of High Purity", *Trans. AIME*, *Inst. Met. Div.*, **93**, 164-197 (1928) (Phase Diagram, Phase Relations, Experimental, 39)

[1931Fin] Fink, W.L., Van Horn, K.R., "Constituents of Aluminium-Iron-Silicon Alloys", *Trans. AIME*, *Inst. Met. Div.*, 383-394 (1931) (Phase Diagram, Phase Relations, Experimental, 12)

[1931Fus] Fuss, V., "The Constitution of Aluminium rich Al-Fe-Si Alloys" (in German), *Z. Metallkd.*, **23**, 231-236 (1931) (Phase Diagram, Experimental, 6)

[1931Wev] Wever, F., Heinzel, A., "Two Examples of Ternary Iron Systems with Closed γ-Loop" (in German), *Mitt. K.-W.-Inst. Eisenforschung*, **13**, 193-197 (1931) (Phase Diagram, Experimental, #, *, 14)

[1932Nis] Nishimura, H., "An Investigation of Al rich Al-Fe-Si Alloys" (in Japanese), *Tetsu to Hagane*, **18**, 849-860 (1932), doi:10.2355/tetsutohagane1915.18.8_849 (Phase Diagram, Experimental, *, 40)

[1933Nis] Nishimura, H., "Investigation of Ternary Aluminium Alloy Systems: Al Rich Al-Fe-Si System", *Mem. Coll. Eng. Kyoto Univ.*, **7**, 285-303 (1933) (Phase Diagram, Experimental, 13)

[1934Fus] Fuess, V., "Aluminium-Iron-Silicon" in "*Metallography of Aluminium and Its Alloys*" (in German), Berlin, 109-117 (1934) (Phase Diagram, Experimental, 6)

[1934Roe] Roehrig, H., Kopernick, E., "On Spherically Precipitated Aluminium-Iron-Silicon Eutectic in Pure Aluminium" (in German), *Metallwirtschaft*, **13**, 591-593 (1934) (Phase Relations, Experimental, 2)

[1936Jae] Jaeniche, W., "On the System Aluminium-Iron-Silicon" (in German), *Alum. Arch.*, (5), 1-21 (1936) (Crystal Structure, Phase Diagram, Experimental, 28)

[1937Koe] Koerber, F., Oelsen, W., Lichtenberg, H., "On the Thermochemistry of Alloys. II. Direct Determination of the Heat of Formation of Ternary Alloys of the System Iron-Nickel-Aluminium-Silicon, as well as Certain Alloys of the Copper-Manganese-Aluminium System" (in German), *Mitt. K.-W.-Inst. Eisenforschung*, **19**, 131-159 (1937) (Experimental, Thermodynamics, 50)

[1937Oel] Oelsen, W., "The Heats of Formation of Binary and Ternary Alloys and Their Importance in Metallurgical Reactions" (in German), *Z. Electrochem.*, **43**, 530-535 (1937), doi:10.1002/bbpc.19370430810 (Experimental, Thermodynamics, 15)

[1937Ura] Urasov, G.G., Shashin, A.V., "Constitution of the (Ternary) Aluminium Alloys with Silicon and Iron" (in Russian), *Metallurg.*, (4), 27-41 (1937) (Phase Diagram, Experimental)

[1940Tak] Takeda, H.P., Mutuzaki, K., "The Equilibrium Diagram of the Iron-Aluminium-Silicon System" (in Japanese), *Tetsu to Hagane*, **26**, 335-361 (1940) (Phase Diagram, Experimental, *, 27)

[1941Pan] Panseri, C., Guastalla, B., "Investigations on the Permanent Modification of Eutectic Aluminium-Silicon Alloys. I.-Influence of Titanium Additions as the Third Component" (in Italian), *Alluminio*, **10**(5), 202-227 (1941) (Phase Diagram, Experimental, Review, 161)

[1943Mon] Mondolfo, L.F., "Aluminum-Iron-Silicon", in "*Metallography of Aluminum Alloys*", John Wiley & Sons, Inc., New York, 95-97 (1943) (Phase Diagram, Review, 27)

[1943Wei] Weill, A.R., "Structure of the Eta Phase of the Iron-Silicon System", *Nature (London)*, **152**(3858), 413 (1943), doi:10.1038/152413a0 (Crystal Structure, Review, 8)

[1946Phi1] Phillips, H.W.L., "The Constitution of Alloys of Aluminium with Magnesium, Silicon and Iron", *J. Inst. Met.*, **72**, 151-227 (1946) (Phase Diagram, Experimental, 86)

[1946Phi2] Phillips, H.W.L., "The Application of Some Thermodynamic Principles to the Liquidus Surfaces of Alloys of Aluminium with Magnesium, Silicon and Iron", *J. Inst. Met.*, **72**, 229-242 (1946) (Theory, Thermodynamics, 21)

[1946Sel] Selisski, Ya.P., "The Lattice Spacing of Solid Solutions of Fe, Si and Al Rich in Fe" (in Russian), *Zh. Fiz. Khim.*, **20**, 597-604 (1946) (Crystal Structure, Experimental, *, 15)

[1948Jen] Jennings, P.H., Pumphrey, W.L., "A Consideration of the Constitution of Aluminium-Iron-Silicon Alloys and Its Relation to Cracking Above the Solidus", *J. Inst. Met.*, **74**, 249-258 (1948) (Experimental, 14)

[1949Cru] Crussard, C., Aubertin, F., "Study of Thermo-electric and Thermodynamic Properties of Aluminium base Alloys Containing Mg, Si, Fe or Ti" (in French), *Rev. Metall.*, **46**, 661-675 (1949) (Phase Diagram, Experimental, #, *, 12)

[1950Gme] *Gmelins Handbook of Inorganic Chemistry*, "Aluminium-Iron-Silicon Alloys. The Al-Fe-Si Phase Diagram" (in German), A(8), System No. 35, Verlag Chemie GmbH, Weinheim, 1334-1370 (1950) (Phase Diagram, Review, 15)

[1950Phr] Phragmen, G., "On the Phase Occurring in Alloys of Aluminium with Copper, Magnesium, Manganese, Iron and Silicon", *J. Inst. Met.*, **77**, 489-552 (1950) (Phase Relations, Experimental, *, 67)

[1951Hol] Holik, L., Nowotny, H., Thury, W., "Investigation of the Microstructure in the Al corner of the System Aluminium-Iron-Silicon" (in German), *Berg- und Huettenmn. Monatsh. Hochsch. Loeben*, **96**, 181-184 (1951) (Phase Diagram, Experimental, 12)

[1951Now] Nowotny, H., Komerek, K., Kromer, J., "An Investigation of the Ternary System: Aluminium-Iron-Silicon" (in German), *Berg- und Huettenmn. Monatsh. Hochsch. Leoben*, **96**, 161-169 (1951) (Crystal Structure, Phase Diagram, Experimental, *, 31)

[1951Oga1] Ogawa, S., Matsuzaki, Y., "Study of the Superlattices in Ternary Iron-Aluminium-Silicon Alloys by X-rays", *Nippon Kinzoku Gakkaishi*, **15**, 242-244 (1951) (Crystal Structure, Experimental, *, 9)

[1951Oga2] Ogawa, S., Matsuzaki, Y., "Study on the Superlattice of Ternary Alloys by X-rays", *Sci. Rep. Research Inst. Tohoku University*, **3A**, 50-54 (1951) (Crystal Structure, Experimental, *, 9)

[1951Pra1] Pratt, J.N., Raynor, G.V., "Intermetallic Compounds in Ternary Aluminium Rich Alloys Containing Transitional Metals", *Proc. Royal Soc.*, **A205**, 103-118 (1951), doi:10.1098/rspa.1951.0020 (Crystal Structure, Phase Relations, Theory, 14)

[1951Pra2] Pratt, J.N., Raynor, G.V., "The Intermetallic Compounds in the Alloys of Aluminium and Silicon with Chromium, Manganese, Iron, Cobalt and Nickel", *J. Inst. Met.*, **79**, 211-232 (1951), doi:10.1098/rspa.1951.0020 (Crystal Structure, Phase Relations, Phase Diagram, Experimental, 32)

[1951Ran] Ransley, C.E., "Determination of Phase Boundaries in Solid Alloy Systems by a Diffusion Technique", *Nature*, **167**, 814 (1951), doi:10.1038/167814a0 (Phase Relations, Experimental, 1)

[1951Sat] Sato, H., Yamamoto, H., "The Behaviours of Fe-Al, Fe-Si and Fe-Al-Si Alloys Considered from the Standpoint of Ferromagnetic Superlattice", *J. Phys. Soc. Jpn.*, **6**, 65-66 (1951), doi:10.1143/JPSJ.6.65 (Experimental, Crystal Structure, Magnetic Properties, *, 2)

[1952Arm] Armand, M., "On the Phases in the Ternary System Aluminium-Iron-Silicon" (in French), *C.R. Seances Acad. Sci.*, **235**, 1506-1508 (1952) (Crystal Structure, Experimental, *, 9)

[1952Han] Hanemann, H., Schrader, A., "*Ternary Alloys of Aluminium*" (in German), Verlag Stahleisen, Duesseldorf, 109-115 (1952) (Phase Diagram, Review, 12)

[1954Gar] Garrod, R.I., Hogan, L.M., "The Superlattice in Sendust", *Acta Metall.*, **2**, 887-888 (1954), doi:10.1016/0001-6160(54)90045-0 (Crystal Structure, Experimental, *, 5)

[1955Arm] Armand, M., "Liquation and Equilibrium Diagram: Applications to the Diagram of Aluminium-Iron-Silicon Alloys" (in French), in *Congress International de l'Aluminium, Revue de l'Aluminium*, **1**, 305-327 (1955) (Crystal Structure, Experimental, *, 9)

[1958Tay] Taylor, A., Jones, R.M., "Constitution and Magnetic Properties of Iron-Rich Iron-Aluminium Alloys", J. Phys. Chem. Solids, **6**, 16-37 (1958), doi:10.1016/0022-3697(58)90213-0 (Crystal Structure, Experimental, Magnetic Properties, Phase Diagram, 49)

[1959Phi] Phillips, H.W.L., "*Annoted Equilibrium Diagrams of Some Al Alloy Systems*", Monograph, Inst. of Met., London, (25), 57-65 (1959) (Phase Diagram, Review, #, *, 18)

[1960Aro] Aronsson, B., "A Note on the Compositions and Crystal Structures of MnB_2, Mn_3Si, Mn_5Si_3 and $FeSi_2$", *Acta Chem. Scand.*, **14**(6), 1414-1418 (1960), doi:10.3891/acta.chem.scand.14-1414 (Crystal Structure, Phase Relations, 15)

[1960Voz] Vozdvizhenskiy, V.M., "The Effect on the Saturation of Solid Solution in Some Al Alloys" (in Russian), *Izv. Vyss. Uchebn. Zaved. Tsvetn. Metall.*, (5), 116-120 (1960) (Phase Diagram, 19)

[1961Sab] Sabirzyanev, A.V., Shumilov, M.A., Geld, P.V., Ozhogikhina, G.V., "Solubility of Al in α-Leoboite", *Phys. Met. Metallogr.*, **12**(5), 81-87 (1961), translated from *Fiz. Met. Metalloved.*, **12**, 714-721 (1961) (Crystal Structure, Experimental, 14)

[1963Wat] Watanabe, H., Yamamoto, H., Ito, K., "Neutron Diffraction Study of Intermetallic Compound FeSi", *J. Phys. Soc. Jpn.*, **18**, 995-999 (1963), doi:10.1143/JPSJ.18.995 (Crystal Structure, Experimental, 10)

[1965Sab] Sabirzyanev, A.V., Shumilov, M.A., "The Solubility of Al and P in Constituents of High-Si Ferrosilicon" (in Russian), *Tr. Ural'sk Politekhn. Inst.*, (144), 35-40 (1965) (Experimental, 14)

[1965Skr] Skripova, E.A., Letun, G.M., "The Solubility of Al in α-Leboite" (in Russian), *Tr. Ural'sk Politekhn. Inst.*, (144), 67-70 (1965) (Crystal Structure, Experimental, 4)

[1965Wal] Walford, L.K., "The Structure of the Intermetallic Phase $FeAl_6$", *Acta Crystallogr.*, **18**, 287-291 (1965), doi:10.1107/S0365110X65000610 (Crystal Structure, Experimental, 13)

[1967Mun] Munson, D., "A Clarification of the Phases Occurring in Aluminium Rich Aluminium-Iron-Silicon Alloys with Particular Reference to the Ternary Phase α-AlFeSi", *J. Inst. Met.*, **95**, 217-219 (1967) (Crystal Structure, Phase Diagram, Experimental, *, 12)

[1967Sun] Sun, C.Y., Mondolfo, L.F., "A Clarification of the Phases Occurring in Al Rich Al-Fe-Si Alloys", *J. Inst. Met.*, **95**, 384 (1967) (Crystal Structure, Experimental, *, 2)

[1968Aru1] Arutyunyan, S.V., Selissky, Ya.P., "The Question of Superstructure in Fe-Si-Al Alloys" (in Russian), *Izv. Akad. Nauk. Arm. SSR, Fiz.*, **3**, 8-11 (1968) (Crystal Structure, Experimental, 5)

[1968Aru2] Arutyunyan, S.V., "Some Features of Atomic Ordering in Ternary Fe-Si-Al Alloys" (in Russian), *Izv. Akad. Nauk Arm. SSR, Fiz.*, **3**, 294-297 (1968) (Crystal Structure, Experimental, 2)

[1968Dri] Drits, M.E., Kadaner, E.S., Turkina, N.I., "The System Al-Fe-Si" in "*Diagrammy Sostoyaniya Metallich. Sistem*" (in Russian), Publ. Nauka, Moscow, **XIV**, 109 (1968) (Phase Diagram, Review, 1)

[1968Lih] Lihl, F., Burger, R., Sturm, F., Ebel, H., "Constitution of Fe Rich Ternary Al-Fe-Si Alloys" (in German), *Arch. Eisenhuettenwes.*, **39**, 877-880 (1968) (Phase Diagram, Experimental, *, 22)

[1968Sab1] Sabirzyanev, A.V., Geld, V.P., "Some Features of the Peritectoid Transformation in β-Leboite ($FeSi_2$) Alloys Alloyed with Al, Ca and P" (in Russian), *Tr. Ural'sk Politekhn. Inst.*, (167), 75-80 (1968) (Experimental, 6)

[1968Sab2] Sabirzyanev, A.V., Geld, V.P., "Nature of Solid Solutions of Aluminium and Phosphorus in Iron Monosilicide" (in Russian), *Izv. Vyss. Uchebn. Zaved. Chern. Metall.*, **11**, 21-26 (1968) (Experimental, 3)

[1969Bed] Bedon., P., Ansara, I., Desre, P., "Isothermal Sections at 1900 K of the Silver - Aluminium - Iron - Silicon and Silver - Aluminium - Nickel - Silicon Metallic Systems, Activity of Aluminium in Molten

Aluminium - Iron - Silver - Silicon and Aluminium - Nickel - Silver Alloys" (in French), *Mem. Sci. Rev. Metall.*, **66**, 907-913 (1969) (Experimental, Thermodynamics, 5)

[1969Pan] Panday, P.K., Schubert, K., "Structure Studies in Some Alloys T-B^3-B^4 (T = Mn, Fe, Co, Ir, Ni, Pd, B^4 = Si, Ge)" (in German), *J. Less-Common Met.*, **18**, 175-202 (1969), doi:10.1016/0022-5088(69)90157-X (Crystal Structure, Experimental, *, 32)

[1969Pol] Polishchuk, V.E., Selissky, YA.P., "High-Temperature Study of the Structure and Electrical Properties of the Fe-Si-Al System" (in Russian), *Ukrain. Fiz. Zhur.*, **14**, 1722-1724 (1969) (Phase Diagram, Experimental, #, *, 9)

[1970Aru] Arutyunyan, S.V., "Transition from Atomic Ordering to Disordering in Fe_3(Al,Si) Alloys Related to the Formation of the K-Effect" (in Russian), *Izv. Akad. Nauk Arm. SSR, Ser. Tekh. Nauk*, **32**, 36-42 (1970) (Crystal Structure, Experimental, 4)

[1970Mit] Mitani, H., Nagai, H., Ohtani, T., "Dry Refining of Aluminium. IV. Activity Measurements of the Ternary Liquid Al-Fe-Si System by the EMF Method" (in Japanese), *Nippon Kinzoku Gakkaishi*, **34**, 165-170 (1970) (Experimental, Thermodynamics, 16)

[1971Gle] Glezer, A.M., Molotilov, B.V., Polishchuk, V.Ye., Selissky, Ya.P., "X-ray and Electron Microscopic Analysis of the Fine Structure of Ordering High-Fe-Al-Si Alloys", *Phys. Met. Metallogr.*, **32**(4), 39-47 (1971), translated from *Fiz. Met. Metalloved.*, **32**, 713-722 (1971) (Experimental, 19)

[1972Ere] Eremenko, V.N., Natanzon, Ya.V., Ryabov, V.R., Dzykovich, I.Ya., "Interaction of Al-Si Melts with Steel" (in Russian), *Liteinoe Proizod.*, (2), 21-22 (1972) (Experimental)

[1973Kat] Katsnelson, A.A., Polishchuk, V.Ye., "Energy Characteristics of Atomic Ordering in Alloys of Iron with Aluminium and Silicon", *Phys. Met. Metallogr.*, **36**(2), 86-90 (1972), translated from *Fiz. Met. Metalloved.*, **36**, 321-325 (1973) (Phase Diagram, Experimental, #, *, 10)

[1973Nag] Nagai, H., Mitani, H., "Activity Measurements of the Ternary Liquid Al-Si-Fe System by the EMF Method", *Trans. Jpn. Inst. Met.*, **14**, 130-134 (1973) (Experimental, Thermodynamics, 9)

[1973Per] Perkins, J., Desre, P., "Determination of Activities in the Al-Fe-Si System by a EMF Method" (in French), *Rev. Int. Hautes Temp. Refract.*, **10**, 79-84 (1973) (Experimental, Thermodynamics, 13)

[1974Mur] Murav'eva, A.A., German, N.V., Zarechnyuk, O.S., Gladyshevskii, E.I., "Ternary Compounds of the Fe-Al-Si System" (in Russian), *Proc. Second All-Union Conf. Crystal Chem. Intermet. Compd.*, L'vov, October, 35-36 (1974) (Crystal Structure, Experimental, *)

[1976Ber] Bergner, R.L., Rao, V.U.S., Sanker, S.G., "Superconducting and Magnetic Properties of $V_{3-x}Fe_xSi$ and $V_{3-x}Mn_xSi$", *Magntsm. and Magn. Mat., AIP, New York*, **29**(1), 325-326 (1976), doi:10.1063/1.30648 (Crystal Structure, Experimental, Magnetic Properties, Superconductivity, 4)

[1977Kud] Kudielka, H., "Crystal-structure of Fe_2Si, its Relationship to Ordered Structures of α-(Fe, Si) Mixed-Crystal and to Fe_5Se_3 Structure" (in German), *Z. Kristallogr.*, **145**(3), 177-189 (1977) (Crystal Structure, Experimental, 16)

[1977Nic1] Niculescu, V., Raj, K., Burch, T., Budnick, J.J., "Hyperfine Interactions and Structural Disorder of $Fe_2Si_{1-x}Al_x$ Alloys", *J. Phys. F, Met. Phys.*, **7**, L73-L76 (1977), doi:10.1088/0305-4608/7/3/004 (Crystal Structure, Experimental, 7)

[1977Nic2] Niculescu, V., Budnick, J.J., "Limits of Solubility, Magnetic Properties and Electron Concentration in $Fe_{3-x}T_xSi$ System", *Solid State Commun.*, **24**, 631-634 (1977), doi:10.1016/0038-1098(77)90378-7 (Crystal Structure, Experimental, Magnetic Properties, 17)

[1977Suw] Suwalski, J., Drabowski, L., Piekoszewski, J., Tucholski, Z., "Study of Order-Disorder Transformation in Fe-Al-Si Alloys by Mössbauer Spectroscopy", *Phys. Status Sol. (A)*, **41**, 191-195 (1977), doi:10.1002/pssa.2210410123 (Experimental, Crystal Structure, Phase Relations, 15)

[1978Suz] Suzuki, H., Kanno, M., Tanabe, H., Itoi, K., "The Effect of Si or Mg Addition on the Metastable to Stable Phase Changes in an Al-0.5% Fe Alloy" (in Japanese), *J. Jpn. Inst. Light Met.*, **28**, 558-565 (1978) (Crystal Structure, Experimental, 7)

[1978Xu] Xu, W.-C., Su, X.-J., "An Investigation on the Structure of Fe-Si-Al Alloy" (in Chinese), *Acta Phys. Sin.*, **27**, 576-582 (1978) (Crystal Structure, Experimental, *, 9)

[1979Bur] Burch, T.J., Raj, K., Jena, P., Budnick, J.I., Niculescu, V., Muir, W.B., "Hyperfine-field Distribution in $Fe_3Si_{1-x}Al_x$ Alloys and a Theoretical Interpretation", *Phys. Rev. B: Solid State*, **19**, 2933-2938 (1979) (Experimental, Theory, 17)

[1979Cow] Cowdery, J.S., Kayser, F.X., "Lattice Parameters of Ferromagnetic $D0_3$-Structured Iron-Aluminium-Silicon Alloys", *Mater. Res. Bull.*, **14**, 91-99 (1979), doi:10.1016/0025-5408(79)90236-8 (Crystal Structure, Experimental, *, 24)

[1980Sud] Sudavsova, V.S., Batalin, G.I., "Aluminium Activity in Liquid Iron Alloys" (in Russian), *Ukr. Khim. Zh.*, **46**, 268-270 (1980) (Experimental, Thermodynamics, 8)

[1981Riv] Rivlin, V.G., Raynor, G.V., "Phase Equilibria in Iron Ternary Alloys 4: Critical Evaluation of Constitution of Aluminium-Iron-Silicon System", *Int. Met. Rev.*, **26**, 133-152 (1981) (Phase Diagram, Review, 56)

[1981Wat] Watanabe, H., Sato, E., "Phase Diagram in Aluminium Alloys" (in Japanese), *J. Jpn. Inst. Light Met.*, **31**, 64-79 (1981) (Phase Diagram, Review, 22)

[1981Zar] Zarechnyuk, O.S., German, N.V., Yanson, T.I., Rykhal, R.M., Murav'eva, A.A., "Some Phase Diagrams of Aluminium with Transition Metals, Rare Earth Metals and Silicon" (in Russian), *Faz. Ravnoves. Metall. Splav.*, Nauka, Moscow, 1981, 69-71 (1981) (Crystal Structure, Phase Diagram, Experimental, *, 5)

[1982Cha] Chang, Y.J., "An Electron Microscopic Investigation of Order-Disorder Transformation in a Fe-Si-Al (SENDUST) Alloy and Its Dislocation Configurations", *Acta Metall.*, **30**, 1185-1192 (1982), doi:10.1016/0001-6160(82)90012-8 (Crystal Structure, Experimental, 17)

[1982Kub] Kubaschewski, O., "Iron-Aluminium" and "Iron-Silicon" in "*Iron-binary Phase Diagrams*", Springer Verlag, Berlin, 5-9 and 136-139 (1982) (Phase Diagram, Review, #, *, 26, 23)

[1982Miy] Miyazaki, T., Tsuzuki, T., Kozakai, T., Fujimoto, Y., "Phase Separation of Fe-Si-Al Ordering Alloys" (in Japanese), *Nippon Kinzoku Gakkai-Si* (*J. Jpn. Inst. Met.*), **46**, 1111-1119 (1982), doi:10.2320/jinstmet1952.46.12_1111 (Crystal Structure, Experimental, #, *, 37)

[1983Gle] Glezer, A.M., Molotilov, B.V., Prokoshin, A.F., Sosnin, V.V., "Structural Features of a SENDUST (Fe-Si-Al) Alloy Obtained by Quenching from the Melt. I. The Study of Atomic Ordering Properties", *Phys. Met. Metallogr.*, **56**(4), 110-117 (1983), translated from *Fiz. Met. Metalloved.*, **56**, 750-757 (1983) (Crystal Structure, Experimental, *, 12)

[1983Per] Perepezko, J.H., Boettinger, J.W., "Use of Metastable Phase Diagrams in Rapid Solidification", in *Alloy Phase Diagrams*, Proc. Mater. Soc. Symp., **19**, 223-240 (1983) (Review, Theory, 52)

[1983Sch] Schneeweiss, O., Zemcik, T., Zak, T., Mager, S., "Atomic Structure and Magnetic Properties of the Pseudobinary Alloys $Fe_3(Al,Si)$", *Phys. Status Solidi (a)*, **79**, 125-129 (1983), doi:10.1002/pssa.2210790113 (Crystal Structure, Magnetic Properties, Experimental, 10)

[1984Ber] Berecz, E., Bader, I., Weberner, Kovacs, E., Hovath, J., Szina, G., "Thermodynamic Examination of Aluminium Alloys by the Electrochemical Method", (in Hungarian), *Banyasz. Kohasz. Lapok*, **117**, 413-417 (1984) (Experimental, Thermodynamics, 10)

[1984Don] Dons, A.L., "AlFeSi-Particles in Commercial Pure Aluminium", *Z. Metallkd.*, **75**, 170-174 (1984), doi:10.1515/ijmr-1984-750210 (Phase Diagram, Experimental, *, 10)

[1984Mat] Matsumura, S., Sonobe, A, Oki, K., Eguchi, T., "Ordering with Phase Separation in an Fe-Al-Si Alloy", in *Phase Transformations in Solids*, Proc. Conf. Materials Research Society, Elsevier, Amsterdam, **Vol. 21**, 269-274 (1984) (Crystal Structure, Experimental, Phase Relations, *, 12)

[1985Cao] Cao, R., Li, G., Wu, X., "Some Thermodynamic Properties in Process of Thermal Reduction of Magnesium with High Aluminium Alloy" (in Chinese), *Acta Metall. Sin.*, **21**, A471-A476 (1985) (Experimental, Thermodynamics, 9)

[1985Riv] Rivlin, V.G., "Assessment of Phase Equilibria in Ternary Alloys of Iron", *J. Less-Common Met.*, **114**, 111-121 (1985), doi:10.1016/0022-5088(85)90395-9 (Phase Diagram, Review, *, 4)

[1986Miy] Miyazaki, T., Kozaki, T., Tsuzuki, T., "Phase Decomposition of Fe-Si-Al Ordered Alloys", *J. Mater. Sci.*, **21**, 2557-2564 (1986), doi:10.1007/BF01114307 (Phase Diagram, Experimental, #, *, 26)

[1986Tak] Takahashi, M., Arai, H., Tanaka, T, Wakiyama, T., "Magnetocrystalline Anisotropy for Fe-Al-Si (SENDUST) Single-Crystals with $D0_3$ Ordered Structure", *IEEE Trans. Magnetics*, **22**, 638-640 (1986), doi:10.1109/TMAG.1986.1064587 (Crystal Structure, Experimental, 7)

[1987Dob] Dobrzynski, L., Giebultowicz, T., Kopcewicz, M., Piotrowski, M., Szymanski, K., "Neutron and Mössbauer Studies of $Fe_{3-x}Al_xSi$ Alloys", *Phys. Status Solidi (A)*, **101**, 567-575 (1987), doi:10.1002/pssa.2211010232 (Crystal Structure, Experimental, 24)

[1987For] Fortnum, R.T., Mikkola, D.E., "Effects of Molybdenum, Titanium and Silicon Additions on The $D0_3$ Reversible $B2$ Transition-Temperature for Alloys Near Fe_3Al", *Mater. Sci. Eng.*, **91**, 223-231 (1987), doi:10.1016/0025-5416(87)90301-6 (Crystal Structure, Experimental, 37)

[1987Gri1] Griger, A., Lendrai, A., Stefaniay, V., Turmezey, T., "On the Phase Diagrams of the Al-Fe and Al-Fe-Si Systems", *Mater. Sci. Forum*, **13/14**, 331-336 (1987) (Phase Diagram, Experimental, 9)

[1987Gri2] Griger, A., "Powder Data for the α_H Intermetallic Phases with Slight Variation in Composition in the System Al-Fe-Si", *Powder Diffr.*, **2**, 31-35 (1987) (Crystal Structure, Experimental, *, 21)

[1987Pri] Prince, A., "Comment on Intermetallic Phases in the Al-side of the AlFeSi-Alloy System", *J. Mater. Sci. Lett.*, **6**, 1364 (1987), doi:10.1007/BF01794621 (Phase Diagram, Theory, 1)

[1987Skj1] Skjerpe, P., "Intermetallic Phases Formed During DC-Casting of an Al-0.25 wt% Fe-0.13 wt% Si Alloy", *Metall. Trans. A*, **18A**, 189-200 (1987) (Crystal Structure, Experimental, 35)

[1987Skj2] Skjerpe, P., Gjonnes, J., "Solidification Structure and Primary Al-Fe-Si Particles in Direct-Chilled-Cast Aluminum Alloys", *Ultramicroscopy*, **22**, 239-250 (1987), doi:10.1016/0304-3991(87)90068-4 (Crystal Structure, Experimental, 21)

[1987Skj3] Skjerpe, P., "An Electron Microscopy Study on the Phase Al_3Fe", *J. Microscopy*, **148**, 33-50 (1987) (Crystal Structure, Experimental, Theory, 12)

[1987Ste] Stefaniay, V., Griger, A., Turmezey, T., "Intermetallic Phases in the Aluminium-side Corner of the AlFeSi-alloy System", *J. Mater. Sci.*, **22**, 539-546 (1987), doi:10.1007/BF01160766 (Crystal Structure, Phase Diagram, Experimental, *, 13)

[1987Tak1] Takahashi, M., Arai, H., Wakiyama, T., "Magnetostriction of Fe-Al-Si Sputtered Thin-Films", *IEEE Trans. Magnetics*, **23**, 3068-3070 (1987), doi:10.1109/TMAG.1987.1065420 (Experimental, 9)

[1987Tak2] Takahashi, M., Arai, H., Wakiyama, T., "Magnetostriction Constants for Fe-Al-Si (SENDUST) Single-Crystals with $D0_3$ Ordered Structure", *IEEE Trans. Magnetics*, **23**, 3523-3525 (1987), doi:10.1109/TMAG.1987.1065759 (Experimental, Magnetic Properties, 5)

[1988Dor] Dorofeyeva, Ye.A., Sasnin, Y.V., Stolokotniy, V.L., "Cross-Relaxation of Magnetic Permeability in Alloy FeSiAl", *Phys. Met. Metallogr.*, **65**(3), 172-174 (1988) (Experimental, 2).

[1988Ray] Raynor, G.V., Rivlin, V.G., "Al-Fe-Si", in "*Phase Equilibria in Iron Ternary Alloys*", Institute of Metals, London, 122-139 (1988) (Phase Diagram, Review, 39)

[1988Zak] Zakharov, A.M., Gulman, I.T., Arnold, A.A., Matsenko, Yu.A., "Phase Diagram of the Aluminium-Silicon-Iron System in the Concentration Range of 10-14% Si and 0-3% Fe", *Russ. Metall.*, (3), 177-180 (1988), translated from *Izv. Akad. Nauk SSSR, Met.*, (3), 178-181 (1988) (Phase Diagram, Experimental, 8)

[1989Bon] Bonnet, M., Rogez, J., Castanet, R., "EMF Investigation of Al-Si, Al-Fe-Si and Al-Ni-Si Liquid Alloys", *Thermochim. Acta*, **155**, 39-56 (1989), doi:10.1016/0040-6031(89)87134-5 (Experimental, Thermodynamics, 15)

[1989Ger1] German, N.V., Bel`skii, V.K., Yanson, T.I., Zarechnyuk, O.S., "Crystal Structure of the Compound $Fe_{1.7}Al_4Si$", *Sov. Phys. Crystallogr.*, **34**(3), 437-438 (1989) (Crystal Structure, Experimental, 5)

[1989Ger2] German, N.V., Zavodnik, V.E., Yanson, T.I., Zarechnyuk, O.S., "Crystal Structure of $FeAl_2Si$", *Sov. Phys. Crystallogr.*, **34**(3), 439-440 (1989) (Crystal Structure, Experimental, 5)

[1991Fuk] Fukaya, M., Miyazaki, T., Kozakai, T., "Phase Diagrams Calculated for Fe Rich Fe-Si-Co and Fe-Si-Al Ordering Systems", *J. Mater. Sci.*, **26**(2), 5420-5426 (1991), doi:10.1007/BF02403939 (Calculation, Phase Relations, 42)

[1991Ger] German, N.V., Zarechnyuk, O.S., Ventskobskyy, O.V., Yanson, T.I., Lysogub, V.O., Manyako, M.B., "Crystal Structure of the Compound $FeAl_{2.4}Si_{0.6}$", *Visn. Lviv. Derz. Univ., Ser. Khim.*, **31**, 8-10 (1991) (Crystal Structure, Experimental) as quoted by [2022Mar]

[1992Gho] Ghosh, G., "Al-Fe-Si Ternary Phase Diagram Evaluation", in *MSI Eureka*, Effenberg, G. (Ed.), MSI, Materials Science International Services GmbH, Stuttgart (1992), Document ID: 10.14596.1.7 (Crystal Structure, Phase Diagram, Phase Relations, Assessment, 138)

[1992Zak] Zakharov, A.M., Guldin, I.T., Arnold, A.A., Matsenko, Yu.A., "Phase Equilibria in Multicomponent Aluminum Systems with Copper, Iron, Silicon, Manganese and Titanium" (in Russian), *Metalloved. Obrab. Tsvetn. Splavov*: *To 90th Anniversary of Academician A.A. Bochvar Birthday*. RAN. Inst. Metallurg., Moscow, 6-17 (1992) (Phase Diagram, Experimental, 14)

[1993Kat] Kattner, U.R., Burton, B.P., "Al-Fe (Aluminum-Iron)" in "*Phase Diagrams of Binary Iron Alloys*", Okamoto, H. (Eds.), Mater. Park OH: ASM Int., 12-28 (1993) (Crystal Structure, Electrical Properties, Magnetic Properties, Mössbauer, Phase Diagram, Review, Thermodynamics, 99)

[1993Sch] Schröer, W., Hartig, C., Mecking, H., "Plasticity of $D0_3$-ordered Fe-Al and Fe-Al-Si Single-Crystals", *Z. Metallkd.*, **84**(5), 294-300 (1993) (Phase Relations, Experimental, 30)

[1994Ang] Anglezio, J.C., Servant, C., Ansara, I., "Contribution to the Experimental and Thermodynamic Assessment of the Al-Ca-Fe-Si System - I. Al-Ca-Fe, Al-Ca-Si, Al-Fe-Si and Ca-Fe-Si Systems", *Calphad*, **18**(3), 273-309 (1994), doi:10.1016/0364-5916(94)90034-5 (Calculation, Phase Diagram, Phase Relations, Thermodynamics, 71)

[1994Bur] Burkhardt, U., Grin, J., Ellner, M., Peters, K., "Structure Refinement of the Iron-Aluminium Phase with the Approximate Composition Fe_2Al_5", *Acta Crystallogr., Sect. B: Struct. Crystallogr. Crys. Chem.*, **B50**, 313-316 (1994), doi:10.1107/S0108768193013989 (Crystal Structure, Experimental, 9)

[1994Koz] Kozakai, T., Miyazaki, T., "Experimental And Theoretical Investigations on Phase Diagrams of Fe Base Ternary Ordering Alloys", *ISIJ Int.*, **34**(5), 373-383 (1994), doi:10.2355/isijinternational.34.373 (Calculation, Phase Diagram, Magn. Prop., 18)

[1994Rag] Raghavan, V., "The Al-Fe-Si System", *J. Phase Equilib.*, **15**(4), 414-416 (1994), doi:10.1007/BF02647566 (Phase Diagram, Review, 27)

[1994Rom] Romming, Chr., Hansen, V., Gjonnes, J., "Crystal Structure of β-$Al_{4.5}FeSi$", *Acta Crystallogr., Sect. B: Struct. Crystallogr. Crys. Chem.*, **B50**(3), 307-312 (1994), doi:10.1107/S0108768193013096 (Crystal Structure, Experimental, 10)

[1995Bel] Belov, N.A., "Analysis of Nonequilibrium Solidification of Subeutectic Sillumines Using Multicomponent Phase Diagrams", *Russ. Metall.* (Engl. Transl.), (1), 41-47 (1995) (Phase Relations, Experimental, 5)

[1995Gue1] Gueneau, C., Servant, C., D'Yvoire, F., Rodier, N., "$FeAl_3Si_2$", *Acta Crystallogr., Sect. C: Cryst. Struct. Commun.*, **C51**, 177-179 (1995), doi:10.1107/S0108270194009030 (Crystal Structure, Experimental, 9)

[1995Gue2] Gueneau, C., Servant, C., "$Fe_2Al_3Si_3$", *Acta Crystallogr., Sect. C: Cryst. Struct. Commun.*, **C51**, 2461-2464 (1995), doi:10.1107/S0108270195007864 (Crystal Structure, Experimental, 8)

[1995Gue3] Gueneau, C., Servant, C., Ansara, I., "Experimental and Thermodynamic Assessments of Substitutions in the AlFeSi, FeMnSi, FeSiZr and AlCaFeSi Systems", *Appl. Thermodyn. Synth. Procee. Mater.*, Proc. Symp., Nash, P., Sundman, B., (Eds.), The Minerals, Metals and Materials Society, Warrendale, Pa, 303-317 (1995) (Experimental, Theory, 19)

[1996All] Allen, C.M., O'Reilly, K.A.Q., Cantor, B., Evans, P.V., "Nucleation of Phases in Al-Fe-Si Alloys", *Mater. Sci. Forum*, **217-222**, 679-684 (1996), doi:10.4028/www.scientific.net/MSF.217-222.679 (Calculation, Phase Relations, 14)

[1996Cho] Choi, Y., Ra, H., "Microstructure of Gas Atomized Al-Fe-Si Alloy Powders" (in Korean), *J. Korean Inst. Met.*, **34**(2), 230-235 (1996) (Experimental, 11)

[1996Fri] Friemelt, K., Ditusa, J.F., Bucher, E., Aeppli, G., "Coulomb Interactions in Al Doped FeSi at Low Temperatures", *Ann. Physik-Leipzig*, **5**(2), 175-183 (1996) (Crystal Structure, Experimental, 25)

[1996Mor] Morris, D.G., Gunther, S., "Order-Disorder Changes in Fe_3Al Based Alloys and the Development of an Iron-Base α-α`` Superalloy", *Acta Mater.*, **44**(7), 2847-2859 (1996), doi:10.1016/1359-6454(95)00382-7 (Crystal Structure, Phase Relations, Experimental, 23)

[1996Szy] Szymanski, K., Baas, J., Dobrzynski, L., Satula, D., "Magnetic and Mössbauer Investigation of $FeSi_{2-x}Al_x$", *Physica B (Amsterdam)*, **225**, 111-120 (1996), doi:10.1016/0921-4526(96)00236-0 (Crystal Structure, Experimental, 20)

[1996Yan] Yanson, T.I., Manyako, M.B., Bodak, O.I., German, N.V., Zarechnyuk, O.S., Cerny, R., Pacheko, J.V., Yvon, K., "Triclinic $Fe_3Al_2Si_3$ and Orthorhombic $Fe_3Al_2Si_4$ with New Structure Types", *Acta Crystallogr., Sect. C: Cryst. Struct. Commun.*, **C52**, 2964-2967 (1996), doi:10.1107/S0108270196008694 (Crystal Structure, Experimental, 15)

[1997All] Allen, C.M., O`Reilly, K.A.Q., Cantor, B., Evans, P.V., "Heterogeneous Nucleation of Solidification of Equilibrium and Metastable Phases in Melt-Spun Al-Fe-Si Alloys", *Mater. Sci. Eng. A*, **A226-228**, 784-788 (1997) (Experimental, Phys. Prop., 10)

[1997Can] Cantor, B., "Impurity Effects on Heterogenous Nucleation", *Mater. Sci. Eng. A*, **A226-228**, 151-156 (1997) (Crystal Structure, Experimental, 38)

[1997Sto] Stone, I.C., Jones, H., "Effect of Cooling Rate and Front Velosity on Solidification Microstructure Selection in Al-3.5wt.%Fe-0 to 8.5wt.%Si Alloys", *Mater. Sci. Eng. A*, **A226-228**, 33-37 (1997) (Phase Relations, Experimental, 10)

[1997Vyb] Vybornov, M., Rogl, P., Sommer, F., "The Thermodynamic Stability and Solid Solution Behavior of the Phases τ_5-$Fe_2Al_{7.4}Si$ and τ_6-$Fe_2Al_9Si_2$", *J. Alloys Compd.*, **247**, 154-157 (1997), doi:10.1016/S0925-8388(96)02602-3 (Crystal Structure, Phase Relations, Experimental, 7)

[1998Akd] Akdeniz, M.V., Mekhrabov, A.O., "The Effect of Substitutional Impurities on the Evolution of Fe-Al Diffusion Layer", *Acta Mater.*, **46**(4), 1185-1192 (1998) (Calculation, Thermodynamics, 55)

[1998Dit] Ditusa, J.F., Friemelt, K., Bucher, E., Aeppli, G., Ramirez, A.P., "Heavy Fermion Metal-Kondo Insulator Transition in $FeSi_{1-x}Al_x$", *Phys. Rev. B*, **58**(16), 10288-10301 (1998) (Crystal Structure, Experimental)

[1998Han] Hansen, V., Hauback, B., Sundberg, M., Romming, Ch., Gjonnes, J., "A Combined Synchrotron Powder Diffraction, Electron Diffraction, High-Resolution Electron Microscopy and Single-Crystal X-ray Diffraction Study of a Faulted Structure", *Acta Crystallogr.*, **54B**, 351-357 (1998) (Crystal Structure, Experimental, 7)

[1998Kol] Kolby, P., "System Al-Fe-Si" in "*COST 507, Thermochemical Database for Light Metal Alloys*", **Vol. 2**, Ansara, I., Dinsdale, A.T., Rand, M.H. (Eds.), Office for official publications of the European Communities, Luxembourg, 1998, ISBN 92-828-3902-8, 319-321 (Assessment, Thermodynamics)

[1999Liu] Liu, Z.-K., Chang, A., "Thermodynamic Assessment of the Al-Fe-Si System", *Metall. Mater. Trans. A.*, **30A**(7), 1081-1095 (1999), doi:10.1007/s11661-999-0160-3 (Calculation, Phase Diagram, Phase Relations, Thermodynamics, 56)

[1999Oht] Ohta, Y., Miura, S., Mishima, Y., "Thermoelectric Semiconductor Iron Disilicides Produced by Sintering Elemental Powders", *Intermetallics*, **7**, 1203-1210 (1999) (Phase Relations, Experimental, Transport Phenomena, 19)

[1999Tay] Taylor, J.A., Schaffer, G.B., St. John, D.H., "The Role of Iron in the Formation of Porosity in Al-Si-Cu-Based Casting Alloys: Part II. A Phase-Diagram Approach", *Metall. Mater. Trans. A*, **30A**, 1651-1655 (1999) (Calculation, Crystal Structure, Experimental, 12)

[2000Bha] Bhattamishra, A.K., Chattoraj, I., Basu, D.K., De, P.K., "Study on the Influence of the Si/Fe Ratio on the Corrosion Behavior of Some Al-Fe-Si Alloys", *Z. Metallkd.*, **91**(5), 393-396 (2000) (Interface Phenomena, Experimental, 23)

[2000Li1] Li, Y., Ochin, P., Quivy, A., Telolahy, P., Legendre, B., "Enthalpy of Formation of Al-Fe-Si Alloys (τ_5, τ_{10}, τ_1, τ_9)", *J. Alloys Compd.*, **298**, 198-202 (2000), doi:10.1016/S0925-8388(99)00657-X (Experimental, Thermodynamics, 20)

[2000Li2] Li, Y., Legendre, B., "Enthalpy of Formation of Al-Fe-Si Alloys II (τ_6, τ_2, τ_3, τ_8, τ_4)", *J. Alloys Compd.*, **302**, 187-191 (2000), doi:10.1016/S0925-8388(00)00682-4 (Experimental, Thermodynamics, 21)

[2000Sri] Sritharan, T., Murali, S., Hing, P., "Synthesis of Aluminium-Iron-Silicon Intermetallics by Reaction of Elemental Powders", *Mater. Sci. Eng. A*, **A286**, 209-217 (2000), doi:10.1016/S0921-5093(00)00823-6 (Crystal Structure, Experimental, 18)

[2000Zhe] Zheng, J.G., Vincent, R., Steeds, J.W., "Crystal Structure of an Orthorhombic Phase in β-(Al-Fe-Si) Precipitates Determined by Convergent-Beam Electron Diffraction", *Philos. Mag. A*, **80**(2), 493-500 (2000), doi:10.1080/01418610008212063 (Crystal Structure, Experimental, 11)

[2001Cho] Cho, H.S., Kim, K.S., Jeong, H.G., Yamagata, H., "Microstructure and Mechanical Properties of Extruded Rapidly Solidified Al-16Si-5Fe Based Alloys", *Key Eng. Mater.*, **189-191**, 479-483 (2001) (Experimental, Mechanical Properties, 5)

[2001Jha] Jha, R., Haworth, C.W., Argent, B.B., "The Formation of Diffusion Coatings on Some Low-Alloy Steels and Their High Temperature Oxidation Behavior: Part 1 Diffusion Coatings", *Calphad*, **25**(4), 651-665 (2001) (Calculation, Phase Diagram, Phase Relations, 9)

[2001Kre] Krendelsberger, N., "Constitution of the Systems Aluminium-Manganese-Silicon, Aluminium-Iron-Silicon, und Aluminium-Iron-Manganese-Silicon", *Thesis*, Inst. of Physical Chemistry, University of Vienna, 2001 (Crystal Structure, Phase Diagram, Experimental, #, *, 83)

[2001Sha] Sha, G., OReilly, K., Cantor, B., Worth, J., Hamerton, R., "Growth Related Metastable Phase Selection in a 6xxx Series Wrought Al Alloy", *Mater. Sci. Eng. A*, **304-306**, 612-616 (2001) (Crystal Structure, Phase Relations, Experimental, 9)

[2002Dut] Dutta, B., Rettenmayr, M., "Microsegregation and Its Effects on Quantity and Morphology of Secondary Phases During Solidification of Al-Fe-Si Alloys", *Mater. Sci. Technol.*, **18**, 1428-434 (2002) (Calculation, Experimental, Morphology, Phase Relations, 22

[2002Gup] Gupta, S.P., "Intermetallic Compound Formation in Fe-Al-Si Ternary System: Part I", *Mater. Charact.*, **49**, 269-291 (2003), doi:10.1016/S1044-5803(03)00006-8 (Experimental, Phase Relations, Phase Diagram, #, *, 22).

[2002Mai] Maitra, T., Gupta, S.P., "Intermetallic Compound Formation in Fe-Al-Si Ternary System: Part II", *Mater. Charact.*, **49**, 293-311 (2003), doi:10.1016/S1044-5803(03)00005-6 (Experimental, Phase Diagram, Phase Relations, #, *, 30)

[2002Rag] Raghavan, V., "Al-Fe-Si (Aluminium-Iron-Silicon)", *J. Phase Equilib.*, **25**(4), 107-112 (2002), doi:10.1361/105497102770331604 (Phase Diagram, Review, 24)

[2003Cie] Cieslar, M., C. Fressengeas, C., Karimi, A., Martin, J.L., "Portevin-Le Chatelier Effect in Biaxially Strained Al-Fe-Si Foils", *Scr. Mater.*, **48**, 1105-1110 (2003) (Experimental, Phase Relations, Mechanical Properties, 19)

[2003Gjo] Gjonnes, J., Hansen, V., Andersen, S.J., Marioara, C.D., Li, X.Z., "Electron Crystallography of Aluminum Alloy Phases", *Z. Kristallogr.*, **218**, 293-307 (2003), doi:10.1524/zkri.218.4.293.20745 (Crystal Structure, Review, 73)

[2003Kan] Kanibolotsky, D.S., Bieloborodova, O.A., Kotova, N.V., Lisnyak, V.V., "Enthalpy of Mixing in Liquid Al-Fe-Si Alloys at 1750 K", *Thermochim. Acta*, **408**(1-2), 1-7 (2003), doi:10.1016/S0040-6031(03)00314-9 (Experimental, Thermodynamics, *, 20)

[2003Mur] Murali, S., Sritharan, T., Hing, P., "Self-Propagating High Temperature Synthesis of AlFeSi Intermetallic Compound", *Intermetallics*, **11**(3), 279-281 (2003) (Experimental, Kinetics, Phase Relations, 10)

[2004Bos] Bosselet, F., Pontevichi, S., Sacerdote-Peronnet, M., Viala, J.C., "Refinement of Experimental Isothermal Section Al-Fe-Si at 1000 K" (in French), *J. Phys. IV, France*, **122**, 41-46 (2004), doi:10.1051/jp4:2004122050 (Experimental, Phase Diagram, Phase Relations, #, *, 21)

[2004Gho] Ghosh, G., "Al-Fe-Si Ternary Phase Diagram Evaluation", in *MSI Eureka*, Effenberg, G. (Ed.), MSI, Materials Science International Services GmbH, Stuttgart (2004), Document ID: 10.14596.2.6 (Crystal Structure, Phase Diagram, Phase Relations, Assessment, 198)

[2004Kaj] Kajihara, K., Sugizaki, Ya., Seki, Yu., "Modelling of Precipitation Behavior of Fe in Commercial Purity Aluminum" (in Japanese), *J. Japan Inst. Light Metals*, **54**(7), 273-279 (2004), doi:10.2464/jilm.54.273 (Calculation, Kinetics, Mechanical Properties, Morphology, Phase Diagram, Phase Relations, Thermodynamics, Transport Phenomena, 25)

[2004Kan] Kanibolotsky, D.S., Stukalo, V.S., Lisnyak, V.V., "Thermodynamic Properties of Eutectic Silumins Doped by Transition Metals", *Z. Naturforschung A.*, **59**, 288-290 (2004) (Experimental, Thermodynamics, 9)

[2004Kha] Khalifa, W., Samuel, F.H., Gruzleski, J.E., "Nucleation of Solid Aluminum on Inclusion Particles Injected into Al-Si-Fe Alloys", *Metall. Mater. Trans. A*, **35A**, 3233-3250 (2004) (Experimental, Morphology, 57)

[2004Luk] Lukas, H., Lebrun, N., "Al-Si Binary Phase Diagram Evaluation", in *MSI Eureka*, Effenberg, G. (Ed.), MSI, Materials Science International Services GmbH, Stuttgart (2004), Document ID: 20.14887.1.6 (Crystal Structure, Phase Diagram, Phase Relations, Assessment, 30)

[2004Pon1] Pontevichi, S., Bosselet, F., Peronnet, M., Viala, J.C., "Thermostability of β-Al5FeSi in the Al-Fe-Si Ternary System", *J. Phys. IV France*, **113**, 81-84 (2004) (in French) (Crystal Structure, Experimental, Morphology, Phase Diagram, Phase Relations, *, 34)

[2004Pon2] Pontevichi, S., Bosselet, F., Barbeau, F., Peronnet, M., Viala, J.C., "Solid-Liquid Phase Equilibria in the Al-Fe-Si System at 727°C", *J. Phase Equilib. Diffus.*, **25**(6), 528-537 (2004), doi:10.1007/s11669-004-0066-0 (Crystal Structure, Experimental, Morphology, Phase Diagram, Phase Relations, *, 34)

[2004Sug] Sugiyama, K., Kaji, N., Hiraga, K., "Crystal Structure of Rhombohedral λ-AlFeSi", *J. Alloys Compd.*, **368**(1-2), 251-255 (2004), doi:10.1016/j.jallcom.2003.08.065 (Crystal Structure, Experimental, Morphology, 26)

[2005Bar] Barros, J., Malengier, B., Van Keer, R., Houbaert, Y., "Modeling Silicon and Aluminum Diffusion in Electrical Steel", *J. Phase Equilib. Diffus.*, **26**(5), 417-422 (2005), doi:10.1007/s11669-005-0028-1 (Experimental, Phase Diagram, Phase Relations, 8)

[2005Kha] Khalifa, W., Samuel, F.H., Gruzleski, J.E., Doty, H.W., Valtierra, S., "Nucleation of Fe-Intermetallic Phases in the Al-Si-Fe Alloys", *Metall. Mater. Trans. A*, **36A**(4), 1017-1032 (2005) (Experimental, Morphology, Phase Relations, 40)

[2005Lu] Lu, L., Dahle, A.K., "Iron rich Intermetallic Phases and Their Role in Casting Defect Formation in Hypoeutectic Al-Si Alloys", *Metall. Mater. Trans. A*, **36A**(3), 819-835 (2005) (Crystal Structure, Experimental, Morphology, Phase Relations, 29)

[2007Gho] Ghosh, G., "Al-Fe-Si Ternary Phase Diagram Evaluation", in *MSI Eureka*, Effenberg, G. (Ed.), MSI, Materials Science International Services GmbH, Stuttgart (2007), Document ID: 10.14596.3.5 (Crystal Structure, Phase Diagram, Phase Relations, Assessment, 224)

[2007Kre] Krendelsberger, N., Weitzer, F., Schuster, J.C., "On the Reaction Scheme and Liquidus Surface in the Ternary System Al-Fe-Si", *Metall. Mater. Trans. A*, **38**(7), 1681-1691 (2007), doi:10.1007/s11661-007-9182-x (Crystal Structure, Experimental, Phase Diagram, #, *, 35)

[2007Ste] Stein, F., Palm, M., "Re-Determination of Transition Temperatures in the Fe-Al System by Differential Thermal Analysis", *Int. J. Mater. Res.* (*Z. Metallkd.*), **98**(7), 580-588 (2007), doi:10.3139/146.101512 (Experimental, Phase Diagram, Phase Relations, *, 59)

[2008Du] Du, Y., Schuster, J.C., Liu, Z.-H., Hu, R., Nash, P., Sun, W., Zhang, W., Wang, J., Zhang, L., Tang, C., Zhu, Z., Liu, S., Ouyang, Y., Zhang, W., Krendelsberger, N., "A Thermodynamic Description of the Al-Fe-Si System over the Whole Composition and Temperature Ranges *via* a

Hybrid Approach of CALPHAD and Key Experiments", *Intermetallics*, **16**(4), 554-570 (2008), doi:10.1016/j.intermet.2008.01.003 (Experimental, Phase Diagram, Thermodynamics, 49)

[2008Gil] Gille, P., Bauer, B., "Single Crystal Growth of $Al_{13}Co_4$ and $Al_{13}Fe_4$ from Al-Rich Solutions by the Czochralski Method", *Cryst. Res. Technol.*, **43**(11), 1161-1167 (2008), doi:10.1002/crat.200800340 (Crystal Structure, Experimental, Morphology, Phase Relations, Theory, 17)

[2008Heg] Hegde, S., Prabhu, K.N., "Modification of Eutectic Silicon in Al-Si Alloys", *J. Mater. Sci.*, **43**(9), 3009-3027 (2008), doi:10.1007/s10853-008-2505-5 (Experimental, Interface Phenomena, Morphology, Phase Relations, 93)

[2009Gom] Gomez, M., Garcia, C.I., Haezebrouck, D.M., Deardo, A.J., "Design of Composition in (Al/Si)-Alloyed TRIP Steels", *ISIJ Int.*, **49**(2), 302-311 (2009), doi:10.2355/isijinternational.49.302 (Calculation, Crystal Structure, Experimental, Kinetics, Morphology, Phase Relations, Physical Properties, 59)

[2009Rag] Raghavan, V., "Al-Fe-Si (Aluminum-Iron-Silicon)", *J. Phase Equilib. Diffus.*, **30**(2), 184-188 (2009) (Phase Diagram, Phase Relations, Review, 14)

[2009Yam] Yamane, H., Yamada, T., "Effects of Stacking Fault on the Diffraction Intensities of β-$FeSi_2$", *J. Alloys Compd.*, **476**(1-2), 282-287 (2009), doi:10.1016/j.jallcom.2008.08.078 (Crystal Structure, Experimental, 18)

[2010Chu] Chumak, I., Richter, K.W., Ehrenberg, H., "Redetermination of Iron Dialuminide, $FeAl_2$", *Acta Crystallogr., Sect. C*, **C66**, i87-i88 (2010), doi:10.1107/S0108270110033202 (Experimental, Crystal Structure, 10)

[2010Du] Du, Y., Wang, J., Ouyang, Y.F., Zhang, L.J., Yuan, Z.H., Liu, S.H., Nash, P., "An Approach to Determine Enthalpies of Formation for Ternary Compounds", *J. Min. Metall., B Metall.*, **46**(1), 1-9 (2010), doi:10.2298/JMMB1001001D (Calculation, Crystal Structure, Experimental, Thermodynamics, 29)

[2010Ele] Eleno, L., Vezely, J., Sundman, B., Cieslar, M., Lacaze, J., "Assessment of the Al Corner of the Ternary Al-Fe-Si System", *Mater. Sci. Forum*, **649**, 523-528 (2010), doi:10.4028/www.scientific.net/MSF.649.523 (Calculation, Phase Diagram, Phase Relations, Thermodynamics, #, *, 25)

[2010Fri] Friak, M., Deges, J., Krein, R., Frommeyer, G., Neugebauer, J., "Combined *Ab Initio* and Experimental Study of Structural and Elastic Properties of Fe_3Al-based Ternaries", *Intermetallics*, **18**(7), 1310-1315 (2010), doi:10.1016/j.intermet.2010.02.025 (Calculation, Crystal Structure, Electronic Structure, Experimental, Mechanical Properties, 21)

[2010Leg] Legarra, E., Apinaniz, E., Plazaola, F., "Magnetic Study of the Influence of Si/Al Substitution in Ordered $Fe_{75}Al_{25}$, $Fe_{70}Al_{30}$ and $Fe_{60}Al_{40}$", *Intermetallics*, **18**(7), 1288-1292 (2010), doi:10.1016/j.intermet.2009.11.007 (Crystal Structure, Experimental, Magnetic Properties, Phase Relations, 22)

[2010Ma] Ma, X.G., Jiang, J.J., Bie, S.W., Miao, L., Zhang, C.K., Wang, Z.Y., "Electronic Structure and Magnetism of $Fe_3Al_{1-x}Si_x$ Alloys", *Intermetallics*, **18**(12), 2399-2403 (2010), doi:10.1016/j.intermet.2010.08.031 (Calculation, Crystal Structure, Electronic Structure, 29)

[2010Mak] Maki, J., Suehiro, M., Ikematsu, Yo., "Alloying Reaction of Aluminized Steel Sheet", *ISIJ Int.*, **50**(8), 1205-1210 (2010), doi:10.2355/isijinternational.50.1205 (Calculation, Crystal Structure, Experimental, Morphology, Phase Diagram, Phase Relations, Physical Properties, 10)

[2010Mal] Malakhov, D.V., Panahi, D., Gallerneault, M., "On the Formation of Intermetallics in Rapidly Solidifying Al-Fe-Si Alloys", *Calphad*, **34**(2), 159-166 (2010), doi:10.1016/j.calphad.2010.01.006 (Calculation, Phase Diagram, Phase Relations, 17)

[2010Mor] Morishita, M., Ishida, H., Yoshida, M., "Modeling of Microsegregation and Precipitation of Iron Metallic Compounds in Al-Fe-Si Ternary Alloy" (in Japanese), *J. Japan Inst. Light Metals*, **60**(4), 157-163 (2010), doi:10.2464/jilm.60.157 (Experimental, Interface Phenomena, Kinetics, Morphology, 11)

[2010Pop] Popcevic, P., Smontara, A., Ivkov, J., Wencka, M., Komelj, M., Jeglic, P., Vrtnik, S., Bobnar, M., Jaglicic, Z., Bauer, B., Gille, P., Borrmann, H., Burkhardt, U., Grin, Yu., Dolinsek, J., "Anisotropic Physical Properties of the $Al_{13}Fe_4$ Complex Intermetallic and its Ternary Derivative $Al_{13}(Fe,Ni)_4$", *Phys. Rev. B: Condens. Matter*, **81**(18), 184203 (2010), doi:10.1103/PhysRevB.81.184203 (Crystal Structure, Electrical Properties, Experimental, Magnetic Properties, Morphology, Physical Properties, Thermodynamics, Transport Phenomena, 42)

[2010Rag] Raghavan, V., "Al-Fe-Si (Aluminum-Iron-Silicon)", *J. Phase Equilib. Diffus.*, **32**(2), 140-142 (2010), doi:10.1007/s11669-010-9823-4 (Review, Phase Diagram, Phase Relations, Thermodynamics, 25)

[2010Ste] Stein, F., Vogel, S.C., Eumann, M., Palm, M., "Determination of the Crystal Structure of the ε Phase in the Fe-Al System by High-Temperature Neutron Diffraction", *Intermetallics*, **18**(1), 150-156 (2010), doi:10.1016/j.intermet.2009.07.006 (Crystal Structure, Experimental, Morphology, Phase Relations, 40)

[2011Lee1] Lee, S., Kim, B., Lee, S., "Prediction of Solidification Paths in Al-Si-Fe Ternary System and Experimental Verification: Part II. Fe-Containing Eutectic Al-Si Alloys", *Mater. Trans.*, **52**(6), 1308-1315 (2011), doi:10.2320/matertrans.M2010423 (Calculation, Crystal Structure, Experimental, Morphology, Phase Diagram, Phase Relations, 27)

[2011Lee2] Lee, S., Kim, B., Lee, S., "Prediction of Solidification Paths in Al-Si-Fe Ternary System and Experimental Verification: Part I. Fe-Containing Hypoeutectic Al-Si Alloys", *Mater. Trans.*, **52**(5), 1053-1062 (2011), doi:10.2320/matertrans.M2010422 (Crystal Structure, Experimental, Morphology, Phase Diagram, Phase Relations, Thermodynamics, 35)

[2011Mar] Marker, M.C.J., Skolyszewska-Kühberger, B., Effenberger, H.S., Schmetterer, C., Richter, K.W., "Phase Equilibria and Structural Investigations in the System Al-Fe-Si", *Intermetallics*, **19**(12), 1919-1929 (2011), doi:10.1016/j.intermet.2011.05.003 (Crystal Structure, Experimental, Morphology, Phase Diagram, Phase Relations, #, *, 42)

[2011Rog1] Roger, J., Bosselet, F., Viala, J. C., "X-rays Structural Analysis and Thermal Stability Studies of the Ternary Compound α-AlFeSi", *J. Solid State Chem.*, **184**(5), 1120-1128 (2011), doi:10.1016/j.jssc.2011.03.025 (Crystal Structure, Experimental, Morphology, Phase Relations, 36)

[2011Rog2] Roger, J., Jeanneau, E., Viala, J.C., "Crystal Structure of the Ternary Compound γ-Al_3FeSi", *Z. Kristallogr.*, **226**(11), 805-813 (2011), doi:10.1524/zkri.2011.1423 (Crystal Structure, Experimental, 43)

[2011Spr] Springer, H., Kostka, A., Payton, E.J., Raabe, D., Kaysser-Pyzalla, A., Eggeler, G., "On the Formation and Growth of Intermetallic Phases during Interdiffusion between Low-carbon Steel and Aluminum Alloys", *Acta Mater.*, **59**(4), 1586-1600 (2011), doi:10.1016/j.actamat.2010.11.023 (Crystal Structure, Experimental, Interface Phenomena, Kinetics, Morphology, Phase Relations, 54)

[2012Leg] Legarra, E., Apinaniz, E., Plazaola, F., "Structural and Magnetic Study of Mechanically Deformed Fe Rich FeAlSi Ternary Alloys", *J. Alloys Compd.*, **536**(Sup. 1), S282-S286 (2012), doi:10.1016/j.jallcom.2011.11.030 (Crystal Structure, Experimental, Magnetic Properties, 17)

[2012Ohn] Ohnuma, I., Abe, S., Shimenouchi, S., Omori, T., Kainuma, R., Ishida, K., "Experimental and Thermodynamic Studies of the Fe-Si Binary System", *ISIJ Int.*, **52**(4), 540-548 (2012), doi:10.2355/isijinternational.52.540 (Calculation, Crystal Structure, Experimental, Interface Phenomena, Magnetic Properties, Morphology, Phase Diagram, Phase Relations, Thermodynamics, Transport Phenomena, 26)

[2012Rag] Raghavan, V., "Al-Fe-Si (Aluminum-Iron-Silicon)", *J. Phase Equilib. Diffus.*, **33**(4), 322-326 (2012), doi:10.1007/s11669-012-0067-3 (Phase Diagram, Phase Relations, Review, 15)

[2013Gho] Ghosh, G., "Al-Fe-Si Ternary Phase Diagram Evaluation", in *MSI Eureka*, Effenberg, G. (Ed.), MSI, Materials Science International Services GmbH, Stuttgart (2013), Document ID: 10.14596.4.9 (Crystal Structure, Phase Diagram, Phase Relations, Assessment, 255)

[2013Zha] Zhang, Y., Jie, J., Gao, Y.., Lu, Y., Li, T., "Effects of Ultrasonic Treatment on the Formation of Iron-Containing Intermetallic Compounds in Al-12%Si-2%Fe Alloys", *Intermetallics*, **42**, 120-125 (2013), doi:10.1016/j.intermet.2013.05.018 (Experimental, Morphology, Phase Relations, 28)

[2014Ami] Amirkhanyan, L., Weissbach, T., Gruber, T., Zienert, T., Fabrichnaya, O., Kortus, J., "Thermodynamic Investigation of the τ_4-Al-Fe-Si Intermetallic Ternary Phase: A Density-Functional Theory Study", *J. Alloys Compd.*, **598**, 137-141 (2014), doi:10.1016/j.jallcom.2014.01.234 (Calculation, Electronic Structure, Experimental, Thermodynamics)

[2014Che] Chen, H.-L., Chen, Q., Du, Y., Bratberg, J., Engström, A., "Update of Al-Fe-Si, Al-Mn-Si and Al-Fe-Mn-Si Thermodynamic Descriptions", *Trans. Nonferrous Met. Soc. China*, **24**(7), 2041-2053 (2014), doi:10.1016/S1003-6326(14)63310-0 (Calculation, Phase Diagram, Phase Relations, Thermodynamics, #, *, 26)

[2014Hao] Hao, D., Hu, B., Zhang, K., Zhang, L., Du, Y., "The Quaternary Al-Fe-Ni-Si Phase Equilibria in Al-rich Corner: Experimental Measurement and Thermodynamic Modeling", *J. Mater. Sci.*, **49**(3), 1157-1169 (2014), doi:10.1007/s10853-013-7795-6 (Calculation, Experimental, Morphology, Phase Diagram, Phase Relations, Thermodynamics, 39)

[2014Li] Li, Z., Li, X., Yin, F., Wu, Y., Zhao, M., "Phase Equilibria of the Al-rich Corner in the Al-Cu-Fe-Si System at 650°C", *J. Phase Equilib. Diffus.*, **35**(3), 248-255 (2014), doi:10.1007/s11669-014-0298-6 (Crystal Structure, Experimental, Morphology, Phase Diagram, Phase Relations, #, *, 30)

[2015Che] Chen, J.K., Hung, H.Y., Wang, C.F., Tang, N.K., "Thermal and Electrical Conductivity in Al-Si/Cu/Fe/Mg Binary and Ternary Al Alloys", *J. Mater. Sci.*, **50**(16), 5630-5639 (2015), doi:10.1007/s10853-015-9115-9 (Electrical Properties, Experimental, Morphology, Transport Phenomena, 29)

[2015Zho] Zhou, Z., Li, Z., Xie, Y., Wang, X., Liu, Y., Long, Z., Yin, F., "Experimental Study of the Phase Relationships in the Al-Rich Corner of the Al-Si-Fe-Cr Quaternary System at 700°C", *Int. J. Mater. Res. (Z. Metallkd.)*, **106**(5), 470-480 (2015), doi:10.3139/146.111202 (Experimental, Phase Diagram, Phase Relations, #, *, 32)

[2015Zou] Zou, Q., Zhao, M., Yin, F., Li, Z., Liu, Y., "Phase Equilibria in the Al-Rich Corner of the Al-Fe-Si-V Quaternary System at 620°C", *J. Phase Equilib. Diffus.*, **36**(3), 274-282 (2015), doi:10.1007/s11669-015-0382-6 (Crystal Structure, Experimental, Morphology, Phase Diagram, Phase Relations, 28)

[2016Leg] Legarra, E., Apinaniz, E., Plazaola, F., "Influence of the Order-Disorder Transition on the Magnetic Properties of $Fe_{75}Al_{25-x}Si_x$ Alloys", *Intermetallics*, **69**, 35-41 (2016), doi:10.1016/j.intermet.2015.10.008 (Crystal Structure, Electronic Structure, Experimental, Magnetic Properties, 42)

[2016Li1] Li, Z., Kuang, X., Liao, C., Yin, F., Zhao, M., "Phase Equilibria of the Al-Fe-Si-Ti Quaternary System at 700°C", *J. Phase Equilib. Diffus.*, **37**(2), 174-185 (2016), doi:10.1007/s11669-015-0443-x (Crystal Structure, Experimental, Morphology, Phase Diagram, Phase Relations, 44)

[2016Li2] Li, X., Scherf, A., Heilmaier, M., Stein, F., "The Al-Rich Part of the Fe-Al Phase Diagram", *J. Phase Equilib. Diffus.*, **37**, 162-173 (2016), doi:10.1007/s11669-015-0446-7 (Crystal Structure, Experimental, Phase Diagram, Phase Relations, 38)

[2016Yu] Yu, J.M., Wanderka, N., Miehe, G., Banhart, J., "Intermetallic Phases in High Purity Al-10Si-0.3Fe Cast Alloys with and without Sr Modification Studied by FIB Tomography and TEM", *Intermetallics*, **72**, 53-61 (2016), doi:10.1016/j.intermet.2016.02.003 (Crystal Structure, Experimental, Morphology, Phase Relations, 40)

[2017Cui] Cui, S., Jung, I., "Critical Reassessment of the Fe-Si System", *Calphad*, **56**, 108-125 (2017), doi:10.1016/j.calphad.2016.11.003 (Calculation, Phase Diagram, Thermodynamics, 157)

[2017Raj] Rajasekar, P., Umarji, A.M., "Effect of Al-doping on Suppression of Thermal Conductivity in Si Dispersed β-$FeSi_2$", *Intermetallics*, **89**, 57-64 (2017), doi:10.1016/j.intermet.2017.04.010 (Crystal Structure, Electrical Properties, Experimental, Morphology, Phase Relations, Physical Properties, Transport Phenomena, 54)

[2017Tod] Todaro, C. J., Easton, M. A., Qiu, D., Wang, G., StJohn, D. H., Qian, M., "The Effect of Ultrasonic Melt Treatment on Macro-Segregation and Peritectic Transformation in an Al-19Si-4Fe Alloy", *Metall. Mater. Trans. A*, **48**(11), 5579-5590 (2017), doi:10.1007/s11661-017-4325-1 (Experimental, Morphology, Phase Relations, 54)

[2019Bec] Becker, H., Bergh, T., Vullum, P. E., Leineweber, A., Li, Y., "β- and δ-Al-Fe-Si Intermetallic Phase, their Intergrowth and Polytype Formation", *J. Alloys Compd.*, **780**, 917-929 (2019), doi:10.1016/j.jallcom.2018.11.396 (Crystal Structure, Electronic Structure, Experimental, Phase Relations, 48)

[2019Ran] Rank, M., Franke, P., Seifert, H.J., "Thermodynamic Investigations in the Al-Fe System: Thermodynamic Modeling Using Calphad", *Int. J. Mater. Res.*, **110**(5), 406-421 (2019), doi:10.3139/146.111765 (Calculation, Crystal Structure, Phase Diagram, Phase Relations, Thermodynamics, 108)

[2019Zie] Zienert, T., Fabrichnaya, O., "Prediction of Heat Capacity for Crystalline Substances", *Calphad*, **65**, 177-193 (2019), doi:10.1016/j.calphad.2019.01.017 (Calculation, Mechanical Properties, Theory, Thermodynamics, 103)

[2020Zha] Zhang, J., Pang, Z.-Y., Wang, L., Sun, C.-C., Liu, N., Chen, H.-M., Cheng, Z.-X., Li, K., "Microstructure and Properties Evolution of Al-17Si-2Fe Alloys with Addition of Quasicrystal Al-Mn-Ti Master Alloy", *Rare Metals*, **39**(10), 1210-1221 (2020), doi:10.1007/s12598-020-01449-7 (Calculation, Crystal Structure, Experimental, Mechanical Properties, Morphology, Phase Diagram, Phase Relations, Thermodynamics, 37)

[2022Ste] Stein, F., "Al-Fe Binary Phase Diagram Evaluation", in *MSI Eureka*, Watson, A. (Ed.), MSI, Materials Science International Services GmbH, Stuttgart (2022), Document ID: 20.10236.2.7 (2022), doi:10.7121/msi-eureka-20.10236.2.7 (Crystal Structure, Phase Diagram, Phase Relations, Assessment, 311)

[2022Mar] Martin, S., Sulik, D., Fang, X.F., Becker, H., Leineweber, A., "Steel - Aluminum Hybrid Die Casting: Microstructures Related to the Applied Al-Si Bond Coating", *Intermetallics*, **151**, 107712 (2022), doi:10.1016/j.intermet.2022.107712 (Crystal Structure, Experimental, Phase Relations, Review, 73)

Table 1: Investigations of the Al-Fe-Si Phase Relations, Structures and Thermodynamics

Reference	Method/Experimental Technique	Temperature/Composition/Phase Range Studied
[1927Gwy]	Metallography, thermal analysis	Al-rich alloys, liquidus surface
[1928Dix]	Metallography, thermal analysis	25 Al-rich alloys, Fe ≤ 11 mass%, Si ≤ 29 mass%, Al = bal., 560°C
[1931Fin]	Metallography, XRD	11 Al rich alloys, Fe: 7.29-36 mass%, Si: 1.85-13.36 mass%, 560-600°C
[1931Fus]	Metallography, thermal analysis	About 50 Al rich alloys, liquidus surface of Al corner
[1932Nis], [1933Nis]	Metallography, thermal analysis	Al-rich alloys, liquidus surface of Al corner
[1937Koe], [1937Oel]	Calorimetry	Heat of formation of liquid alloys
[1937Ura]	Metallography, thermal analysis	Alloys up to 68 mass% Fe, liquidus surface of Al corner
[1940Tak]	Dilatometry, magnetometry, metallography, thermal analysis, XRD	About 150 alloys, entire composition range
[1946Phi1], [1946Phi2]	Metallography, XRD	Al-rich alloys., liquidus surface of Al-corner
[1949Cru]	Thermoelectric power	3 Al-rich alloys, Fe ≤ 0.51 mass%, Si ≤ 0.35 mass%, Al = bal., 420-640°C
[1950Phr]	Metallography, XRD	Al-rich alloys, liquidus surface of Al corner
[1951Oga1], [1951Oga2]	Metallography, thermal analysis	Al-rich alloys, liquidus surface of Al corner
[1951Pra1]	Metallography, chemical analysis, XRD	11 Al-rich alloys, liquidus surface of Al corner
[1951Pra2]	Metallography, chemical analysis, XRD	11 Al-rich alloys, liquidus surface of Al corner
[1952Arm]	Thermal analysis, chemical analysis	Al-rich alloys, liquidus surface of Al-corner
[1967Mun]	EPMA, TEM, XRD	Al-rich alloys, (Fe + Si) ≤ 22 mass%, Al = bal.
[1967Sun]	Chemical analysis, XRD	Al-rich alloys
[1968Lih]	DTA, magnetometry, microhardness, XRD	Fe corner, Al ≤ 50 at.%, Si ≤ 35 at.%, Fe = bal., up to solidus temperature (≈1500°C)
[1969Pan]	XRD	Crystal structure of $FeAl_3Si_2$
[1969Pol]	High-temperature XRD, resistivity	15 Fe-rich alloys, $Fe_3(Al_xSi_{1-x})$, $0 \le x \le 1$, order-disorder transition
[1970Mit], [1973Nag]	Galvanic cell	35 Al-rich alloys with Fe/Si ratio (in mass%) 0.133, 0.338, 0.561, 1, 1.667, 3.04, 6.94, activity of Al in liquid alloys, 785-1100°C
[1973Kat]	High-temperature XRD	15 Fe-rich alloys, $Fe_3(Al_xSi_{1-x})$, $0 \le x \le 1$, order-disorder transition, up to 1325°C
[1974Mur]	XRD	Crystal structure and homogeneity ranges of $Fe_3Al_2Si_3$, γ-$FeAl_3Si$, $FeAl_2Si$, $FeAl_3Si_2$, α-FeAlSi, β-$FeAl_{4.5}Si$, $Fe_2Al_3Si_3$, $Fe_3Al_2Si_4$, $Fe_{1.7}Al_4Si$
[1977Nic1], [1977Nic2]	NMR, magnetometry, XRD	$Fe_3(Al_xSi_{1-x})$, x = 0, 0.04, 0.08, 0.15, 0.25, Fe_3Al phase
[1977Suw]	Mössbauer spectroscopy	$Fe_{73}Al_{11}Si_{16}$ and $Fe_{68}Al_{22}Si_{10}$, Fe_3Al phase
[1979Bur]	XRD, magnetic measurements	$Fe_3Al_xSi_{1-x}$ at $0 \le x \le 1$
[1979Cow]	XRD	16 alloys of $Fe_3(Al_xSi_{1-x})$, $0 \le x \le 1$, Fe_3Al phase
[1980Sud]	Galvanic cell	Activity of Al in an Fe-1 mass% Al-1 mass% Si alloy

Reference	Method/Experimental Technique	Temperature/Composition/Phase Range Studied
[1981Zar]	XRD	Isothermal section at 600°C
[1982Cha]	TEM	$Fe_3(Al_{0.392}Si_{0.608})$, order-disorder transitions
[1982Miy]	TEM	20 Fe-rich alloys, Al = 0.5-33 at.%, Si = 2.8-15.1 at.%, Fe = bal., 450-700°C, order-disorder transitions
[1983Gle]	TEM, Mössbauer spectroscopy	Fe-5.4Al-9.6Si (mass%), order-disorder transitions
[1983Sch]	Mössbauer spectroscopy	8 alloys along Fe_3Al-Fe_3Si, Fe_3Al phase
[1984Ber]	Galvanic cell	Al-2.5Fe-6Si (mass%) alloy, activity of Al, 660-900°C
[1984Don]	TEM	3 Al-rich alloys, Fe = 0.21-0.6 mass%, Si = 0.14-0.59 mass%, Al = bal., 400-600°C
[1986Miy]	Hardness, TEM	20 Fe-rich alloys, Al = 0.5-33 at.%, Si = 2.8-15.1 at.%, Fe = bal., 450-700°C, order-disorder transitions
[1986Tak]	Magnetometry	$Fe_3(Al_xSi_{1-x})$ alloys, order-disorder transitions
[1987Dob]	Neutron diffraction, Mössbauer spectroscopy	$Fe_{73.6}Al_{2.9}Si_{23.5}$, $Fe_{70.8}Al_{5.8}Si_{23.4}$ and $Fe_{69.4}Al_{7.2}Si_{23.4}$, Fe_3Al phase
[1987Gri1]	DTA, EPMA, XRD	Al-rich alloys, Fe = 18-35 mass%, Si = 4-12 mass%, Al = bal., 600°C
[1987Ste]	SEM, EPMA, XRD	9 Al-rich alloys, Fe = 17.8-34.9 mass%, Si = 3.9-14.1 mass%, Al = bal., 570-600°C
[1988Zak]	DTA, XRD	15 Al-rich alloys, Fe = 1-3 mass%, Si = 10-14 mass%, Al = bal., Al corner liquidus surface and vertical sections
[1989Bon]	Galvanic cell	Al-rich alloys, Fe = 3.6-11.8 at.%, Si = 6.9-23.7 at.% Si, Al = bal., activity of Al in liquid alloys
[1989Ger2]	Single crystal XRD	Crystal structure of $FeAl_2Si$
[1994Ang]	Calphad modeling	Vertical sections at x_{Al}/x_{Si}=3/1 and at x_{Si} = 0.85
[1995Gue3]	Calphad modeling	Isothermal and vertical sections
[1996Mor]	DSC, TEM	$Fe_{82}Al_{17}Si_1$, TEM, order-disorder transitions
[1996Szy]	XRD, magnetic susceptibility, Mössbauer measurements	$FeAl_xSi_{2-x}$ at x = 0–0.06
[1996Yan]	XRD	Crystal structures of $Fe_3Al_2Si_3$ and $Fe_3Al_2Si_4$
[1997Vyb]	Calorimetry	Heat of formation of α-FeAlSi and β-$FeAl_{4.5}Si$
[1998Han]	Single crystal XRD	Crystal structure of β-FeAl4.5Si
[1999Liu]	Calphad modeling	Isothermal and vertical sections, reaction scheme
[2000Li1] [2000Li2]	Calorimetry	Heat of formation of $Fe_3Al_2Si_3$, γ-$FeAl_3Si$, $FeAl_2Si$, $FeAl_3Si_2$, α-FeAlSi, β-$FeAl_{4.5}Si$, $Fe_3Al_2Si_4$, and τ_1
[2000Zhe]	TEM	Crystal structure of β-FeAl4.5Si
[2001Kre]	SEM, EDX, powder XRD	100 alloys containing up to 50 at.% Fe, isothermal section at 550°C
[2002Gup]	EPMA	Diffusion couples, 1020-1115°C
[2002Mai]	EPMA	Diffusion couples, 600-900°C
[2003Gjo]	TEM	Crystal structure of β-$FeAl_{4.5}Si$
[2003Kan]	Calorimetry	Heat of mixing of liquid alloys at 1477°C
[2004Bos]	XRD, OM, SEM/EPMA, DTA	Isothermal section at 727°C, temperature of formation of τ_1
[2004Kan]	Galvanic cell	$Fe_x(Al_{0.879}Si_{0.121})_{1-x}$, $0.0249 \le x_{Fe} \le 0.0512$, activity of Al in liquid alloys
[2004Pon1] [2004Pon2]	Optical microscopy, SEM/EPMA, DTA, XRD	18 ternary alloys, solid-liquid phase equilibria at 727°C
[2004Sug]	Single crystal XRD, SEM/EPMA	Crystal structure of γ-$FeAl_3Si$

Reference	Method/Experimental Technique	Temperature/Composition/Phase Range Studied
[2007Kre]	Powder XRD, EDX, SEM, DTA	More than 80 alloys containing up to 50 at.% Fe, isothermal section at 550°C, reaction scheme and partial liquidus surface
[2008Du]	Calorimetry and first-principles calculations	Heat of formation ternary intermetallics
[2008Du]	Calphad modeling	Isothermal, vertical sections, liquidus surface and enthalpies of formation of phases
[2010Ele]	Calphad modeling	Liquidus surface of Al-corner, isothermal sections at 500 and 727°C, vertical sections at 13.5 mass% Si and 5 mass% Fe.
[2010Mak]	SEM/EDS	Aluminization of mild steel at 600°C. $Fe_3Al_2Si_3$ and γ-$FeAl_3Si$ phases
[2011Lee1]	Optical microscopy, SEM/EDS	The effects of Fe content and cooling rate on the solidification path and formation behavior of the β-$FeAl_{4.5}Si$ phase in two Fe-containing eutectic Al-Si alloys
[2011Lee2]	SES, OM, SEM/EDS, thermal analysis, thermodynamic calculations	The effects of Fe content and cooling rate on the solidification path and formation of the β-$FeAl_{4.5}Si$ phase in two Fe-containing hypoeutectic Al-Si alloys.
[2011Mar]	DTA, EPMA, SEM and XRD	73 ternary alloys, isothermal sections at 800 and 900°C, vertical sections, and a partial reaction scheme
[2011Rog1]	XRD, DTA	Crystal structure temperature of formation of α-FeAlSi
[2011Rog2]	XRD	Single crystals of γ-$FeAl_3Si$
[2011Spr]	OM, SEM, EBSD, and STEM	Interdiffusion between Al-5 mass% Si and mild steel at 600 and 675°C. $Fe_3Al_2Si_3$, $FeAl_2Si$, α-FeAlSi and β-$FeAl_{4.5}Si$ in the interdiffusion zone
[2013Zha], [2017Tod]	EPMA	Effects of ultrasonic treatment (USMT) and cooling rate on morphology and composition of iron-containing intermetallic compounds were investigated by EPMA
[2014Ami]	DFT, DSC	Heat capacity of $FeAl_3Si_2$
[2014Che]	Calphad modeling	Based on the work of [2008Du], vertical section at 5 mass% Fe, vertical section at 10 mass% Si, vertical section at 13.5 mass% Si, liquidus surface in Al-rich corner, liquidus surface over entire composition range, vertical section at 35 mass% Fe
[2014Hao]	XRD, SEM/EDS, EPMA Calphad modeling	2 Al-rich alloys, as-cast alloys analysis, vertical section at 13.5 mass% Si in the Al-rich corner, liquidus projection in Al-rich corner
[2014Li]	XRD, SEM/EDS	3 Al-rich alloys, isothermal section of the Al-rich corner at 650°C
[2015Zho]	XRD, SEM/EDS	5 Al-rich alloys, isothermal section of the Al-rich corner at 700°C
[2015Zou]	XRD, SEM/EDS	5 Al-rich alloys, isothermal section of the Al-rich corner at 600°C
[2016Leg]	XRD, Mössbauer spectroscopy, magnetic measurement	Intermetallic $Fe_{75}Al_{25-x}Si_x$ alloys (x =7.5, 12.5, 17.5, 25), annealed at 770°C for 2 h then cooled down to 570°C and kept there for 10 h
[2016Li1]	XRD, SEM/EDS	4 Al-rich alloys annealed at 700°C
[2016Yu]	TEM/EDX	Intermetallic phases in Al-10Si-0.3Fe alloys, γ-$FeAl_3Si$ and α-FeAlSi

Reference	Method/Experimental Technique	Temperature/Composition/Phase Range Studied
[2017Tod]	SEM/EDS	Effect of the ultrasonic melt treatment on macro-segregation and intermetallic transformations of Al-19Si-4Fe alloys
[2019Bec]	SEM/EDS, EBSD, TEM	Crystal structure characteristics of coexisting $FeAl_3Si_2$ and β-$FeAl_{4.5}Si$ phase were investigated in a purely intermetallic Al-Fe-Si alloy
[2019Zie]	Calculated by an algorithm	Heat capacity of Fe_2Al_5, Fe_5Al_8 and $FeAl_3Si_2$, calculated by an algorithm based on zero-Kelvin properties (V_0, B_0), the Debye temperature and the thermal expansion coefficient at Debye temperature
[2020Zha]	OM, SEM/EDS, Thermodynamic calculations	The microstructural evolution of an as-cast Al-7Si-2Fe alloy

Table 2: Crystallographic Data of Solid Phases

Phase/ Temperature Range (°C)	Pearson Symbol/ Space Group/ Prototype	Lattice Parameters (pm)	Comments/References
(Al) < 660.452	*cF*4 $Fm\bar{3}m$ Cu	*a* = 404.96	pure Al at 25°C [Mas2] solubility for Fe (the Al-Fe system): 0.023 at.% [2019Ran] solubility for Si in (the Al-Si system): 1.5 at.% [2004Luk]
(αδFe) < 1540	*cI*2 $Im\bar{3}m$ W		Strukturbericht designation: *A*2 [2007Ste]
αFe < 912		*a* = 286.65	at 25°C [Mas2]
δFe 1538 - 1394		*a* = 293.15	[Mas2] solubility for Al (the Al-Fe system): 45.0 at.% [1993Kat, 2007Ste] solubility for Si (the Fe-Si system): ~19 at.% [2017Cui]
(γFe) 1394 - 912	*cF*4 $Fm\bar{3}m$ Cu	*a* = 364.67	at 915°C [V-C2, Mas2] solubility for Al in the Al-Fe system: 1.35 at.% [1993Kat]
(Si) < 1414	*cF*8 $Fm\bar{3}m$ C (diamond)	*a* = 543.06	at 25°C [Mas2]
Fe_5Al_8 1231 - 1095	*cI*52 $I\bar{4}3m$ Cu_5Zn_8	*a* = 897.57 ± 0.02	sometimes named γ phase Strukturbericht designation: $D8_2$ at 1120°C and 59.4 at.% Al [2010Ste] 56.0 to 64.5 at.% Al [2016Li2]
$FeAl_2$ < 1146	*aP*19 $P\bar{1}$ $FeAl_2$	*a* = 487.45 *b* = 645.45 *c* = 873.61 α = 87.930° β = 74.396° γ = 83.062°	sometimes named ζ phase at 66.4 at.% Al [2010Chu] 64.7 to 66.7 at.% Al

Phase/ Temperature Range (°C)	Pearson Symbol/ Space Group/ Prototype	Lattice Parameters (pm)	Comments/References
Fe_2Al_5	*oC*24		sometimes named η phase
1159 - ~331	*Cmcm*	*a* = 765.59 ± 0.08	at 71.5 at.% Al [1994Bur]
	Fe_2Al_5	*b* = 641.54 ± 0.06	
		c = 421.84 ± 0.04	
			68.4 to 72.5 at.% Al
Fe_4Al_{13}	*mC*102		referred to as $FeAl_3$ in old literature before ~1995
< 1150	*C*2/*m*		sometimes named θ phase
	Fe_4Al_{13}		single crystal grown by Czochralski technique
		a = 1548.8 ± 0.1	[2008Gil, 2010Pop]
		b = 808.66 ± 0.05	
		c = 1247.69 ± 0.08	
		β = (107.669±0.004)°	74.5 to 76.9 at.% Al
$FeAl_6$	*oC*28		metastable
	$Cmc2_1$	*a* = 744.0	85.7 at.% Al [1965Wal]
	$FeAl_6$	*b* = 646.4	
		c = 877.9	
Fe_2Si	*hP*6	*a* = 405.2 ± 0.2	at 1062 ± 10°C [1977Kud]
1212 - 1040	$P6_3/mmc$	*c* = 508.55 ± 0.25	
	Fe_2Si		~32.8-~33.8 at.% Si [1982Kub]
Fe_5Si_3	*hP*16	*a* = 674.16 ± 0.06	[1943Wei]
1060 - 825	$P6_3/mcm$	*c* = 470.79 ± 0.06	
	Mn_5Si_3		
FeSi	*cP*8	*a* = 450.0 ± 0.5	at room temperature [1963Wat]
<1409	$P2_13$		~49.0 to 51.8 at.% Si [1982Kub]
	FeSi		
Fe_3Si_7	*tP*3		Also called Fe_2Si_5. High-temperature modification of $FeSi_2$
1208 - 955	*P*4/*mmm*		
	$FeSi_2$	*a* = 268.4	single crystal [1960Aro]
		c = 512.8	~69 to ~73 at.% Si [1982Kub]
$FeSi_2$	*oC*48	*a* = 987.75 ± 0.03	[2009Yam]
< 986	*Cmca*	*b* = 781.27 ± 0.02	
	$FeSi_2$	*c* = 782.73± 0.02	
$Fe_3(Al,Si)$	*cF*16		sometimes named α_1 phase
	$Fm\bar{3}m$		Strukturbericht designation: $D0_3$
Fe_3Al	BiF_3	*a* = 579.30	at 23.1 at.% Al, water-quenched from 250°C [1958Tay]
< 545			
		a = 578.86	at 35.0 at.% Al, water-quenched from 250°C [1958Tay]
			~24 to ~34 at.% Al at 400°C [1993Kat]
Fe_3Si		*a* = 565.0	[1976Ber]
< 1210			~13.5 at.% at 600°C [2012Ohn]
			~28.8 at.% at 1047°C [2017Cui]
Fe(Al,Si)	*cP*2		sometimes named α_2 phase
	$Pm\bar{3}m$		Strukturbericht designation: *B*2
FeAl	CsCl	*a* = 289.53 to 290.90	at 36.2 to 50.0 at.% Al, water-quenched from 250°C [1958Tay]
< 1318			23.5 to ~53 at.% Al [2007Ste]
FeSi’		-	~12 at.% at 700°C [2012Ohn]
< 1285			~26 at.% at 1210°C [2017Cui]

Phase/ Temperature Range (°C)	Pearson Symbol/ Space Group/ Prototype	Lattice Parameters (pm)	Comments/References
*$Fe_3Al_2Si_3$, < 1052	*aP*16 $P\bar{1}$ $Fe_3Al_2Si_3$		Denoted as K_1 [1940Tak], D, E [1974Mur, 1981Zar], τ_1, τ_9 [2002Gup, 2002Mai], τ_1 [2011Mar]
		a = 465.12 ± 0.16 *b* = 632.61 ± 0.24 *c* = 749.9 ± 0.3 α = (101.375±0.023)° β = (105.923±0.017)° γ = (101.237±0.019)°	Single crystal [1996Yan]
		a = 469.3 to 458.3 *b* = 632.2 to 633.4 *c* = 748.4 to 752.4 α = (100.5 to 101.6)° β = (105.1 to 106.5)° γ = (101.7 to 100.2)°	24.5-41.5 at.% Si [2011Mar] (as read from figure)
			21-45 at.% Al, 37.5-36.5 at.% Fe, 41.5-18.5 at.% Si at 727°C [2004Bos]
*γ-$FeAl_3Si$, < 900-934	*h** $R\bar{3}$ -		Denoted as K_5 [1940Tak], K [1974Mur, 1981Zar], τ_2 [2002Gup, 2002Mai, 2011Mar], γFeAlSi [1967Mun, 1987Ste], γ$Fe_2Al_5Si_2$ or γ [2004Pon1, 2004Pon2], λ-AlFeSi [2004Sug]
		a = 1022.2±0.2 *c* = 1966.7±0.2	single crystal [2004Sug]
		a = 1022.23±0.02 *c* = 1967.91±0.04	single crystal with average composition $Fe_{20.4}Al_{65.0}Si_{14.6}$ (at.%) [2011Rog2]
		a = 1018.52±0.02 *c* = 1921.48±0.07	powder sample with composition $Fe_{21.5}Al_{52.4}Si_{26.1}$ (at.%) [2011Rog2]
			52.4-64.7 at.% Al, 21.5-20.1 at.% Fe, 26.1-15.2 at.% Si [2011Rog2]
*$FeAl_2Si$ < 940	*oC*128 *Cmma* $FeAl_2Si$		Denoted as K_2 of [1940Tak], G [1974Mur, 1981Zar], τ_3 [2001Kre, 2007Kre, 2011Mar]
		a = 799.5±0.2 *b* = 1516.2±0.6 *c* = 1522.1±0.1	single crystal taken from the $Fe_{25}Al_{50}Si_{25}$ (at.%) alloy [1989Ger2]
		a = 799.57±0.01 to 799.55±0.01 *b* = 1517.89±0.05 to 1520.67±0.01 *c* = 1522.59±0.06 to 1523.78±0.01	51.8-54.5 at.% Al, 25.2-26.6 at.% Fe, 23-18.9 at.% Si at 800°C [2011Mar]

Phase/ Temperature Range (°C)	Pearson Symbol/ Space Group/ Prototype	Lattice Parameters (pm)	Comments/References
*$FeAl_3Si_2$ < 875	*o** *Pbcn*		Denoted as $Fe_2Al_6Si_3$ by [1931Fus], $FeAl_4Si_2$ [1936Jae, 1988Zak], K_4 by [1940Tak], t-FeAlSi by [1950Phr], A by [1974Mur, 1981Zar], τ_4 by [2001Kre, 2002Gup, 2002Mai, 2007Kre], δ-$FeAl_3Si_2$ by [2004Pon1, 2004Pon2], δ by [1967Sun, 2019Bec]
		a = 606.1±0.1 *c* = 952.5±0.1	Ordered superstructure measured from single crystal $FeAl_{2.7}Si_{2.3}$ [1995Gue1]
			If superstructure reflections are neglected, the average structure can be refined in the tetragonal *I*4/*mcm* structure of $PdGa_5$ firstly reported by [1969Pan]
			15.5-16.5 at.% Fe, 54-45.5 at.% Al, 30.5-39 at.% Si [2007Kre]
*α-FeAlSi < 772	*hP** $P6_3/mmc$		Average chemical formula $Fe_2Al_{7.1}Si$ [2011Rog1] Denoted as c-FeAlSi by [1950Phr], M by [1974Mur, 1981Zar], α_H-FeAlSi by [1987Gri2], τ_5 by [1997Vyb, 2001Kre, 2002Gup, 2002Mai, 2007Kre 2014Li, 2015Zho, 2015Zou, 2016Li1], α-$Fe_2Al_{7.4}Si$ by [2004Pon1, 2004Pon2], Fe_2Al_8Si by [2014Hao].
		a = 1234.6±0.2 *c* = 2621.0±0.3	Single crystal $Fe_2Al_{7.1}Si$ [2011Rog1]
			18-19.5 at.% Fe, 72-68 at.% Al, 10-12.5 at.% Si [2007Kre]
*β-$FeAl_{4.5}Si$ < 665	- *A*2/*a*		Denoted as K_6 by [1940Tak], m-FeAlSi by [1950Phr], β($FeAl_5Si$), β($FeAl_{4.5}Si$), β-$FeAl_3Si$ by [1967Sun, 1988Zak, 1994Rom, 1998Han, 2004Pon1, 2004Pon2, 2019Bec], L by [1974Mur, 1981Zar], β-FeAlSi [1987Ste, 2000Zhe], τ_6 by [1997Vyb, 2001Kre, 2002Gup, 2002Mai, 2011Mar, 2014Li, 2015Zho, 2015Zou, 2016Li1].
		a = 616.1±0.3 *b* = 617.5±0.3 *c* = 2081.3±0.6 β = (90.42±0.03)°	Indexing of EBSD data was done with a tetragonal structure mimicking the diffraction effects due to a disordered stacking sequence [1994Rom]
			Exhibits polytype structures. [2019Bec] formulated structural models for these structures based on ordering of the constituting double layers being shifted by a/2 or b/2 displacements leading to 4 different double layer positions A, B, C, and D.
			64.5-67.5 at.% Al, 16.5-15.5 at.% Fe, 17-19 at.% Si [2007Kre]

Phase/ Temperature Range (°C)	Pearson Symbol/ Space Group/ Prototype	Lattice Parameters (pm)	Comments/References
*$Fe_2Al_3Si_3$ < 934	$P2_1/n$ *mP*64 $Fe_2Al_3Si_3$	a = 717.9±0.2 b = 835.4±0.2 c = 1445.5±0.4 β = (93.8±0.2)°	Denoted as K_3 by [1940Tak], B by [1974Mur, 1981Zar], τ_7 by [2001Kre, 2007Kre, 2011Mar]. Small single crystals [1995Gue2]
		a = 718.29±0.01 to 732.57±0.01 b = 835.69±0.03 to 827.92±0.01 c = 1445.64±0.06 to 1460.96±0.03 β = (93.81 to 93.71)°	41.3-46.6 at.% Al, 23.8-26.1 at.% Fe, 34.9-27.3 at.% Si at 800°C [2011Mar]
			24.0-26.0 at.% Fe, 41.0-46.5 at.% Al, 35.0-27.5 at.% Si [2011Mar]
*$Fe_3Al_2Si_4$ < 1010	*oC*48 *Cmcm* $Fe_3Al_2Si_4$	a = 366.87±0.15 b = 1238.5±0.7 c = 1014.7±0.5	Denoted as C by [1974Mur, 1981Zar], τ_8 by [2001Kre, 2007Kre, 2011Mar] Single crystals [1996Yan]
		a = 366.89±0.01 to 365.99±0.04 b = 1232.45±0.02 to 1247.29±0.05 c = 1014.07±0.01 to 11015.68±0.02	23.2-28.6 at.% Al, 34.5-34.1 at.% Fe, 42.3-37.3 at.% Si at 800°C [2011Mar]
			23.0-28.5 at.% Al, 33.5-34.5 at.% Fe, 42.5-37.5 at.% Si [2011Mar]
* $FeAl_{2.4}Si_{0.6}$ (τ_1)	*hP*8 $P6_3/mmc$ Na_3As	a = 406.0 c = 773.8	τ_{10} by [2001Kre, 2002Gup, 2004Bos, 2007Kre] [1991Ger]
			24-25 at.% Fe, 59-57 at.% Al, 17-18 at.% Si at 727°C [2004Bos]
* $Fe_{1.7}Al_4Si$ 997 - ?	*hP*28 $P6_3/mmc$ Co_2Al_5	a = 750.9±0.3 c = 759.4±0.3	Denoted as F by [1974Mur, 1981Zar], τ_{11} [2004Bos, 2007Kre, 2011Mar]. Single crystal [1989Ger1]
		a = 752.53±0.01 to 753.55±0.01 b = 756.05±0.02 to 758.05±0.02	62.3-64.7 at.% Al, 25.9-26.1 at.% Fe, 11.8-9.2 at.% Si at 800°C [2011Mar]
			26.0 at.% Fe, 62.5-65 at.% Al, 11.5-9.0 at.% Si [2011Mar]
* Fe_2Al_3Si 1005 - 720	*cF*96 $Fd\bar{3}m$ $NiTi_2$	a = 1080.6±0.2	Single crystal [2011Mar]

Table 3: Invariant Equilibria

Reaction	T (°C)	Type	Phase	Composition (at.%)		
				Al	Fe	Si
L+Fe_2Si ⇌ Ord + FeSi	~1192	U_1	L	4.7	64.9	30.4
L + Fe_5Al_8 ⇌ Ord + Fe_2Al_5	1120	U_2	L	62.6	33.5	3.9
Fe_2Al_5 + Fe_5Al_8 ⇌ Ord + $FeAl_2$	1095< T <1120	U_3	–	–	–	–
L + Ord + FeSi ⇌ $Fe_3Al_2Si_3$	1052	P_1	L	42.0	32.8	25.2
L + Ord ⇌ $Fe_3Al_2Si_3$ + Fe_2Al_5	1036	U_4	L	50.2	30.2	19.6
L + Fe_2Al_5 ⇌ $Fe_3Al_2Si_3$ + Fe_4Al_{13}	1028	U_5	L	52.0	29.0	19.0
L + Fe_3Si_7 ⇌ $Fe_3Al_2Si_4$	1010	p_5, max	L	21.9	32.8	45.4
L + FeSi ⇌ Fe_3Si_7 + $Fe_3Al_2Si_3$	1005	U_6	L	21.3	34.8	42.9
Ord+ Fe_2Al_5 + $Fe_3Al_2Si_3$ ⇌ Fe_2Al_3Si	1005	P_2	–	–	–	–
L + Fe_4Al_{13} + $Fe_3Al_2Si_3$ ⇌ $Fe_{1.7}Al_4Si$	997	P_3	L	56.3	23.9	19.8
L + Fe_3Si_7 ⇌ $Fe_3Al_2Si_3$ + $Fe_3Al_2Si_4$	989	U_7	L	24.2	33.9	42.0
L + $Fe_3Al_2Si_3$ + $Fe_{1.7}Al_4Si$ ⇌ $FeAl_2Si$	940	P_4	L	51.0	23.0	26.0
L + $Fe_3Al_2Si_3$ + $FeAl_2Si$ ⇌ $Fe_2Al_3Si_3$	934	P_5	L	49.0	20.6	30.4
L + $Fe_3Al_2Si_3$ ⇌ $Fe_2Al_3Si_3$ + $Fe_3Al_2Si_4$	928	U_8	L	47.1	18.2	34.7
L + $Fe_{1.7}Al_4Si$ ⇌ $FeAl_2Si$ + Fe_4Al_{13}	914	U_9	L	59.9	21.7	18.4
L + $Fe_2Al_3Si_3$ + $FeAl_2Si$ ⇌ γ-$FeAl_3Si$	900< T <934	P_6	L	63.9	13.8	22.3
L + $FeAl_2Si$ ⇌ γ-$FeAl_3Si$ + Fe_4Al_{13}	900	U_{10}	L	65.9	15.1	18.9
L + Fe_3Si_7 ⇌ $Fe_3Al_2Si_4$ + (Si)	885	U_{11}	L	51.3	12.7	36.0
L + $Fe_3Al_2Si_4$ ⇌ $Fe_2Al_3Si_3$ + (Si)	< 885	U_{12}	L	52.5	12.3	35.2
L + $Fe_2Al_3Si_3$ + (Si) ⇌ $FeAl_3Si_2$	875	P_7	L	57.0	10.5	32.5
L + $Fe_2Al_3Si_3$ ⇌ $FeAl_3Si_2$ + γ-$FeAl_3Si$	858	U_{13}	L	66.1	10.9	23.0
L + γ-$FeAl_3Si$ + Fe_4Al_{13} ⇌ α-FeAlSi	772	P_8	L	81.8	6.5	11.7
Fe_3Si_7+$Fe_3Al_2Si_3$⇌$Fe_3Al_2Si_4$+FeSi	700< T <727	U_{14}	–	–	–	–
Fe_3Si_7+FeSi⇌$Fe_3Al_2Si_4$+$FeSi_2$	700< T <727	U_{15}	–	–	–	–
Fe_2Al_3Si ⇌ Ord+ Fe_2Al_5 + $Fe_3Al_2Si_3$	720	E_1	–	–	–	–
Fe_3Si_7 ⇌ $Fe_3Al_2Si_4$ + (Si) + $FeSi_2$	600< T <700	E_2	–	–	–	–
$Fe_2Al_3Si_3$+$FeAl_2Si$⇌$Fe_3Al_2Si_3$+γ-$FeAl_3Si$	600< T <700	U_{16}	–	–	–	–
L + γ-$FeAl_3Si$ + $FeAl_3Si_2$ ⇌ β-$FeAl_{4.5}Si$	665	P_9	L	83.9	1.8	14.3
L + γ-$FeAl_3Si$ ⇌ α-FeAlSi + β-$FeAl_{4.5}Si$	648	U_{17}	L	88.2	1.7	10.2
L + Fe_4Al_{13} ⇌ α-FeAlSi + (Al)	636	U_{18}	L	93.6	1.1	5.2
L + α-FeAlSi ⇌ β-$FeAl_{4.5}Si$ + (Al)	609	U_{19}	L	91.2	1.1	7.7
L + $FeAl_3Si_2$ ⇌ β-$FeAl_{4.5}Si$ + (Si)	596	U_{20}	L	85.3	0.6	14.1
L ⇌ (Al) + (Si) + β-$FeAl_{4.5}Si$	577	E_3	L	87.7	0.3	12.0

Note: "Ord" denotes ordered (Fe,Al)Si or Fe_3(Al,Si) phases

Most of the compositions of the liquid phase are as-read from the figure of [2007Kre].

The composition of the liquid phase for U_2 is accepted after [1988Ray]

Table 4: Selected Data of Heat of Mixing of Liquid Alloys

Reaction	Temperature (°C)	$\Delta_{mix}H$ (kJ·(g-at)$^{-1}$)	Comments
xFe(l) + yAl(l) + zSi(l) ⇌ Fe$_x$Al$_y$Si$_z$(l)	1477	–29.4	x = 0.36, y = 0.36, z = 0.28
		–27.9	x = 0.32, y = 0.38, z = 0.30
		–28.9	x = 0.40, y = 0.40, z = 0.20
		–28.3	x = 0.39, y = 0.42, z = 0.19
		–17.3	x = 0.15, y = 0.48, z = 0.37
		–23.3	x = 0.25, y = 0.50, z = 0.25
		–17.2	x = 0.154, y = 0.538, z = 0.308
		–20.6	x = 0.22, y = 0.58, z = 0.20
		–19.3	x = 0.20, y = 0.60, z = 0.20
		–21.5	x = 0.25, y = 0.60, z = 0.15
		–14.9	x = 0.15, y = 0.70, z = 0.15
		–16.2	x = 0.18, y = 0.72, z = 0.10
			High-temperature isoperibolic calorimeter [2003Kan]

Table 5: Standard Heat of Formation of Ternary Intermetallics

Reaction	T (K)	$\Delta_f H^{298.15}$ (kJ·(g-at)$^{-1}$)	Comments
xFe(s) + yAl(s) + zSi(s) ⇌ Fe$_x$Al$_y$Si$_z$(s)	298.15	–34.3 ± 2	x = 2, y = 7.4, z = 1 (α-FeAlSi)
		–24.5 ± 2	x = 2, y = 9, z = 2 (β-FeAl$_{4.5}$Si)
			Isoperibolic high-temperature solution calorimeter [1997Vyb]
xFe(s) + yAl(s) + zSi(s) ⇌ Fe$_x$Al$_y$Si$_z$(s)	298.15	–35.731 ± 1.381	x = 0.39, y = 0.42, z = 0.19 (Fe$_3$Al$_2$Si$_3$)
		–34.176 ± 1.570	x = 0.40, y = 0.40, z = 0.20 (Fe$_3$Al$_2$Si$_3$)
		–36.704 ± 1.860	x = 0.36, y = 0.36, z = 0.28 (Fe$_3$Al$_2$Si$_3$)
		–24.440 ± 1.387	x = 0.18, y = 0.72, z = 0.10 (α-FeAlSi)
		–30.384 ± 1.869	x = 0.25, y = 0.60, z = 0.15 (Fe$_3$Al$_2$Si$_{30}$)
			Setaram microcalorimeter of the Tian-Calvet type [2000Li1]
xFe(s) + yAl(s) + zSi(s) ⇌ Fe$_x$Al$_y$Si$_z$(s)	298.15	–25.273 ± 1.556	x = 0.20, y = 0.60, z = 0.20 (γ-FeAl$_3$Si)
		–28.392 ±1.891	x = 0.22, y = 0.58, z = 0.20 (γ-FeAl$_3$Si)
		–20.475 ± 1.208	x = 0.154, y = 0.538, z = 0.308 (FeAl$_3$Si$_2$)
		–19.222 ± 1.253	x = 0.15, y = 0.48, z = 0.37 (FeAl$_3$Si$_2$)
		–29.634 ± 0.929	x = 0.25, y = 0.50, z = 0.25 (FeAl$_2$Si)
		–20.209 ± 0.926	x = 0.15, y = 0.70, z = 0.15 (β-FeAl$_{4.5}$Si)
		–35.845 ± 1.760	x = 0.32, y = 0.38, z = 0.30 (Fe$_3$Al$_2$Si$_4$)
			Setaram microcalorimeter of the Tian-Calvet type [2000Li2]

Table 6: Investigations of the Al-Fe-Si Materials Properties

Reference	Method/Experimental Technique	Type of Property
[1968Aru1], [1968Aru2], [1970Aru]	Resistivity measurements	Electrical resistivity
[1968Lih]	Magnetometry	Curie temperature
[1977Nic2]	Magnetometry	Saturation magnetization
[1983Sch]	Magnetometry	Saturation magnetization

Reference	Method/Experimental Technique	Type of Property
[1986Tak], [1987Tak1], [1987Tak2]	Magnetometry	Magnetostriction, magnetocrystalline anisotropy
[1988Dor]	Magnetometry	Magnetic permeability
[1993Sch]	Mechanical tests	Critical resolved shear stress up to 720°C
[1996Fri]	Electrical tests	Metal/insulator transition
[1996Szy]	Magnetometry	Magnetic susceptibility
[1998Dit]	Electrical and magnetic	Electrical conductivity, Hall effect, magneto-resistance, magnetic susceptibility
[1999Oht]	Electrical tests	Thermoelectric power
[2000Bha]	Electrochemical tests	Corrosion
[2001Cho]	Mechanical tests	Hardness, strength, and elongation up to 520°C
[2003Cie]	Mechanical tests	Dynamic strain aging
[2003Mur]	Mechanical tests	Hardness and indentation fracture toughness
[2010Fri]	First-principles calculation of elastic properties	Youngs modulus
[2010Leg]	Mössbauer spectroscopy	Magnetic property
[2012Leg]	Mössbauer spectroscopy, X-ray diffraction, magnetic measurement	Magnetic and structural properties
[2015Che]	Thermal and electrical tests	Thermal and electrical conductivity
[2017Raj]	Van der Pauw four probe method, laser flash technique	Electrical resistivity, thermal diffusivity

Table 7: Coordinates of the γ/(α+γ) and (α+γ)/α Phase Boundaries in the Al-Fe-Si System. γ and α denote (γFe) and (αδFe)

Composition (mass%)		Temperature (°C) of the	
Al	Si	γ/(α+γ) boundary	(α + γ)/α boundary
0.16	0.25	905	1385
0.19	0.58	952	1351
0.31	0.93	1014	1300
0.44	0.19	935	1350
0.44	0.53	976	1326
0.48	0.13	948	1347
0.64	0.23	1030	1275
0.71	0.65	1048	1270
0.74	0.24	1000	1303

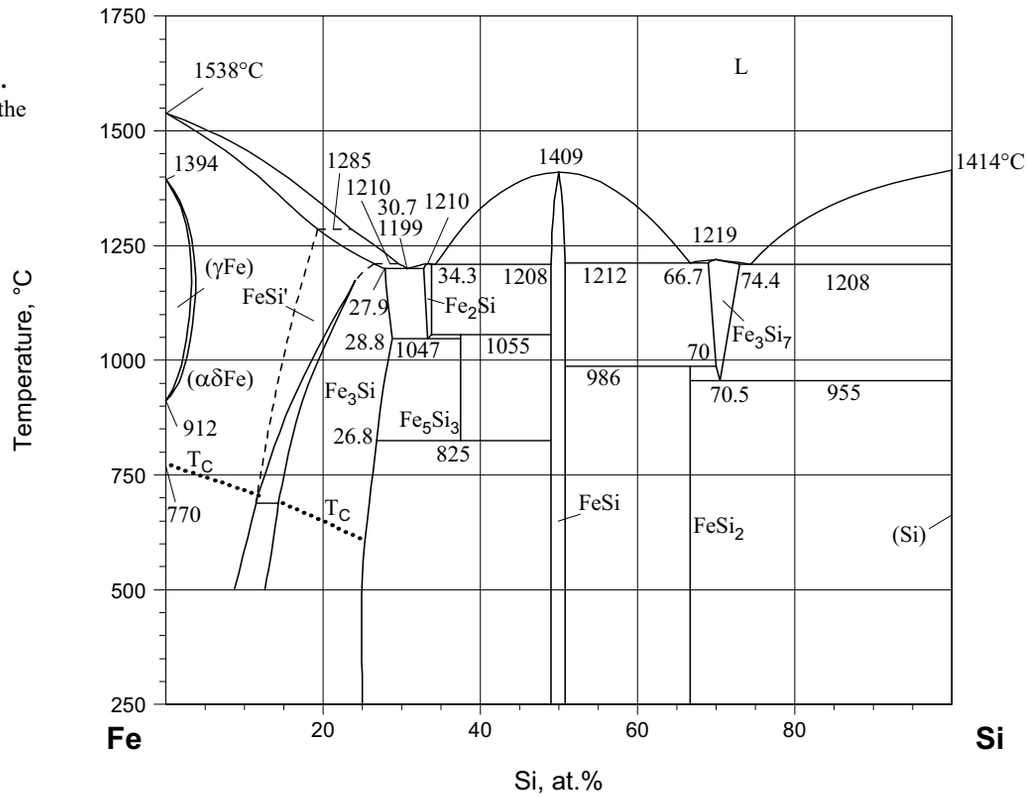

Fig. 1: Al-Fe-Si. Phase diagram of the Fe-Si system

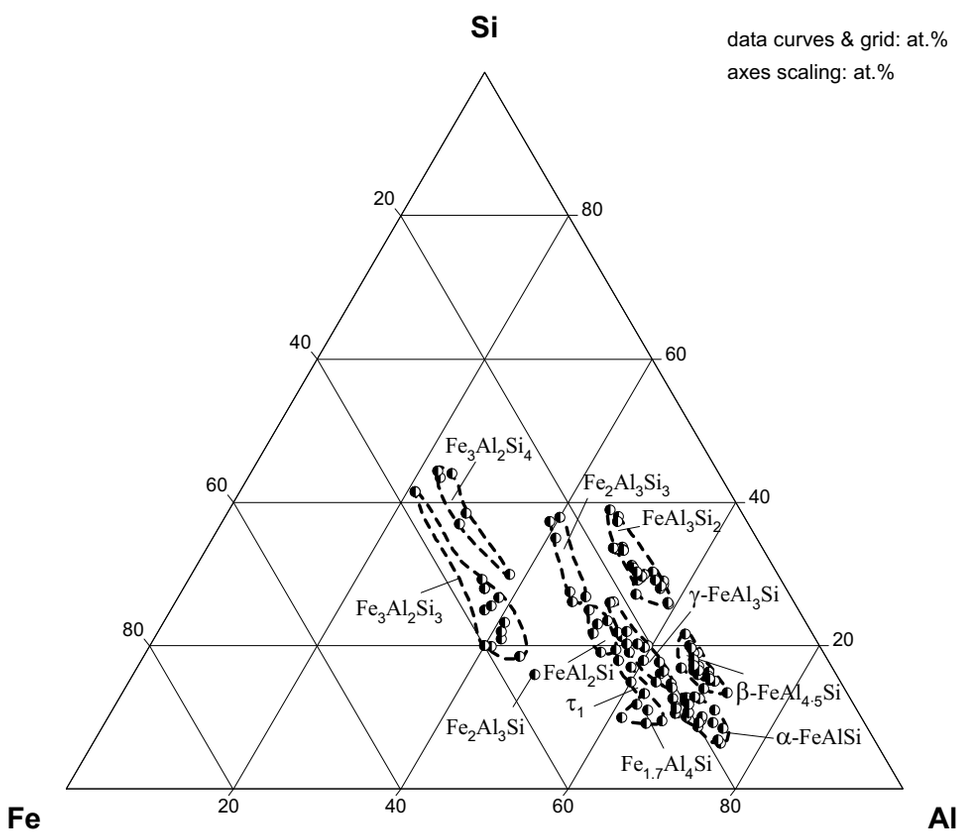

Fig. 2: Al-Fe-Si. Distribution of the equilibrium ternary phases, as reported by different authors

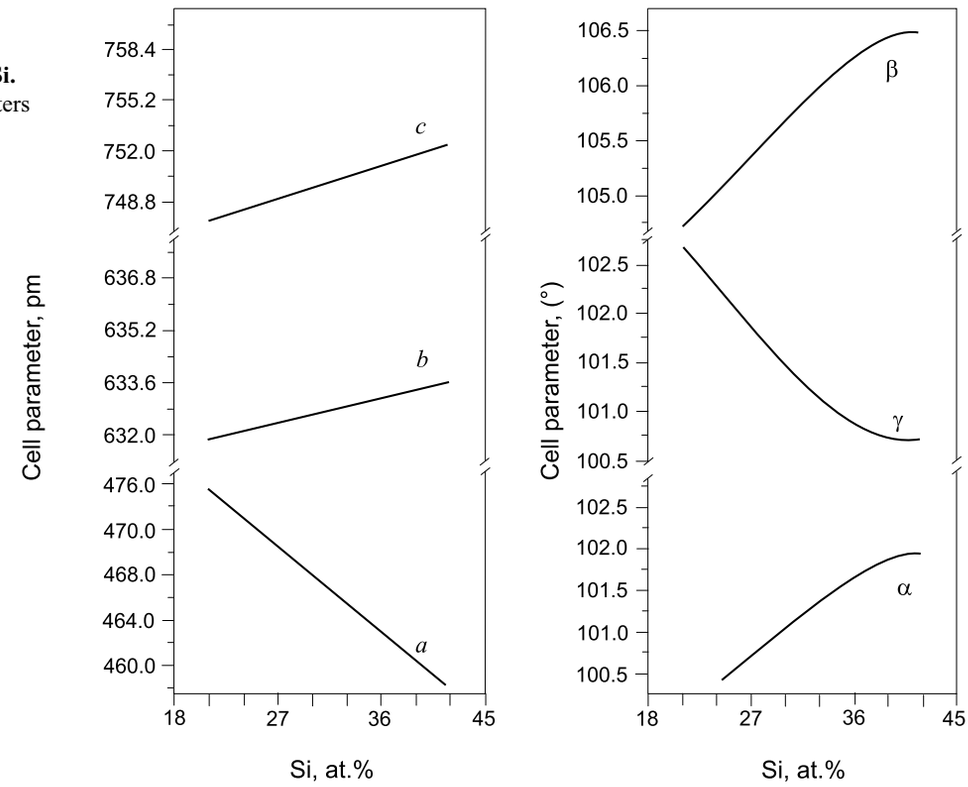

Fig. 3: Al-Fe-Si. Unit-cell parameters of the $Fe_3Al_2Si_3$ compound as a function of the composition according to [2011Mar]

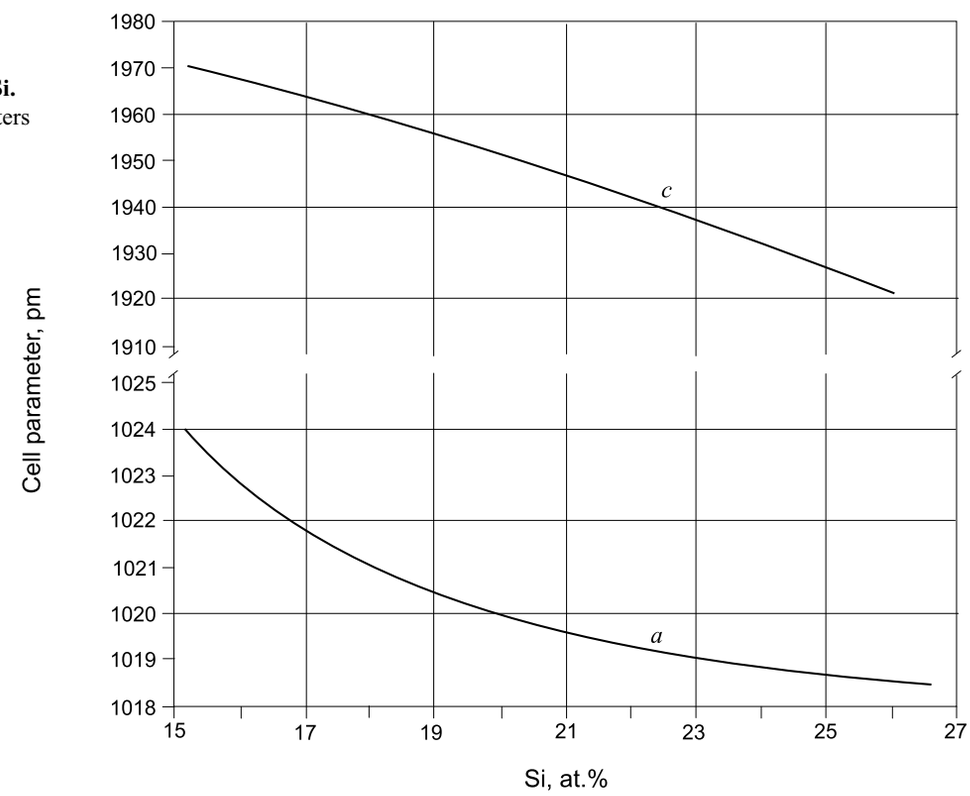

Fig. 4: Al-Fe-Si. Unit-cell parameters of the $\gamma FeAl_3Si$ compound as a function of the composition according to [2011Rog2]

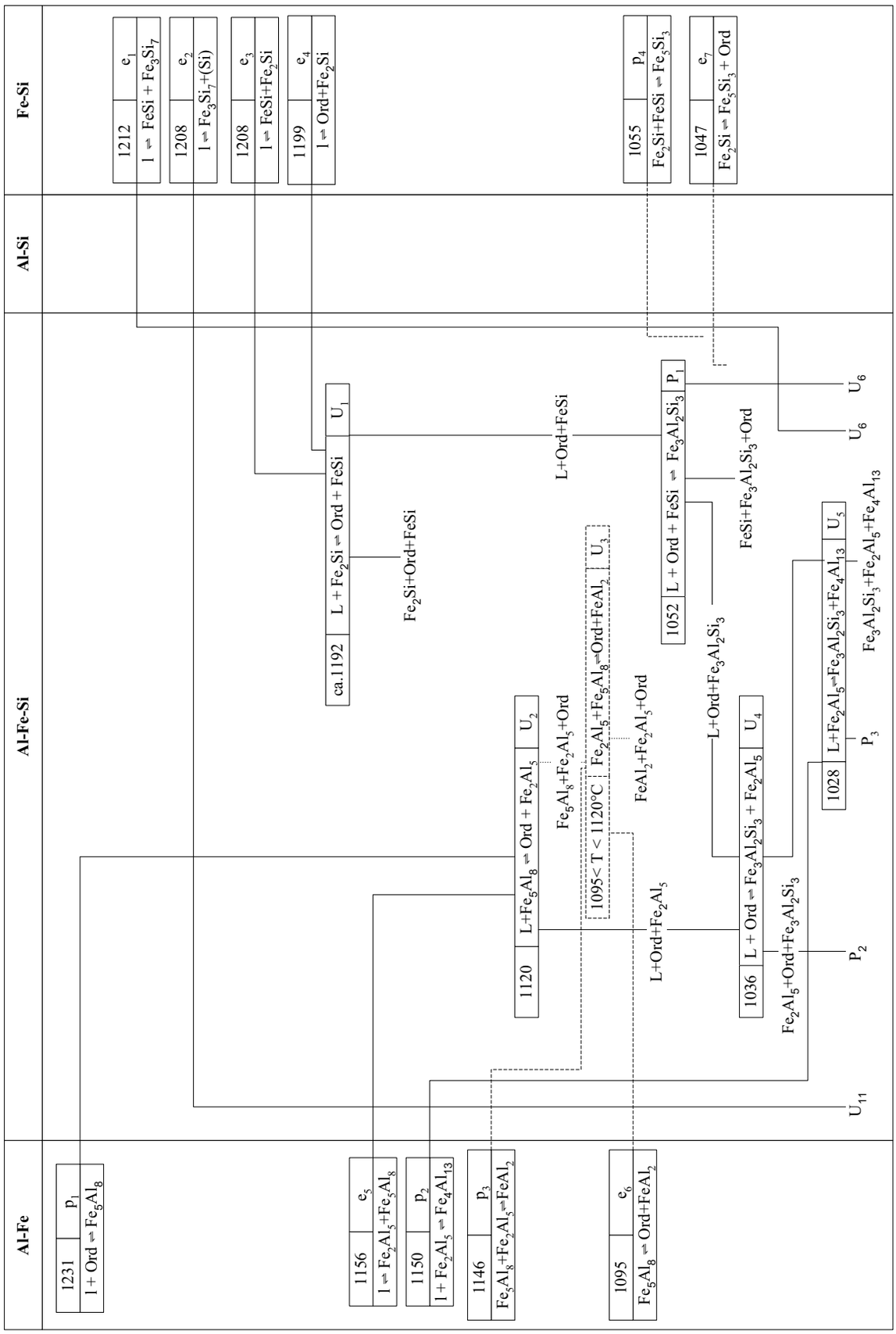

Fig. 5a: Reaction scheme. "Ord" denotes ordered Fe(Al,Si) or $Fe_3(Al,Si)$ phases

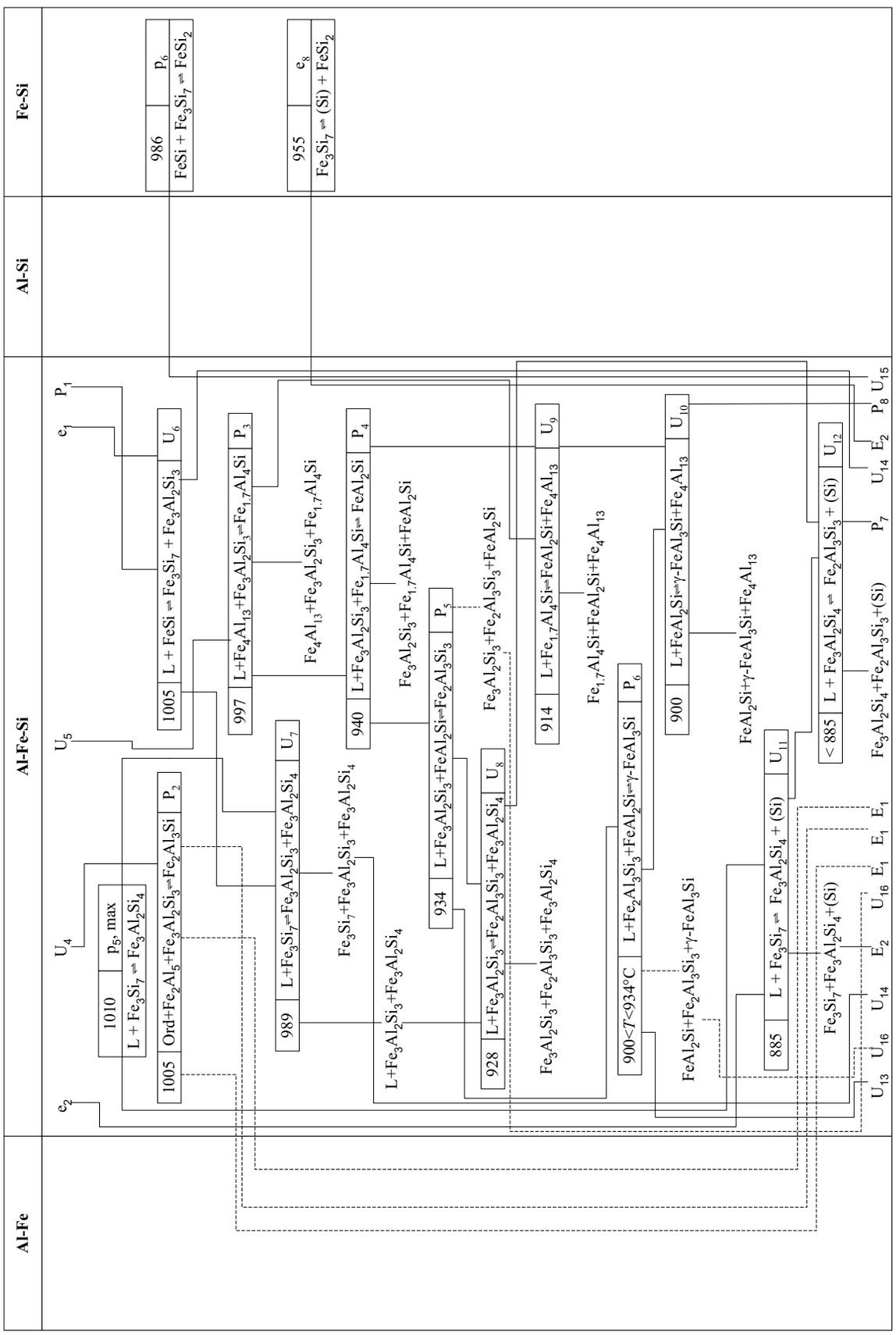

Fig. 5b: Reaction scheme. "Ord" denotes ordered Fe(Al,Si) or $Fe_3(Al,Si)$ phases

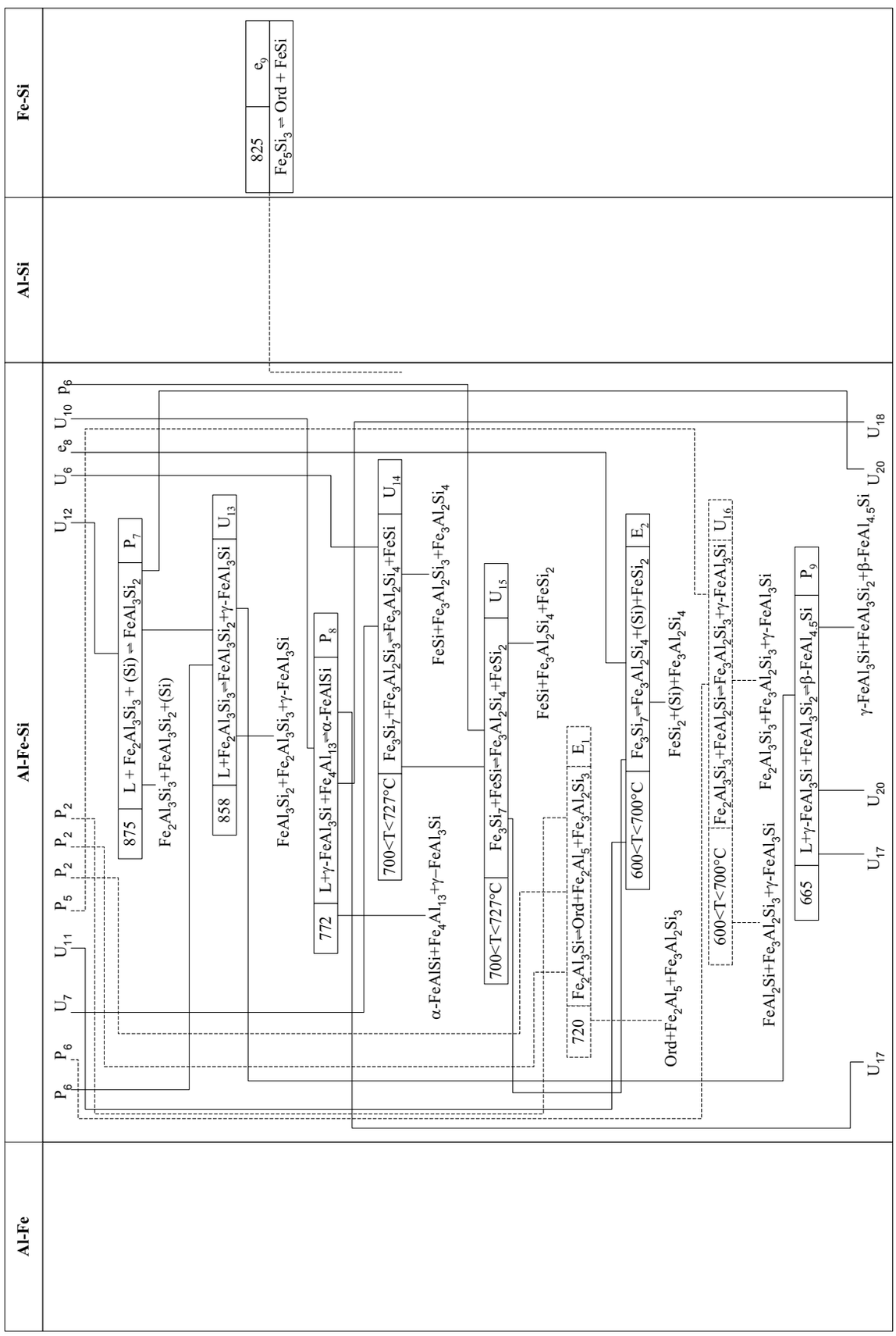

Fig. 5c: Reaction scheme. "Ord" denotes ordered Fe(Al,Si) or $Fe_3(Al,Si)$ phases

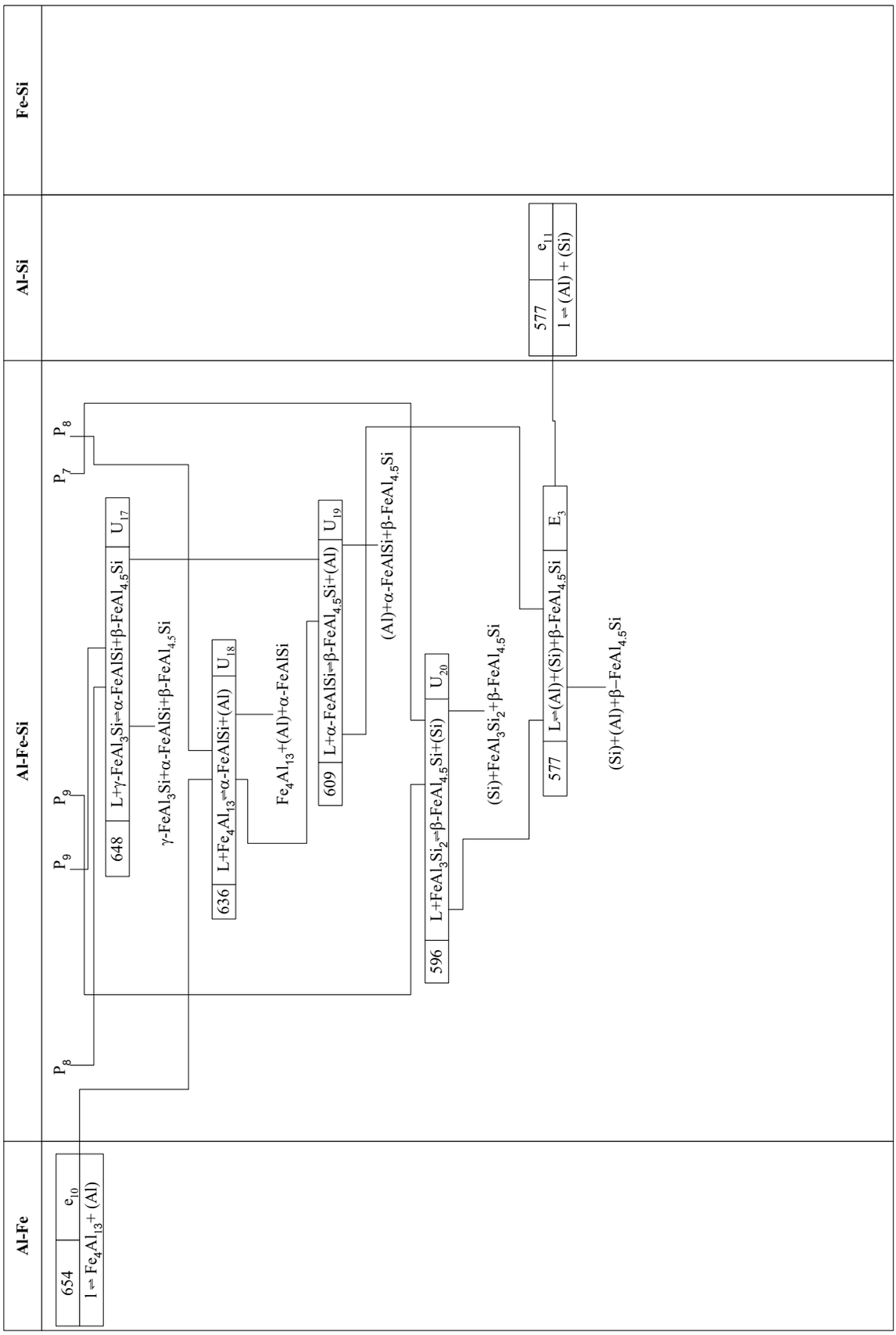

Fig. 5d: Reaction scheme. "Ord" denotes ordered Fe(Al,Si) or $Fe_3(Al,Si)$ phases

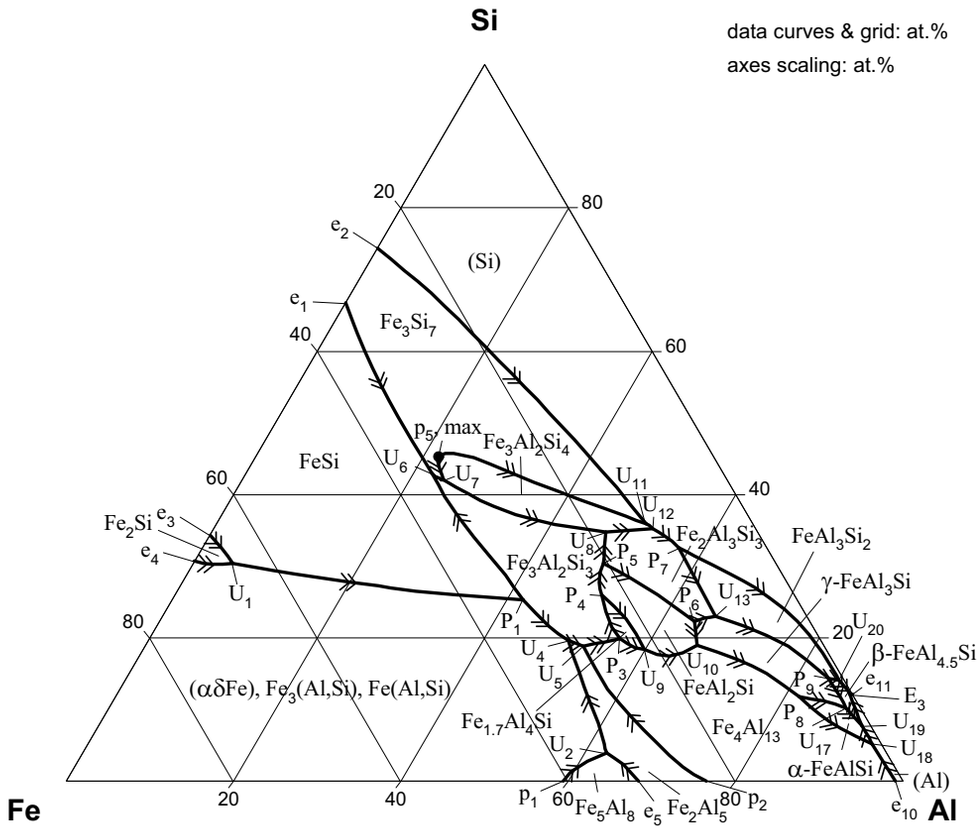

Fig. 6: Al-Fe-Si. Liquidus surface projection

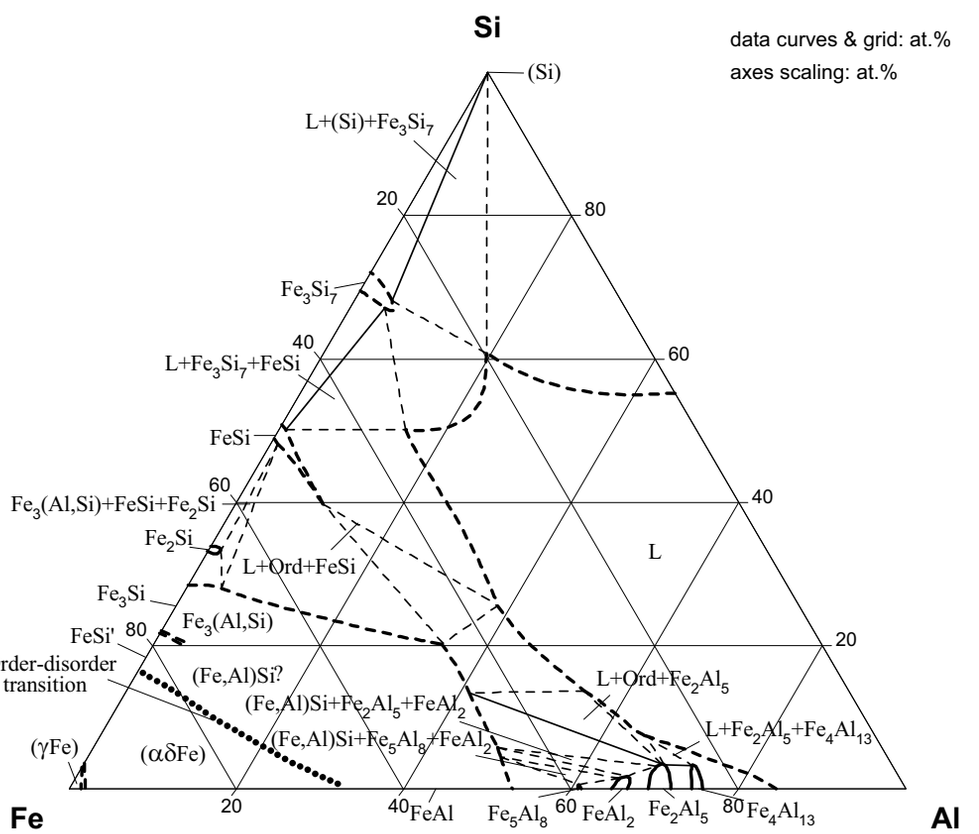

Fig. 7: Al-Fe-Si. Isothermal section at 1100°C

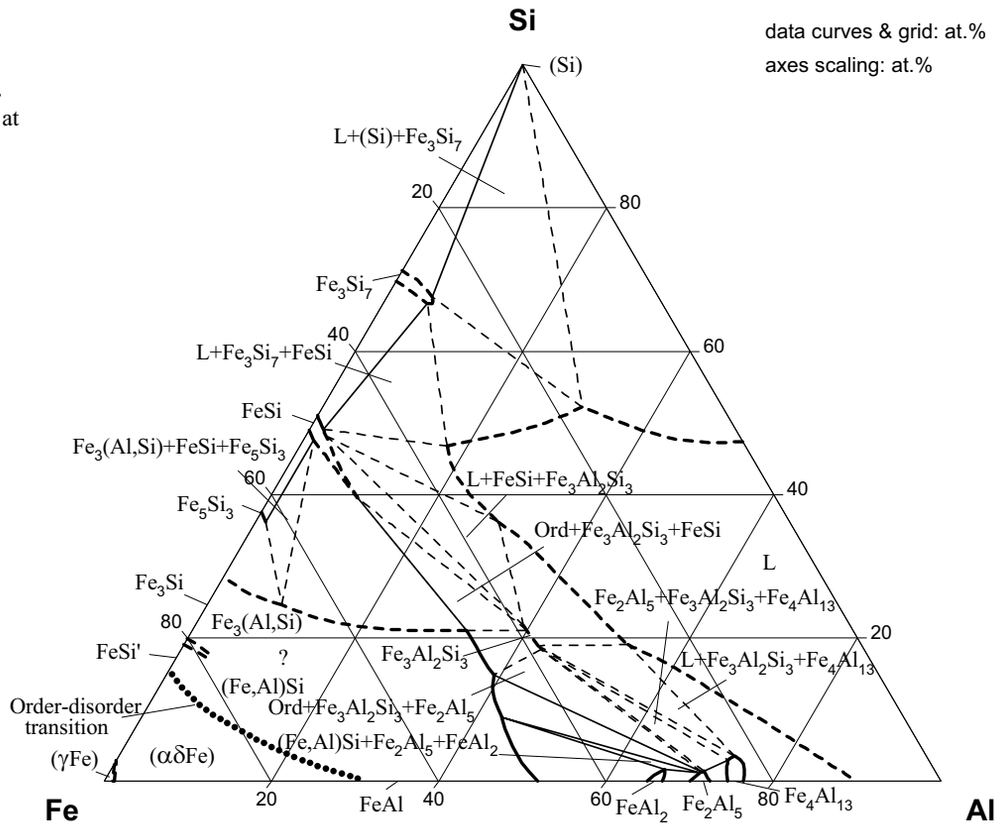

Fig. 8: Al-Fe-Si.
Isothermal section at 1020°C

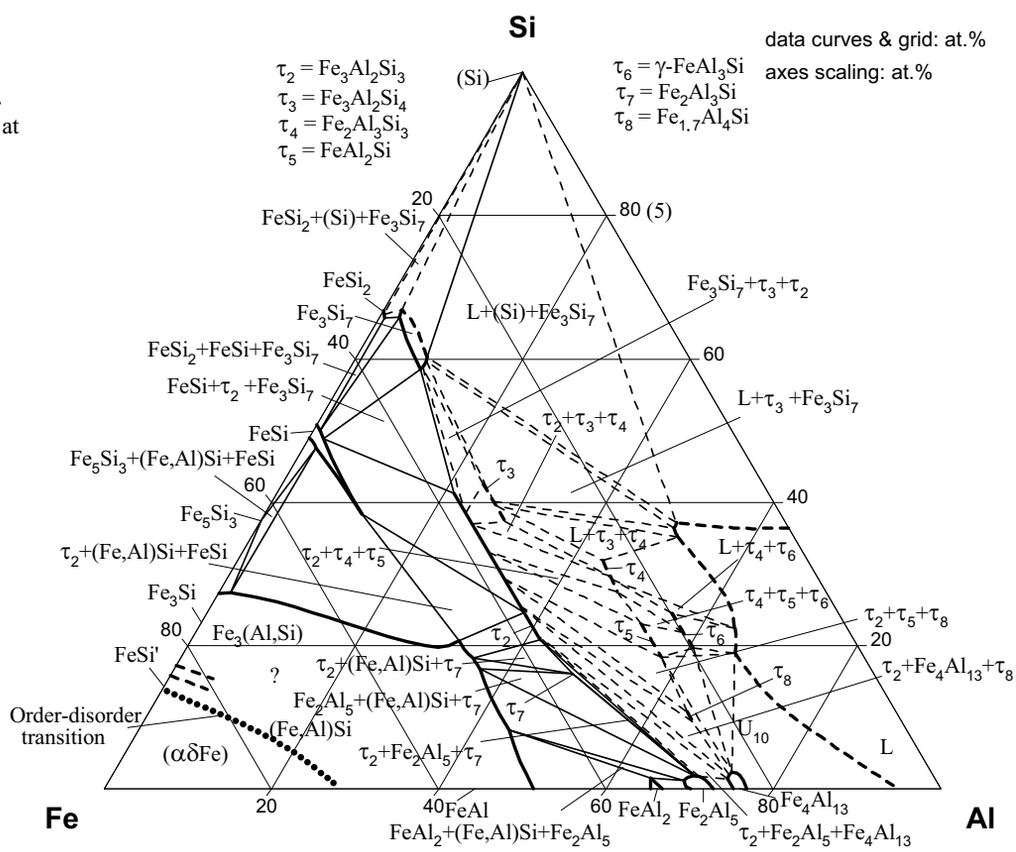

Fig. 9: Al-Fe-Si.
Isothermal section at 900°C

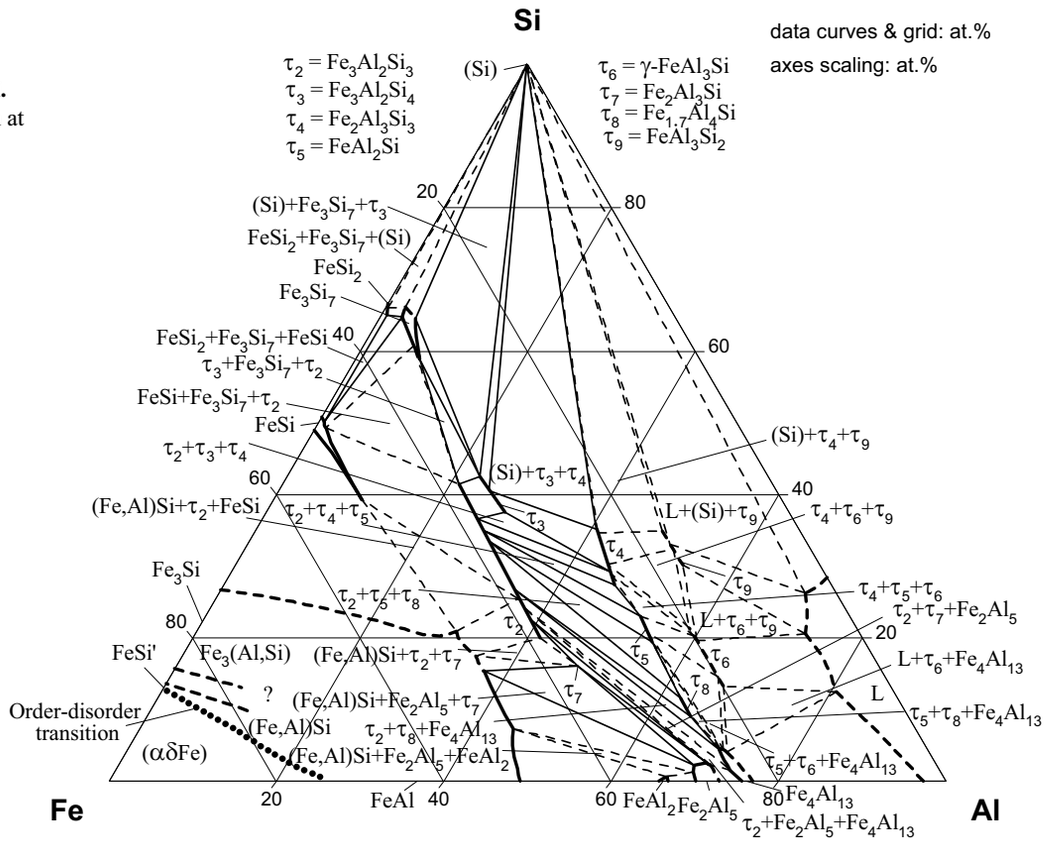

Fig. 10: Al-Fe-Si.
Isothermal section at 800°C

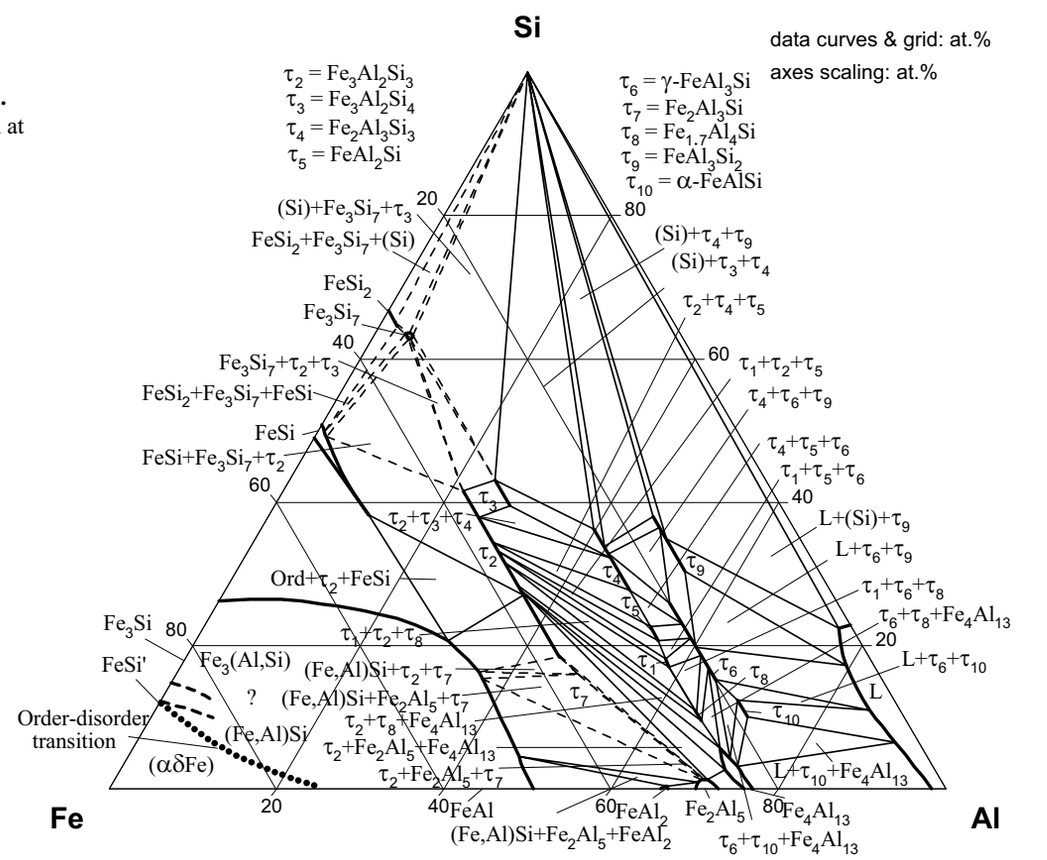

Fig. 11: Al-Fe-Si.
Isothermal section at 727°C

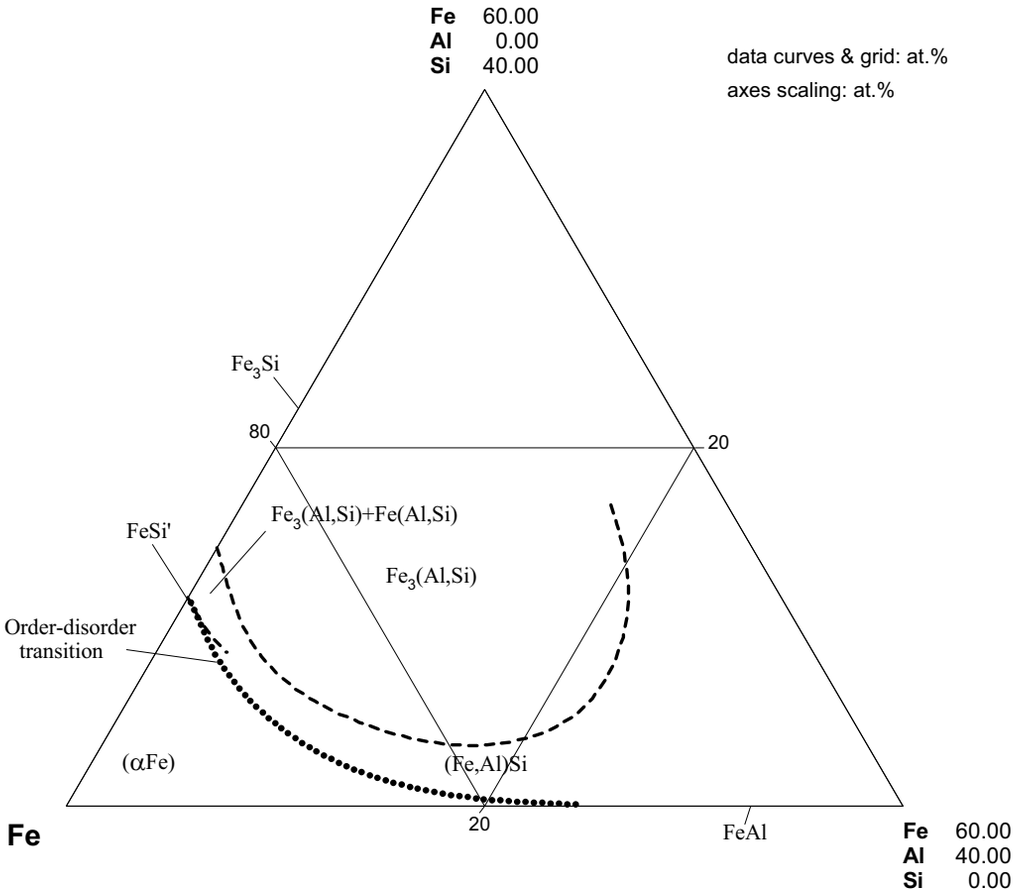

Fig. 12: Al-Fe-Si. Partial isothermal section at 700°C

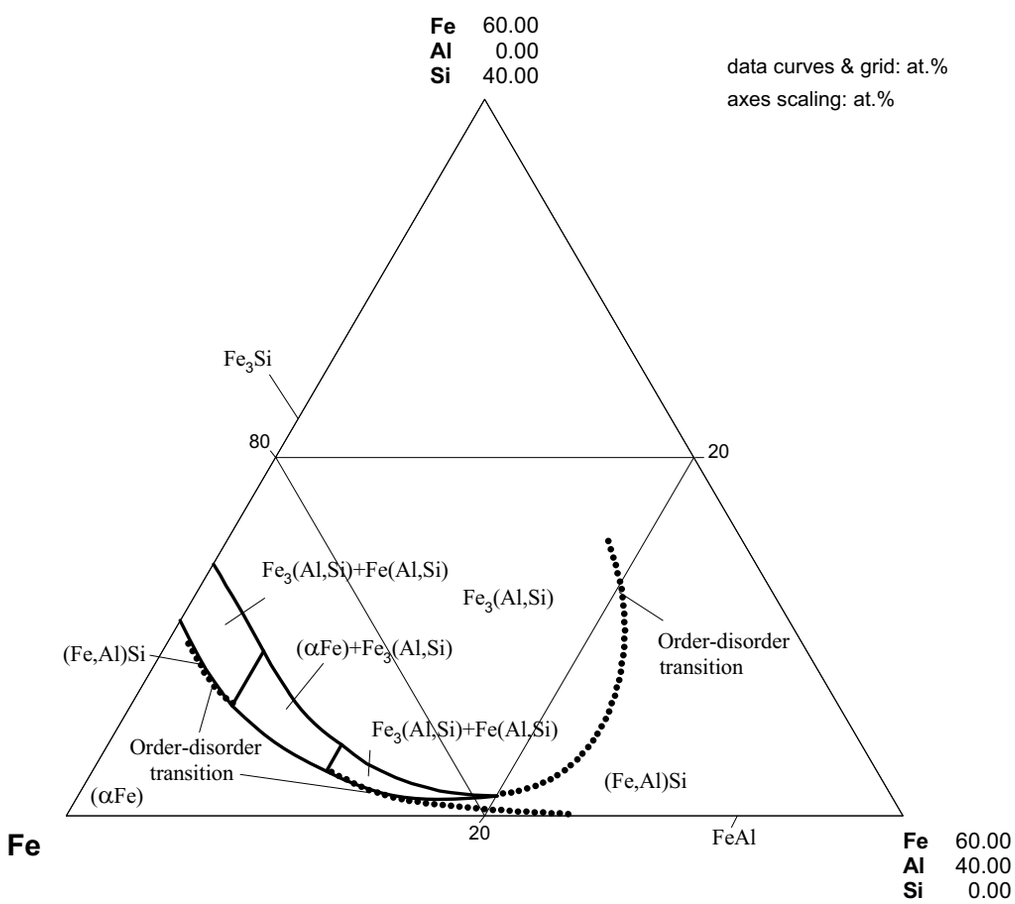

Fig. 13: Al-Fe-Si. Phase equilibria in the Fe corner at 650°C

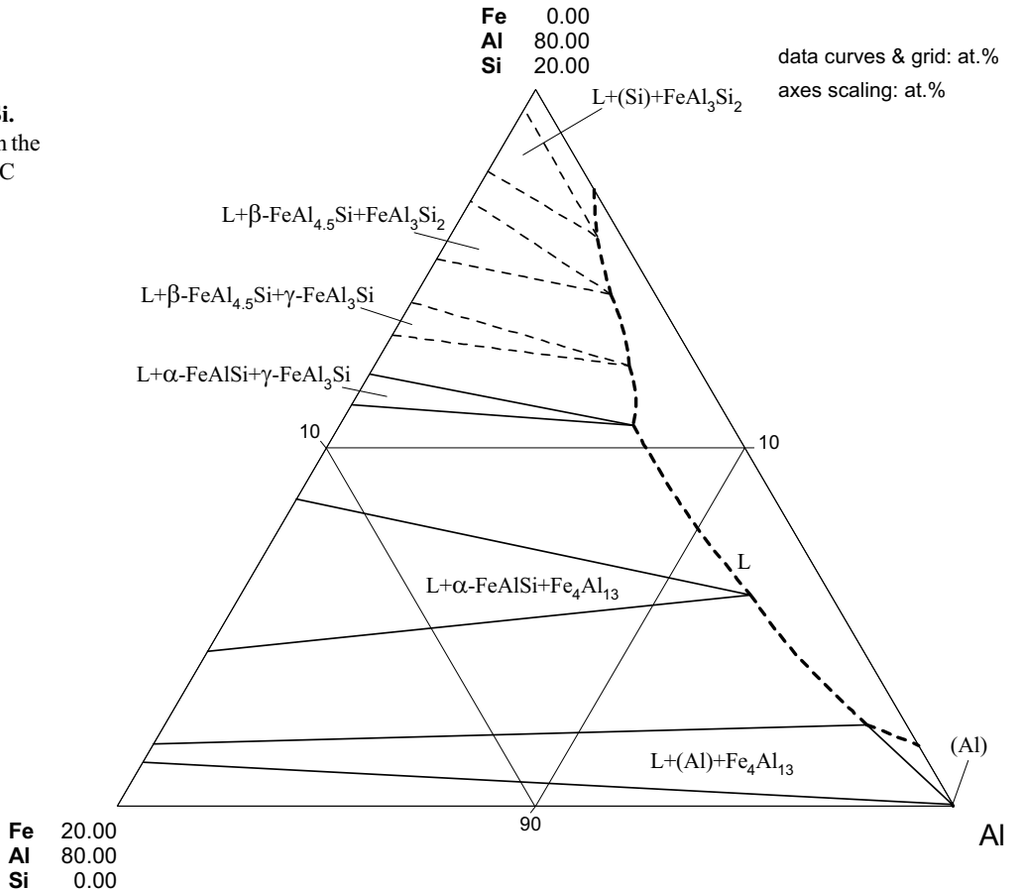

Fig. 14: Al-Fe-Si.
Phase equilibria in the Al corner at 650°C

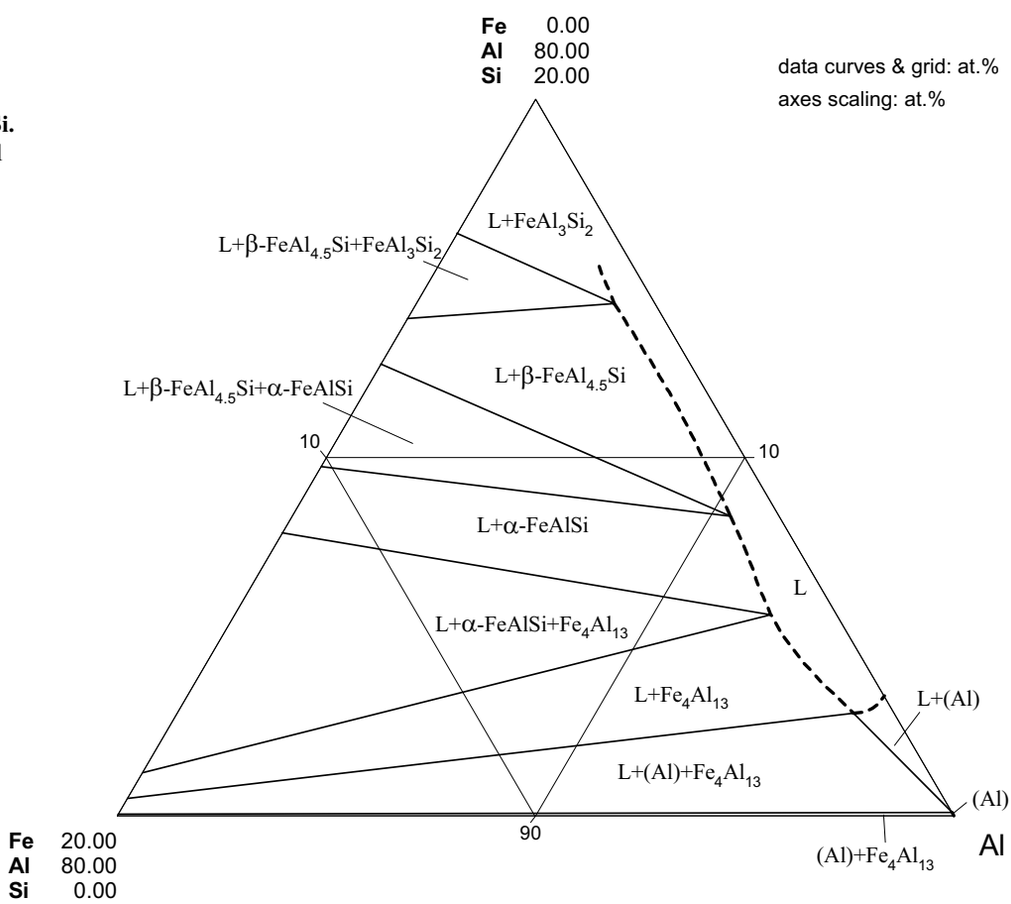

Fig. 15: Al-Fe-Si.
Partial isothermal section at 640°C

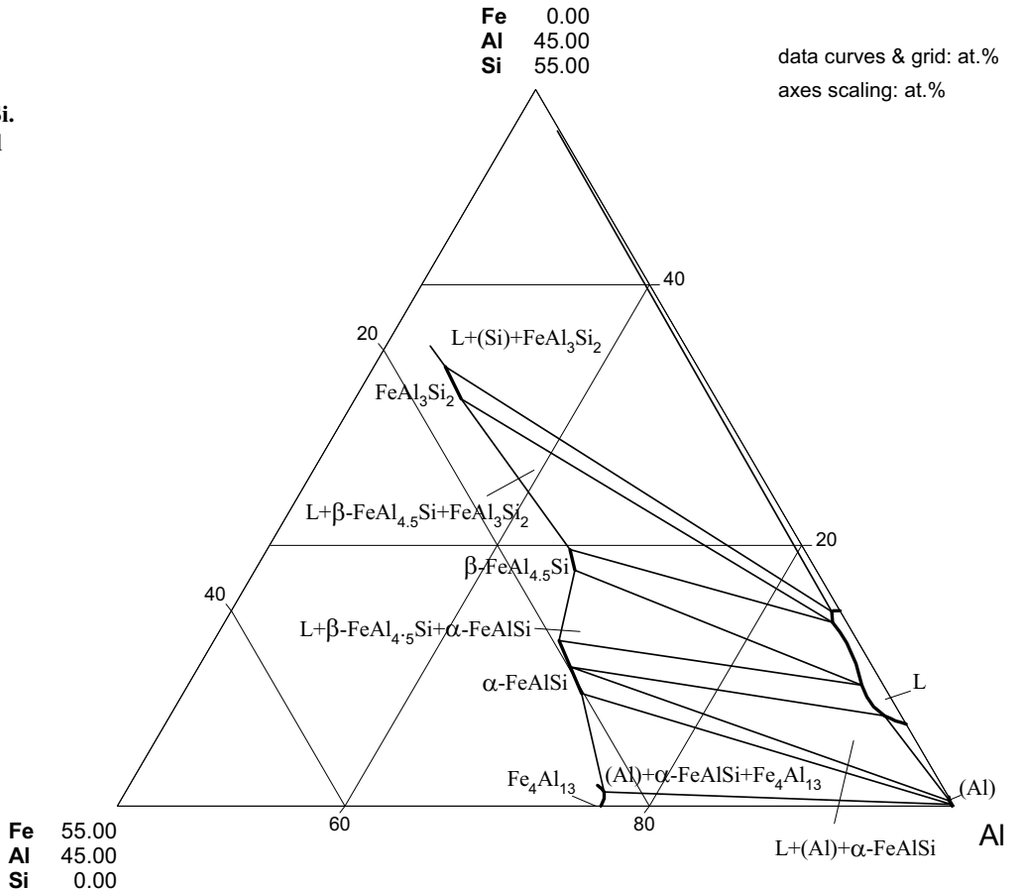

Fig. 16: Al-Fe-Si.
Partial isothermal section at 620°C

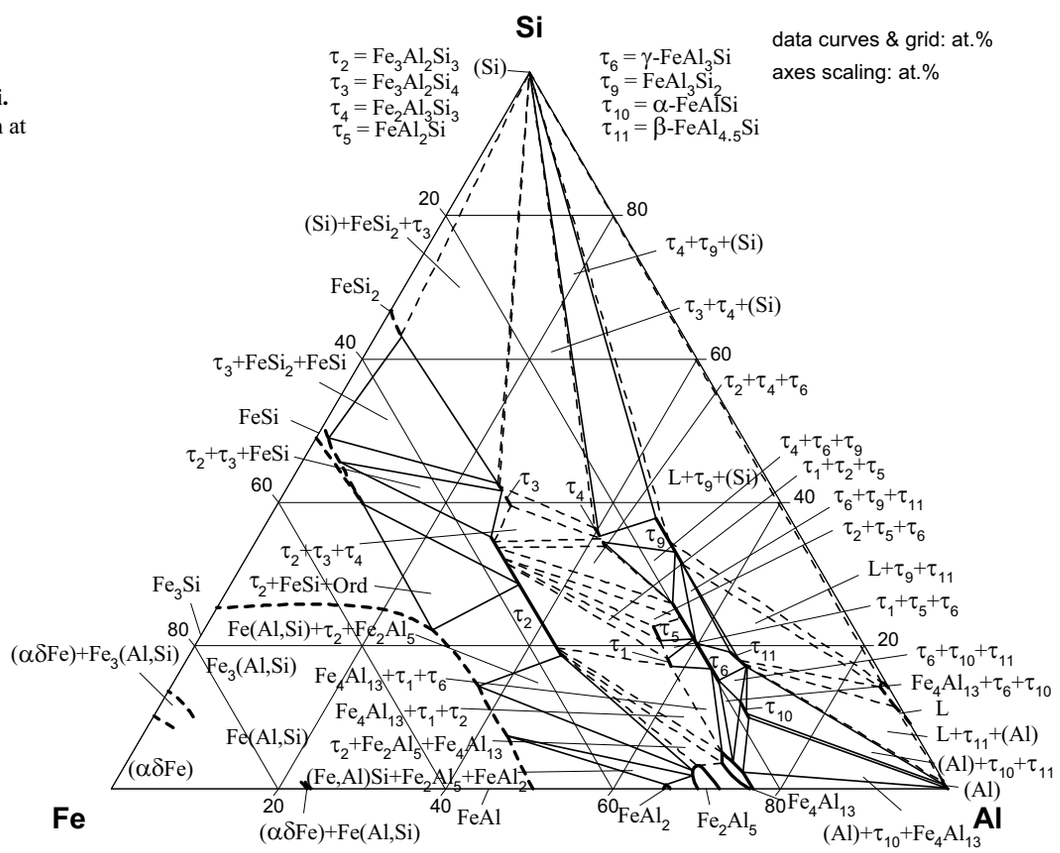

Fig. 17: Al-Fe-Si.
Isothermal section at 600°C

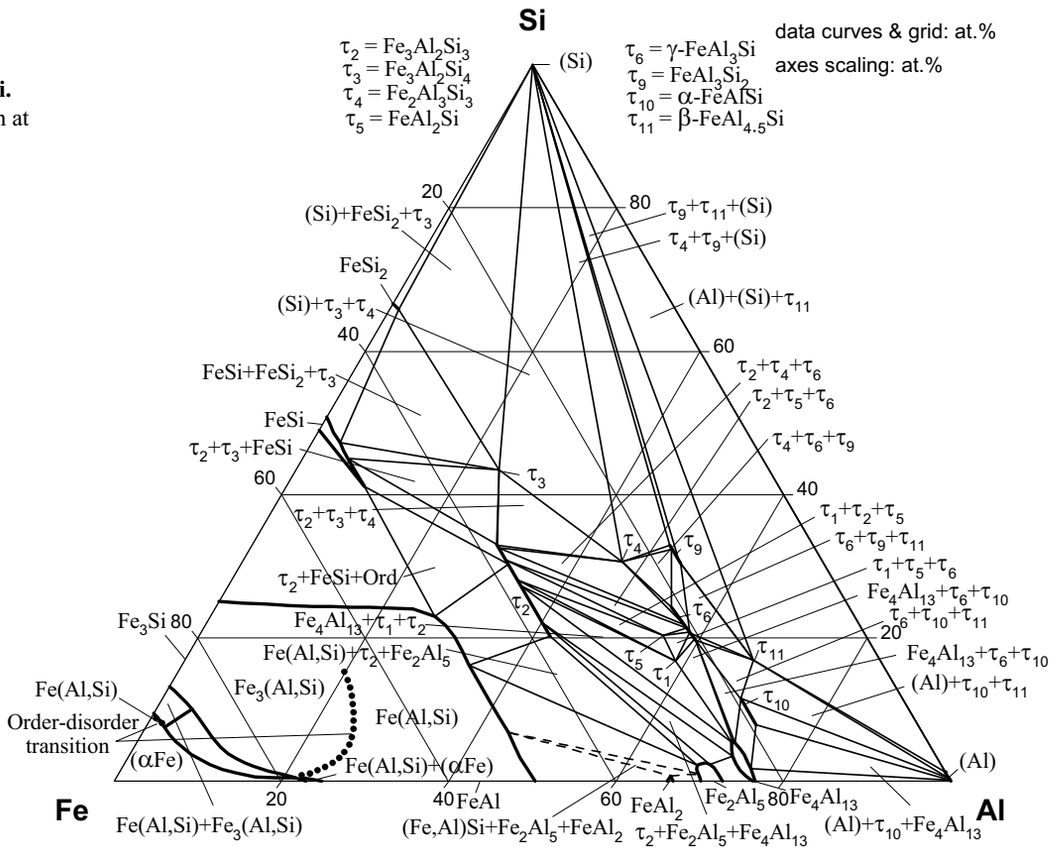

Fig. 18: Al-Fe-Si.
Isothermal section at 550°C

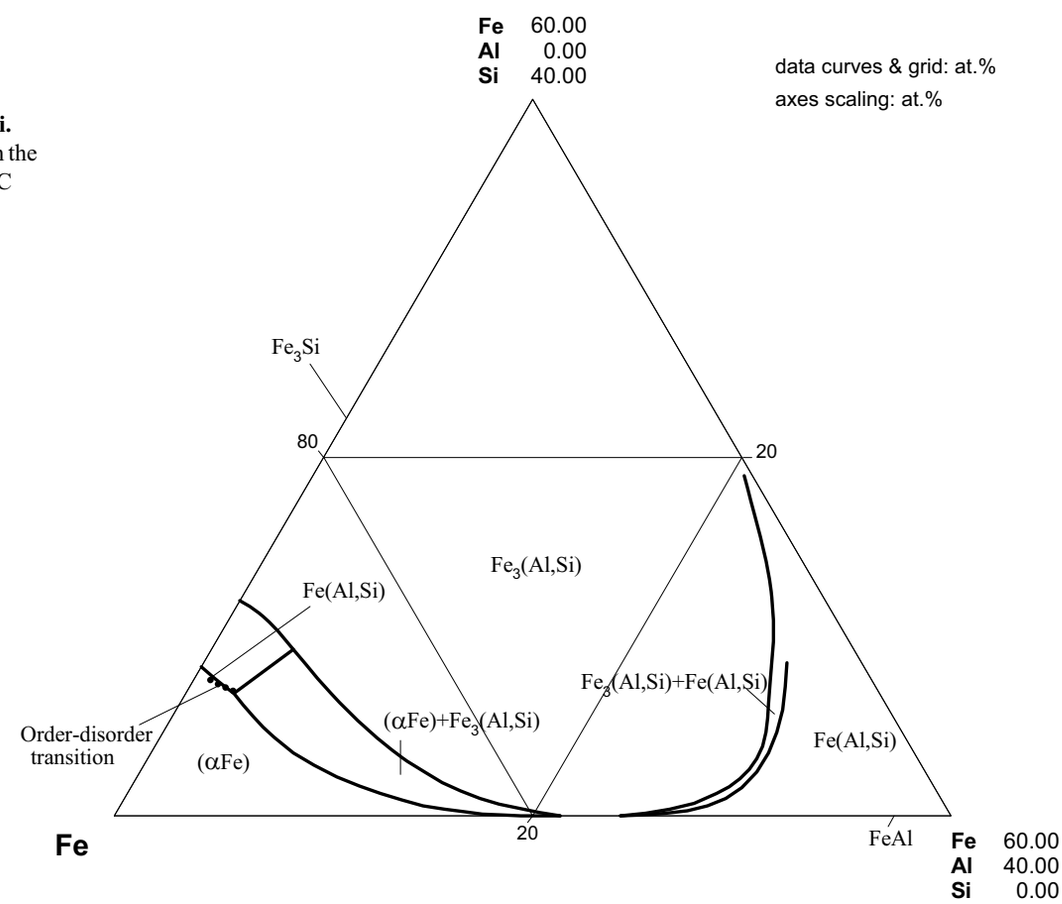

Fig. 19: Al-Fe-Si.
Phase equilibria in the Fe corner at 450°C

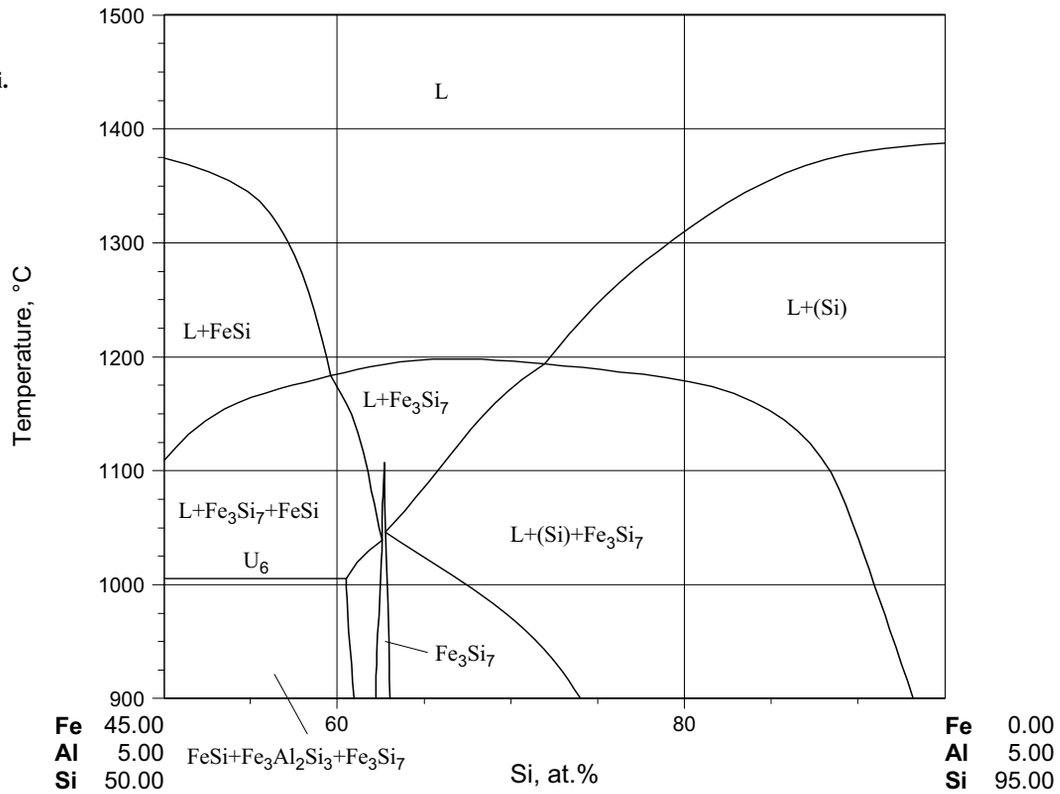

Fig. 20: Al-Fe-Si. Partial isopleth at 5 at.% Al

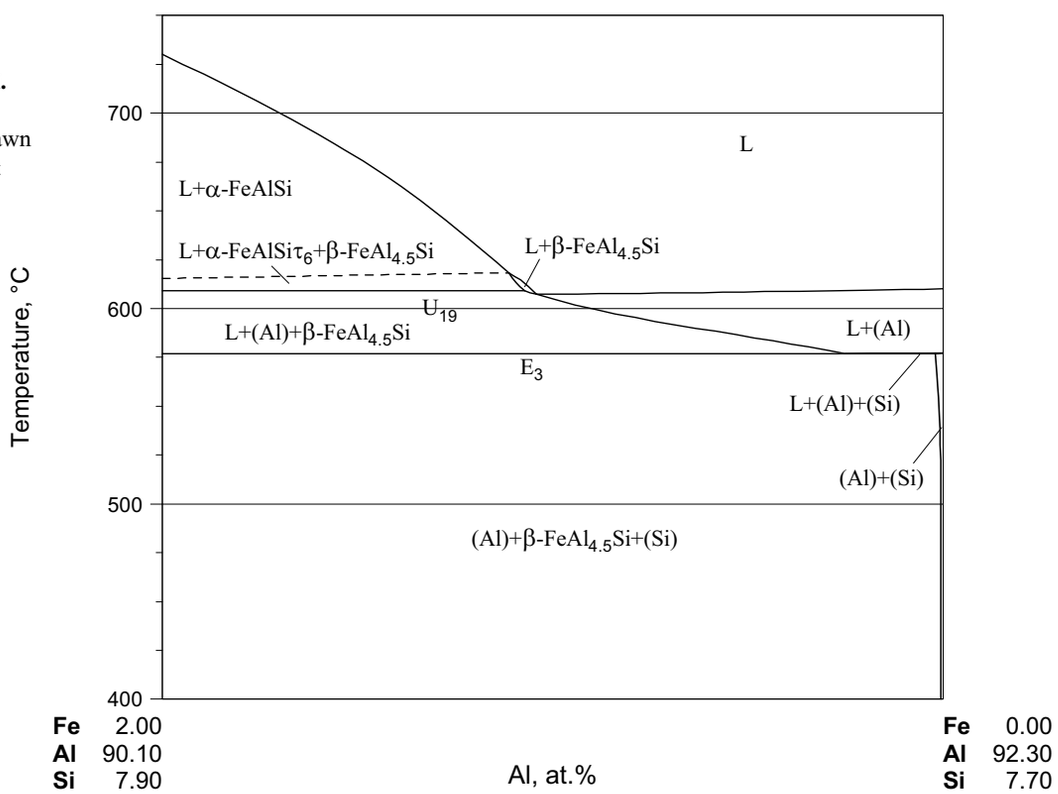

Fig. 21: Al-Fe-Si. Partial isopleth at 8 mass% Si. Redrawn for atomic percent

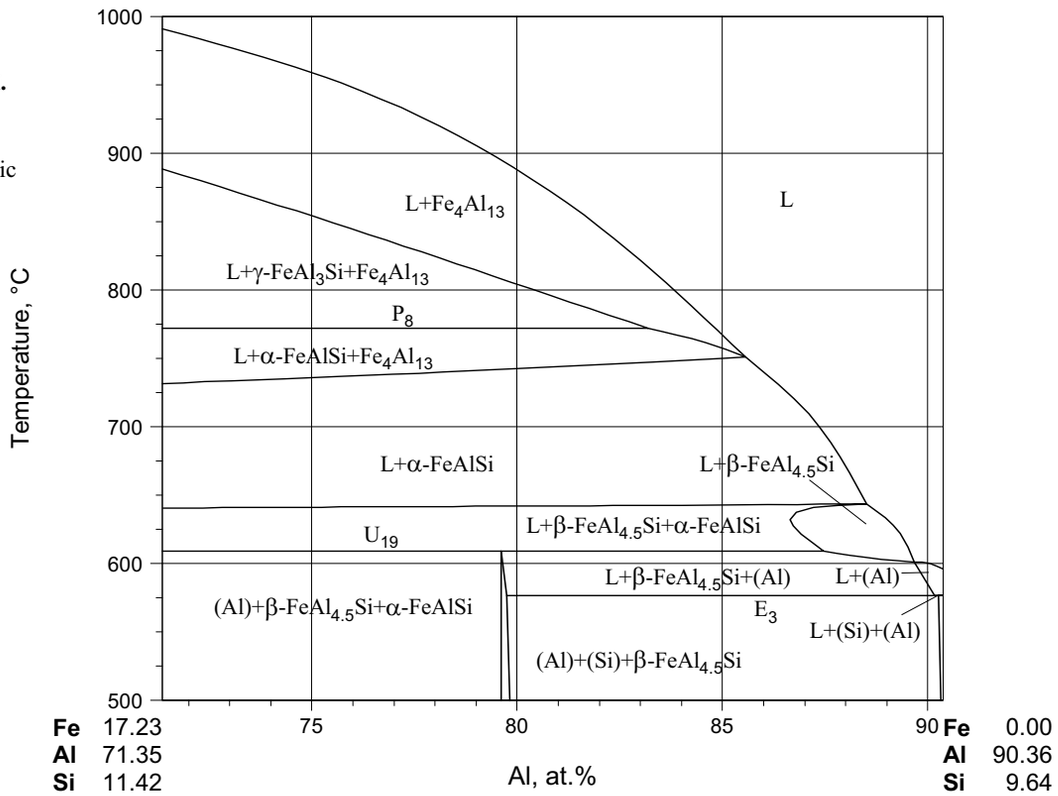

Fig. 22: Al-Fe-Si. Partial isopleth at 10 mass% Si. Redrawn for atomic percent

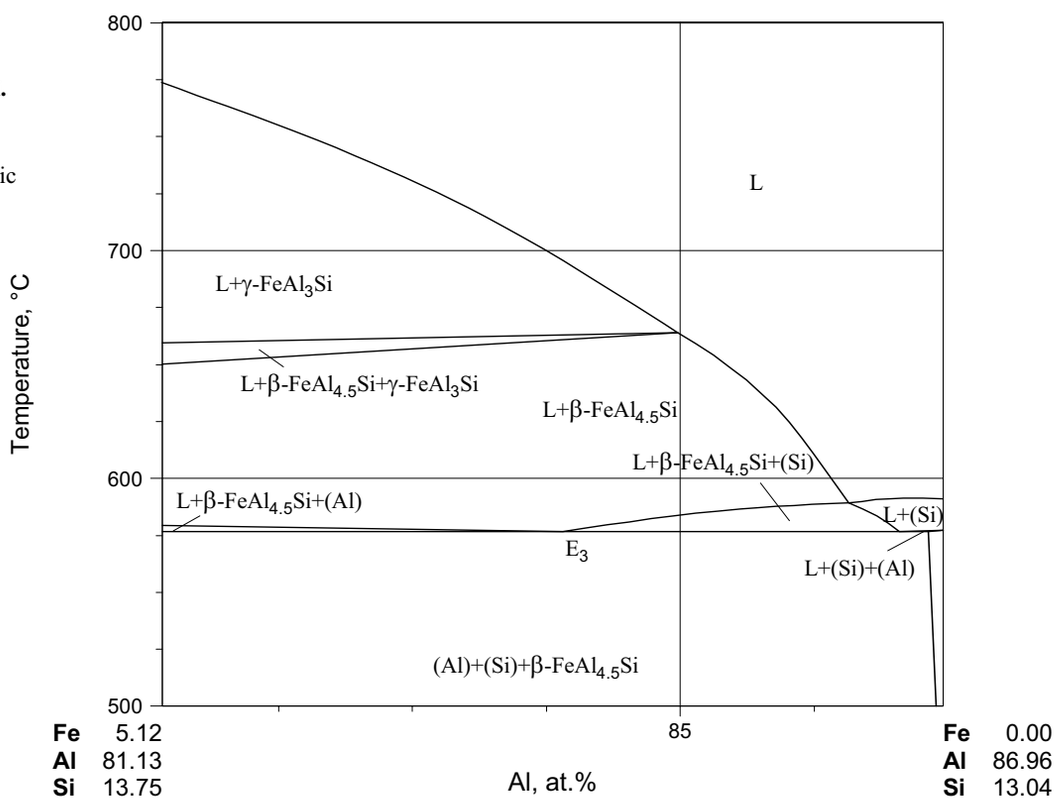

Fig. 23: Al-Fe-Si. Partial isopleth at 13.5 mass% Si. Redrawn for atomic percent

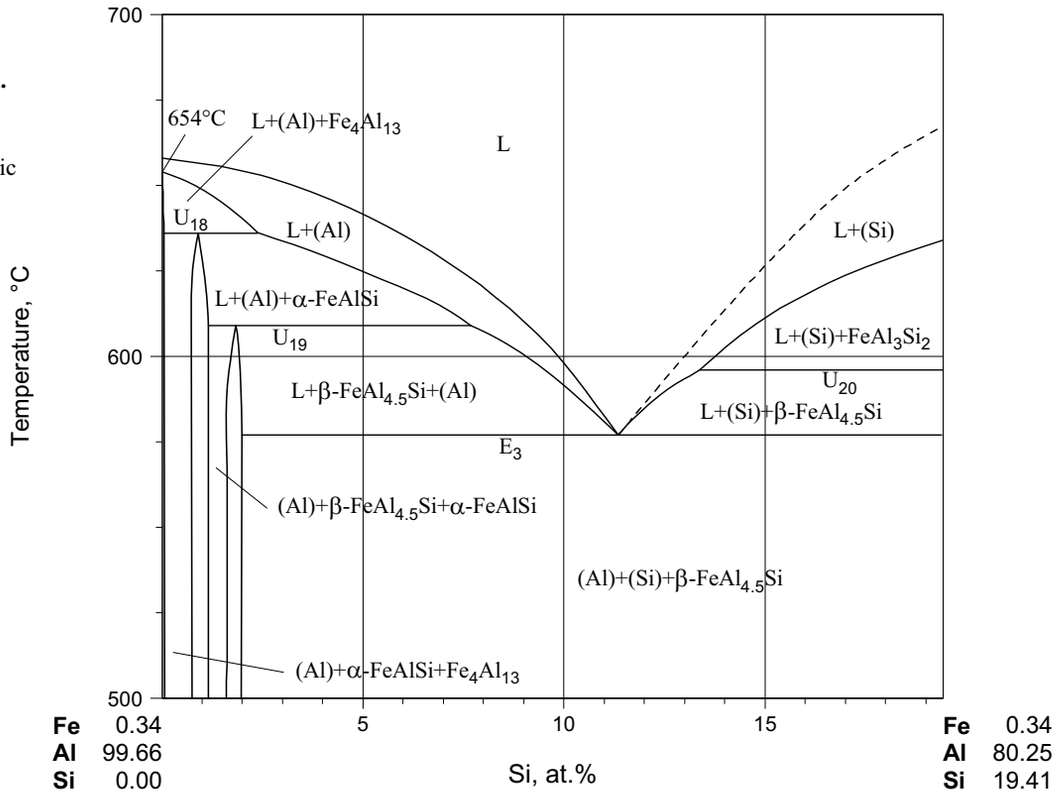

Fig. 24: Al-Fe-Si. Partial isopleth at 0.7 mass% Fe. Redrawn for atomic percent

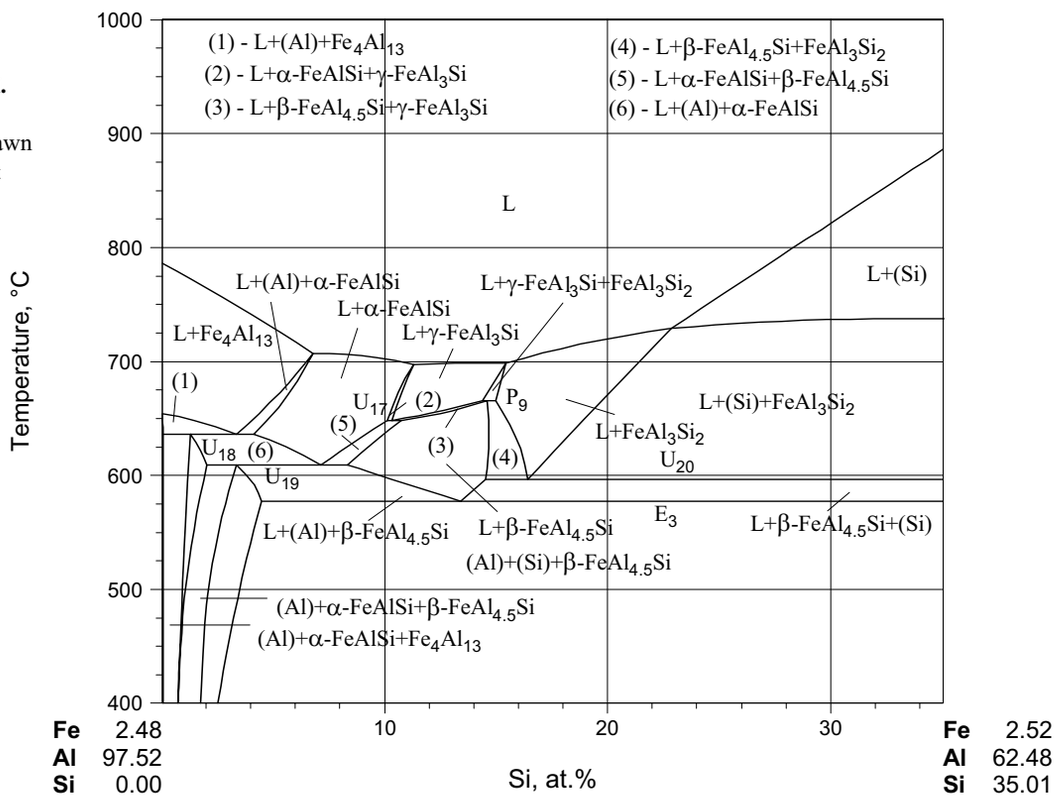

Fig. 25: Al-Fe-Si. Partial isopleth at 5 mass% Fe. Redrawn for atomic percent

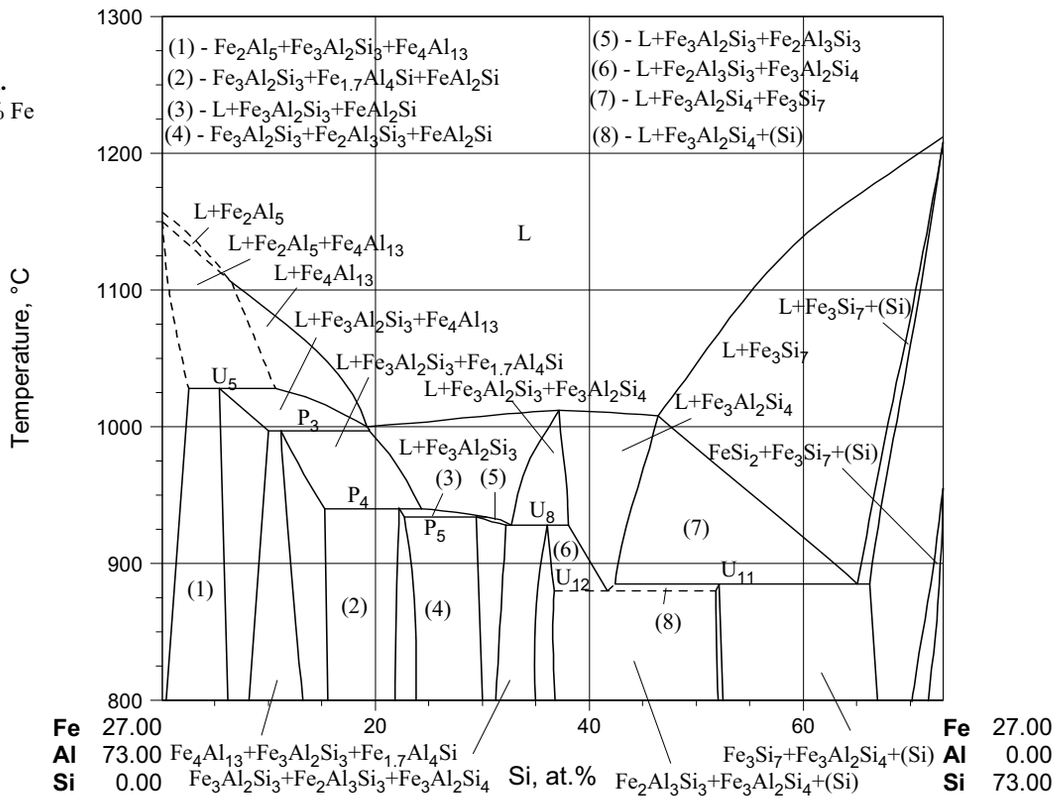

Fig. 26: Al-Fe-Si.
Isopleth at 27 at.% Fe

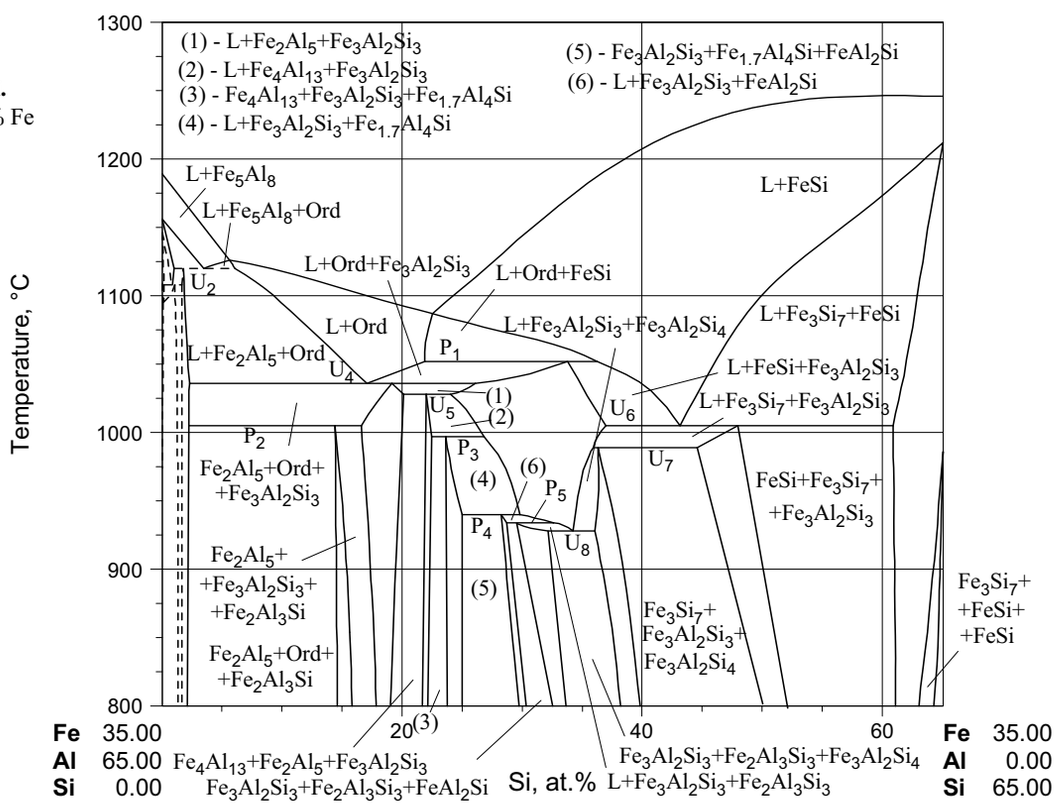

Fig. 27a: Al-Fe-Si.
Isopleth at 35 at.% Fe

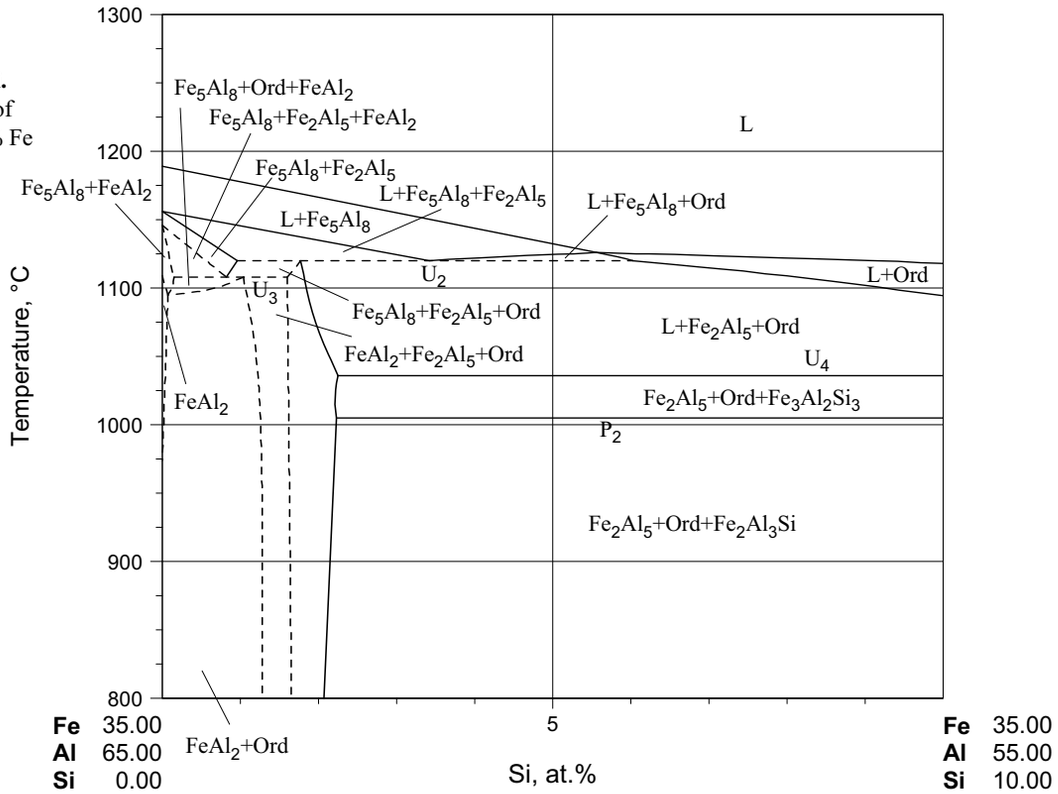

Fig. 27b:Al-Fe-Si.
Enlarged portion of isopleth at 35 at.% Fe

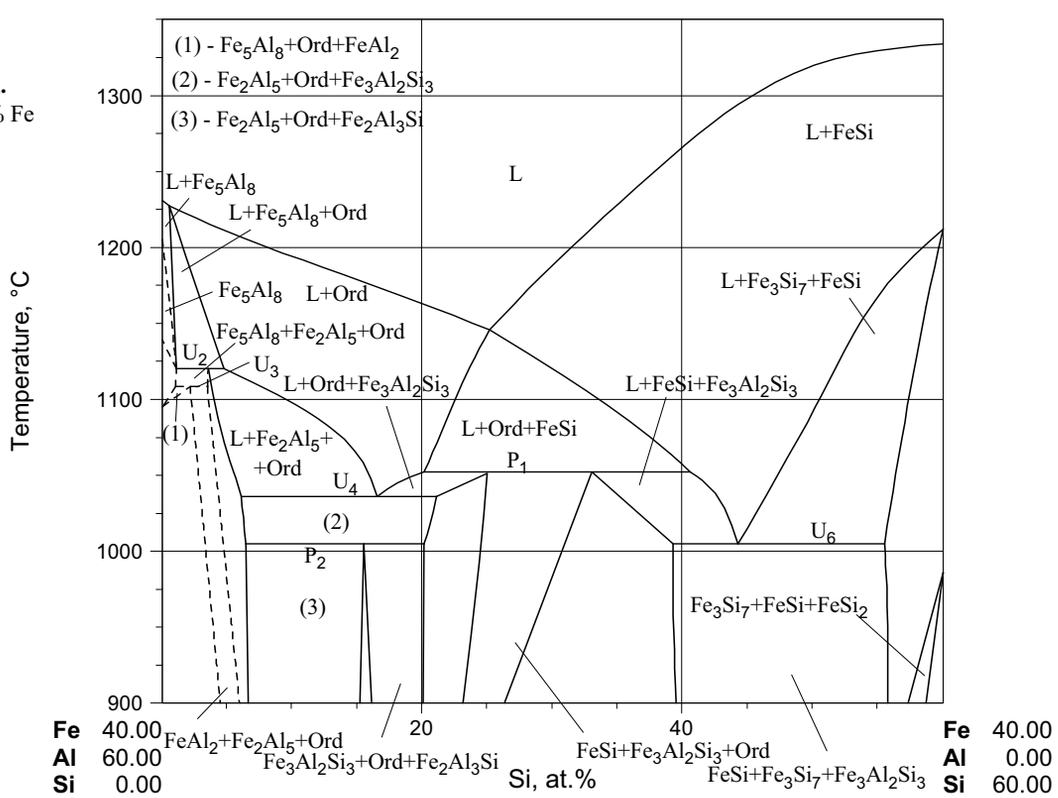

Fig. 28: Al-Fe-Si.
Isopleth at 40 at.% Fe

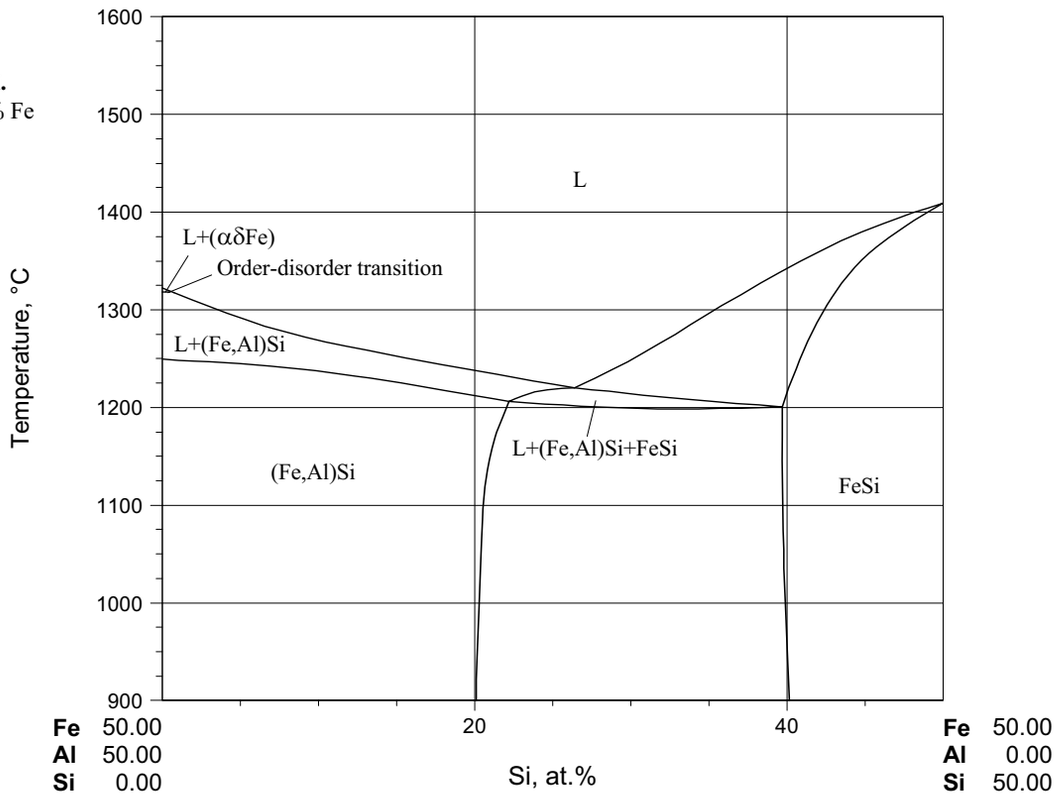

Fig. 29: Al-Fe-Si. Isopleth at 50 at.% Fe

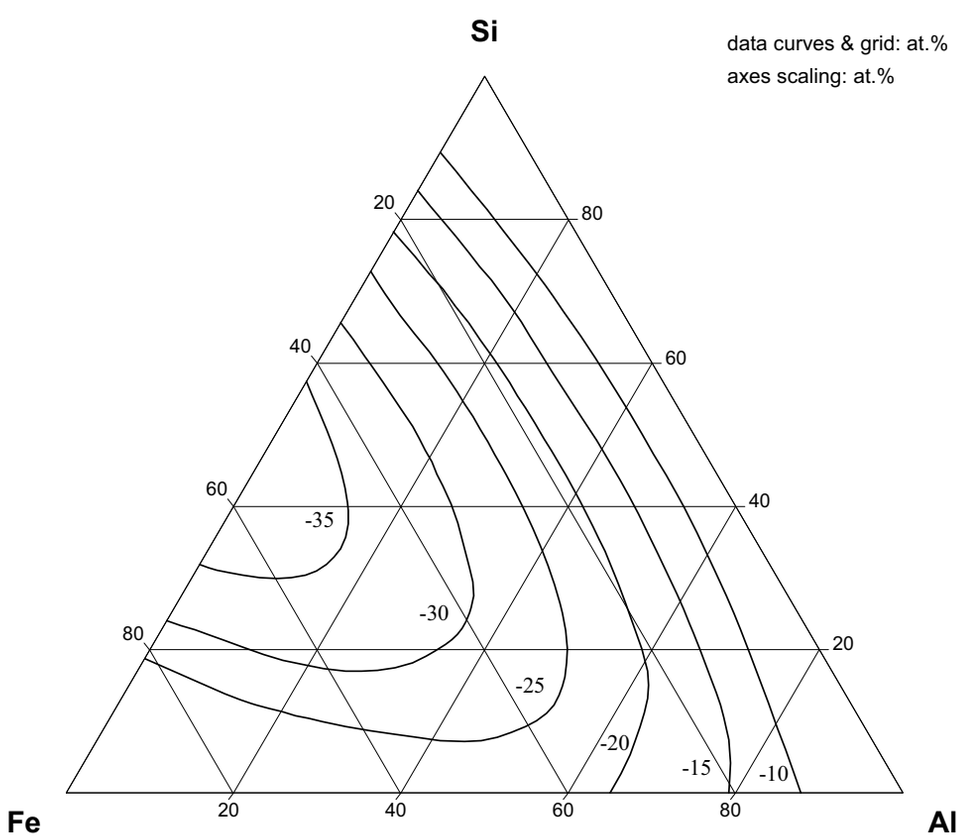

Fig. 30: Al-Fe-Si. Integral enthalpy of mixing of liquid alloys at 1477°C, in kJ/mol of atoms